



Working Report 2011-84

Quality Control and Characterization of Bentonite Materials

Leena Kiviranta
Sirpa Kumpulainen

December 2011

Working Report 2011-84

Quality Control and Characterization of Bentonite Materials

Leena Kiviranta
Sirpa Kumpulainen
B+Tech Oy

December 2011

Working Reports contain information on work in progress
or pending completion.

The conclusions and viewpoints presented in the report
are those of author(s) and do not necessarily
coincide with those of Posiva.

QUALITY CONTROL AND CHARACTERIZATION OF BENTONITE MATERIALS

ABSTRACT

Before bentonite material is taken into use in performance testing, the quality of the material needs to be checked. Three high grade bentonite materials: two natural Na-bentonites from Wyoming, and one natural Ca-bentonite from Milos, were characterized. Each material was characterized using duplicate or triplicate samples in order to study variability in material quality in batches. The procedure consisted of basic acceptance testing (water ratio, CEC, swelling index, liquid limit, and granule size distribution), advanced acceptance testing (exchangeable cations, chemical and mineralogical composition, density, swelling pressure and hydraulic conductivity) and complementary testing (herein surface area, water absorption capacity, montmorillonite composition, grain size distribution and plastic limit).

All three materials qualified the requirements set for buffer bentonite for CEC, smectite content, swelling pressure, and hydraulic conductivity. Wyoming bentonites contained approximately 88 wt.% of smectite, and Milos bentonite 79 wt.% of smectite and 3 wt.% of illite. Precision of smectite analyses was $\pm 2\%$, and variances in composition of parallel samples within analytical errors, at least for Wyoming bentonites. Accuracy of quantitative analyses for trace minerals such as gypsum, pyrite or carbonates, was however low. As the concentrations of these trace minerals are important for Eh or pH buffering reactions or development of bentonite pore water composition, normative concentrations are recommended to be used instead of mineralogically determined concentrations.

The swelling pressures and hydraulic conductivities of different materials were compared using EMDD. Swelling pressure was relatively higher for studied Ca-bentonite than for the studied Na-bentonites and the difference could not be explained with different smectite contents. Hydraulic conductivities seemed to be similar for all materials.

The results of index tests correlated with the smectite content. Thus, in a certain extent, index tests can be used to determine the smectite content indicatively for quality control purposes. Previously set acceptance testing requirement limits for swelling index, liquid limit and CEC should be reconsidered, since Ca-bentonite tested in this study did not fulfill the requirement for swelling index, the previously set liquid limit requirement value was way below the values measured in this study, and because the previously set CEC requirement limits were based on a technique that needed different requirement limits for Na- and Ca-bentonites, on contrary to the method used in this study.

Keywords: Quality control, characterization, bentonite, index test, composition, swelling pressure, hydraulic conductivity.

BENTONIITTIMATERIAALIEN LAADUNVALVONTA JA KARAKTERISOINTI

TIIVISTELMÄ

Bentoniittimateriaalin laatu täytyy tarkastaa ennen kuin se otetaan käyttöön toimintakyky-analyyseissä. Kolme korkealaatuista bentoniittimateriaalia: kaksi Na-bentoniittia Wyomingista ja yksi Ca-bentoniitti Milokselta, karakterisoitiin. Jokaisesta materiaalista karakterisoitiin kaksi tai kolme rinnakkaisnäytettä, jotta materiaalien laadun vaihtelua voitiin arvioida. Karakterisointimenetelmä sisälsi perushyväksyntätestauksen (vesipitoisuus, CEC, paisuntaindeksi, juoksuraja ja raekokojakauma), jatkohyväksyntätestauksen (vaihtuvat kationit, kemiallinen ja mineraloginen koostumus, tiheys, paisuntapaine ja vedenjohtavuus) ja täydentävän testauksen (tässä tutkimuksessa pinta-ala, veden absorptiokyky, montmorilloniitin koostumus, partikkelikokojakauma ja plastisuusraja).

Kaikki kolme materiaalia täyttivät bentoniittipuskurin CEC:lle, smektiittipitoisuudelle, paisuntapaineelle ja vedenjohtavuudelle asetetut vaatimukset. Wyoming-bentoniitit sisälsivät noin 88 % smektiittiä, ja Milos-bentoniitti 79 % smektiittiä ja 3 % illiittiä. Smektiitin pitoisuusmäärittysten toistettavuus oli ± 2 %, ja rinnakkaisnäytteiden välinen koostumuksen vaihtelu analyttisen virheen rajoissa, ainakin Wyoming-bentoniiteilla. Kvantitatiivisten analyysien tarkkuus hivenmineraaleille, kuten kipsille, rikkikiisulle tai karbonaateille oli kuitenkin alhainen. Koska näiden hivenmineraalien pitoisuudet ovat tärkeitä bentoniitin Eh tai pH puskurireaktioille tai huokosveden koostumuksen kehitykselle, niille suositellaan käytettävän normatiivisia pitoisuuksia mineralogisesti määritettyjen pitoisuuksien sijaan.

Eri materiaalien paisuntapaineita ja vedenjohtavuuksia vertailtiin EMDD:n avulla. Tutkitun Ca-bentoniitin paisuntapaine oli suhteessa suurempi kuin tutkittujen Na-bentoniittien, eikä eroa voitu selittää erilaisilla smektiittipitoisuuksilla. Kaikkien tutkittujen materiaalien vedenjohtokyky näytti olevan samaa suuruusluokkaa.

Indeksitestien tulokset korreloivat smektiittipitoisuuden kanssa. Niinpä, tietyssä laajuudessa, indeksitestejä voidaan käyttää indikoivaan smektiittipitoisuuden arviointiin laaduntarkkailutarkoituksessa. Aikaisemmin asetettuja paisuntaindeksin, juoksurajan ja CEC:n hyväksyntärajoja kannattaisi harkita uudelleen, koska tässä tutkimuksessa analysoidut Ca-bentoniitit eivät täyttäneet vaatimuksia paisuntaindeksille, aikaisemmin asetettu juoksurajan hyväksyntäraja oli huomattavasti alhaisempi kuin tässä tutkimuksessa määritetyt juoksurajat, ja koska aikaisemmin asetetut CEC:n hyväksyntäraajat perustuivat tekniikkaan, jonka seurauksena tarvittiin eri hyväksyntäraajat Na- ja Ca-bentoniiteille, päinvastoin kuin esimerkiksi tässä tutkimuksessa käytetyssä menetelmässä.

Avainsanat: Laadunvalvonta, bentoniitti, karakterisointi, indeksitesti, koostumus, paisuntapaine, vedenjohtavuus.

TABLE OF CONTENTS

ABSTRACT
TIIVISTELMÄ

LIST OF ABBREVIATIONS	3
PREFACE.....	5
1 INTRODUCTION	7
1.1 Quality requirements for buffer and backfill.....	7
1.2 Method selection	9
1.3 Materials.....	11
2 METHODS	13
2.1 Basic acceptance testing.....	13
2.1.1 Water ratio.....	13
2.1.2 CEC.....	13
2.1.3 Swelling index	14
2.1.4 Liquid limit	14
2.1.5 Granule size distribution by dry sieving.....	14
2.2 Advanced quality assurance testing.....	14
2.2.1 Original exchangeable cations	14
2.2.2 Chemical composition	15
2.2.3 Mineralogical composition.....	15
2.2.4 Grain density	16
2.2.5 Swelling pressure, hydraulic conductivity, dry density and EMDD.....	17
2.3 Complementary testing	21
2.3.1 Specific surface area by EGME-method	21
2.3.2 Water absorption capacity by Enslin-Neff device.....	21
2.3.3 Plastic limit	22
2.3.4 Composition of montmorillonite.....	22
2.3.5 Grain size distribution by laser diffraction	24
2.3.6 FTIR, Greene-Kelly test and the amount of illite	24
3 RESULTS	27
3.1 Basic acceptance testing.....	27
3.1.1 Water ratio, CEC, swelling index, liquid limit and granule size distribution by dry sieving.....	27
3.1.2 Comparison to acceptance requirements	29
3.2 Further quality assurance testing	29
3.2.1 Original exchangeable cations	29
3.2.2 Chemical composition	30

3.2.3	Mineralogical composition.....	31
3.2.4	Grain density	37
3.2.5	Swelling pressure, hydraulic conductivity, dry density and EMDD.....	37
3.2.6	Comparison to acceptance requirements	40
3.3	Complementary testing	40
3.3.1	Specific surface area, water absorption capacity and plastic limit	40
3.3.2	Composition of montmorillonite.....	40
3.3.3	Grain size distribution.....	42
3.3.4	FTIR, Greene-Kelly test and amount of illite	44
4	DISCUSSION.....	47
4.1	Index tests to determine smectite content.....	47
4.2	Index testing requirement limits.....	51
4.3	Determination of trace mineral contents.....	52
5	CONCLUSIONS.....	55
	REFERENCES	57
	LIST OF APPENDICES	61

LIST OF ABBREVIATIONS

CBD	Citrate-bicarbonate-dithionite extraction
CEC	Cation exchange capacity
EC	Electric conductivity
EG	Ethylene glycol
EGME	Ethylene glycol monoethyl ether
EMDD	Effective montmorillonite dry density
FTIR	Fourier transform infrared spectroscopy
HC	Hydraulic conductivity
IC	Ion chromatography
ICP-AES	Inductively coupled plasma atomic emission spectroscopy
LL	Liquid limit
MBI	Methylene blue index
PP	Polypropene
SSA	Specific surface area
SC	Sodium carbonate extraction
SP	Swelling pressure
WAC	Water absorption capacity
XRD	X-ray diffraction

PREFACE

This report includes the descriptions of test methods to be used for quality control of chemical, mineralogical and physical properties of buffer and backfill materials. As an example, it includes characterization of three material batches, two Wyoming bentonites and one Ca-bentonite from Milos that are used in various Posiva buffer performance testing projects, and assessment of analytical errors for part of the test methods. Finally, semiquantitative determination of smectite content using index tests is discussed and recommendations given to update some of previously given requirement limits for these tests.

1 INTRODUCTION

1.1 Quality requirements for buffer and backfill

Buffer

Buffer and backfill performance targets and requirements have been discussed extensively by Posiva (Posiva 2010 and related reference documents). Because this work is focused on the quality control of bentonite materials upon acquisition to ensure that the quality fulfils the specified requirements, a few of the key performance targets are reviewed here.

The most important task of the buffer is to protect the copper canister and, if any canister damage occurs, to prevent harmful substances from escaping outside the buffer (Posiva 2010). The buffer should be plastic enough to cushion the canister against minor rock movements, it should ensure tightness to support the canister and prevent it from sinking and it should have self-sealing ability. The buffer should prevent the formation of internal flow paths and avoid significant advective transport of solute material. It should have a sufficiently fine pore structure in order to prevent microbial activity and colloid facilitated radionuclide transport. All transport in the buffer should be diffusion controlled. The thermal conductivity of the buffer must be sufficient to allow heat transport from the canister surface to the bedrock. Finally, the buffer shouldn't compromise the operation of other release barriers in any way.

In order to function as designed, the buffer requires counter-pressure produced by backfill installed in the deposition tunnel (Posiva 2010). The pressure should limit the expansion of buffer and keep it in place so that the density requirements of buffer are met. Also backfill should limit radionuclide transport in case of canister failure. All transport should be diffusion-dominated and advective solute transport through the backfill should not occur. The backfill should enhance the mechanical stability of the deposition tunnels and the near-field rock. It should be able to provide tight contact between the backfill and the rock and it should have self-sealing ability. The backfill should, in general, maintain favourable conditions for the buffer and canister.

In addition to the mentioned performance targets, buffer and backfill requirements arise from the conditions in the repository, material properties at the initial state, system restrictions (which can't be changed, e.g., canister diameter), estimated long-term buffer behaviour, manufacture and installation requirements (Posiva 2010).

On the basis of studies conducted so far, some limit values for buffer properties have been set. In order to perform according to the requirements, the buffer must, in spite of the salinity variations to be expected in the Olkiluoto groundwater, fulfil the following conditions (Posiva 2010).

- Hydraulic conductivity of the buffer $<10^{-12}$ m/s.
- Swelling pressure of buffer >2 MPa.
- Montmorillonite content above 75 %.
- Saturated density above 1950 kg/m^3 but below 2050 kg/m^3 .

- The buffer must be sufficiently ductile to protect the canister in the canister deposition hole from damage due to any potential rock dislocations up to a 100-mm shear-type dislocation.
- The entire disposal system must be designed in such a manner that the temperature of the buffer remains below 100 °C.

In addition, bentonite should have no harmful effect on other barriers and particularly not on the canister. Therefore, the quantity of harmful components that bentonite may contain needs to be low (Posiva, 2010). Such quality requirements, at least for the amount of organic carbon, total sulphur and sulphur as sulphides, have been proposed by SKB (2009).

In terms of specific quality requirements for bentonite buffer material, Ahonen et al. (2008) provided “preliminary required values” for a set of eight tests (see Table 1). Note that some of the required values in Table 1 actually reflect minimum performance targets (updated to Posiva 2010) and not quality control metrics. Ideally, quality control requirements should ensure that minimum performance targets will be met.

Backfill

The following requirements exist for backfill materials (Posiva 2010).

- Hydraulic conductivity $<10^{-10}$ m/s.
- The consolidation of the backfill as a result of the swelling of the buffer must remain small enough for the buffer density not to decrease below 1950 kg/m³.

In addition, backfill material must not contain organic, oxidizing or other potentially harmful agents in amounts that would significantly impair the functioning of the buffer, copper canister or the surrounding rock (Posiva 2010). The limits on the chemical composition of the backfill material are the same as for buffer.

Table 1. Preliminary required values for buffer bentonite. Separate requirements for Na-/Ca-bentonite (Ahonen et al. 2008; Posiva 2010; Laaksonen 2010; SKB 2009).

Test	Required average value for Na-bentonite	Single test, minimum/maximum value for Na-bentonite	Required average value for Ca-bentonite	Single test, minimum/maximum value for Ca-bentonite
Water Content	≤ 13 %	max. 15 %	≤ 13 %	max. 15 %
Swelling Index	≥ 20 ml/2g	min. 15 ml/2g	≥ 15 ml/2g	min. 10 ml/2g
Smectite Content	≥ 75 %	min. 65 %	≥ 75 %	min. 65 %
Liquid Limit	≥ 250 %	min. 200 %	≥ 80 %	min. 60 %
Cation Exchange Capacity (CEC)	≥ 70 meq/100 g	min. 60 meq/100 g	≥ 60 meq/100 g	min. 50 meq/100 g
Hydraulic Conductivity (HC)**	≤ 10 ⁻¹² m/s	max. 10 ⁻¹¹ m/s	≤ 10 ⁻¹² m/s	max. 10 ⁻¹¹ m/s
Swelling Pressure (SP)**	≥ 2 MPa		≥ 2 MPa	
Thermal Conductivity*	≥ 1.0 W/Km	min. 1.0 W/Km	≥ 1.0 W/Km	min. 0.9 W/Km
Organic carbon	< 1 %		< 1 %	
Sulphur in sulphides	≤ 0.5 %		≤ 0.5 %	
Total sulphur	≤ 1 %		≤ 1 %	

* In dry density of 1655 kg/m³, water content 17 % and degree of saturation 70 % or in dry density of 1754 kg/m³, water content 17 % and degree of saturation 81 %. After saturation thermal conductivity of buffer block should be 1.3 W/Km.

** Dry density of buffer blocks 1655 – 1754 kg/m³.

1.2 Method selection

In addition to the tests enumerated in Table 1, Ahonen et al. (2008) describe numerous other mineralogical, chemical, and geotechnical tests and discuss them in the context of quality control of bentonite material as well. Based on these discussions, the set of tests presented in Table 2 was compiled. Some of the test methods proposed in Ahonen et al. (2008) were replaced with equivalent methods (e.g. laser diffraction instead of x-ray monitoring of gravity sedimentation for particle size distribution) or those thought to be more suitable (e.g. Cu(II)-triethylenetetramine method instead of MBI for CEC measurement). In addition, some complementary test methods were introduced.

The selected methods were divided into three categories; basic, advanced and complementary acceptance testing. A potential quality control process for bentonite material, encompassing basic, advanced, and complementary testing, is displayed schematically in Figure 1. As indicated, basic and advanced acceptance testing are to be performed for all materials and complementary testing can be performed if needed. As discussed previously, a set of “preliminary required values” exist for some of the basic and advanced acceptance tests. Basic tests can be done relatively fast (from hours to couple of days) and they are supposed to give an indication of the smectite content as well as exchangeable cation population. Advanced testing deepens the knowledge of smectite content, exchangeable cation population, swelling properties and hydraulic conductivity, but their performance usually takes more time (from days to weeks). A

limit value exists also for thermal conductivity (Table 1). However it was not tested in this study.

The complementary tests selected for this study are presented in Table 2. Purified material tests and additional mineralogical tests were selected to support the mineralogical interpretation. Specific surface area, water absorption capacity and plastic limit were selected in order to test their potential as index tests, i.e. if they could be used instead of the current basic tests. Grain size distribution was selected to get additional information and to assess the success of the separation of clay sized particles.

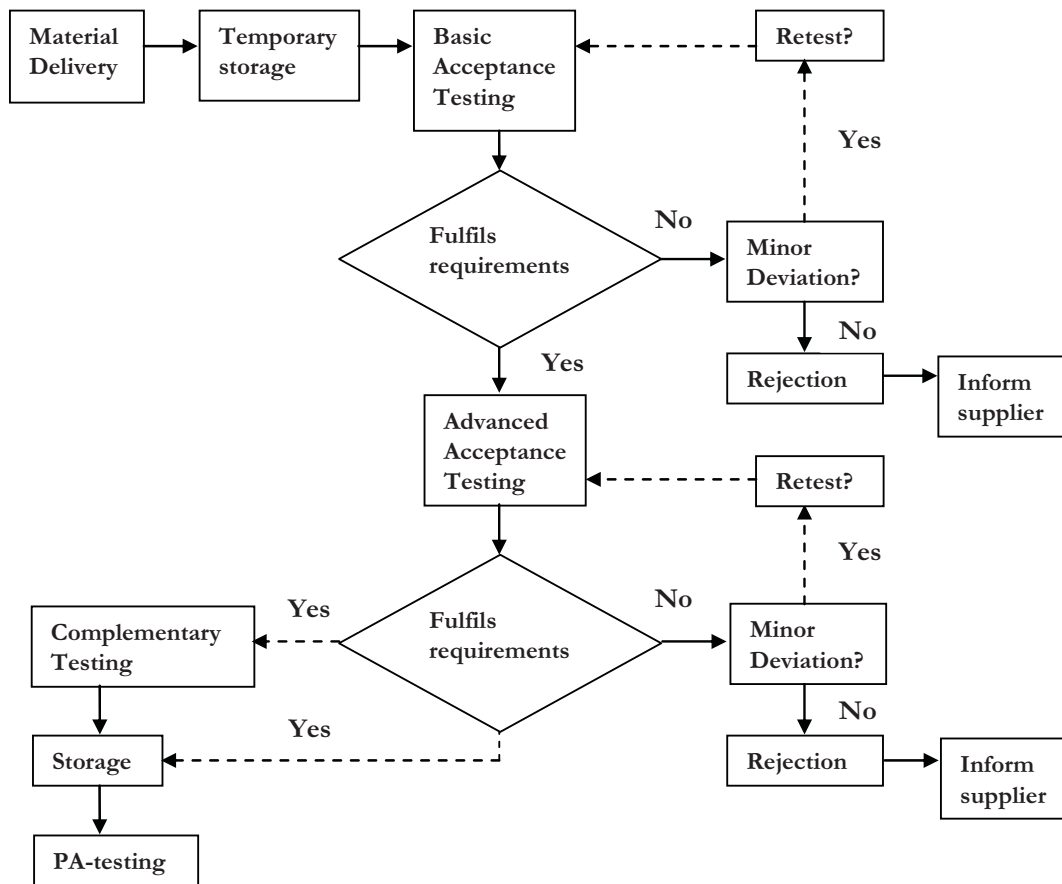


Figure 1. Quality control process for bentonite material (modified from Ahonen et al. 2008).

Table 2. Selected test methods for basic, advanced and complementary acceptance testing.

A) Basic Acceptance Testing:	Reference or standard method for the test
Water Ratio	Based on CEN ISO/TS 17892-1:2004
CEC	Ammann et al., 2005; Meier and Kahr, 1999
Swelling Index	Based on ASTM D 5890 – 06
Liquid Limit	Based on CEN ISO/TS 17892-12:2004
Granule Size Distribution (Dry Sieving)	CEN ISO/TS 17892-4:2004
B) Advanced Acceptance Testing:	
Exchangeable Cation Analysis (NH ₄ Cl-method)	Belyayeva, 1967; Jackson, 1975
Chemical Composition: ICP/AES, LOI, Leco (Total S, Inorg.C and Org. C), IC (SO ₄ ²⁻), Fe ²⁺ /Fe ³⁺	Kumpulainen et al., 2011
Mineralogy: Quantitative XRD Optical Microscopy	Kumpulainen et al., 2011
Grain Density	Based on CEN ISO/TS 17892-3:2004 and Karnland et al., 2006
Swelling Pressure	ASTM D 4546-08; Karnland et al., 2006
Hydraulic Conductivity	ASTM D 5084-03; Karnland et al., 2006
Bulk Density (after SP- and HC measurement)	Based on CEN ISO/TS 17892-2:2004
Thermal Conductivity	Based on ASTM D 5334-08
C) Complementary testing (this study):	
Specific Surface Area: EGME	Cerato and Lutenegger, 2002
Water Absorption Capacity (Enslin-Neff)	Based on DIN 18132
Plastic Limit	Based on CEN ISO/TS 17892-12:2004 and ASTM D 4318-05
Purified Material Tests (Calculation of molecular structure of smectite): Chemical Composition, CEC, CBD-extraction, Na ₂ CO ₃ -extraction	Kumpulainen et al., 2011
Grain Size Distribution by Laser Diffraction	
Mineralogy: FTIR, Greene-Kelly Test	Kumpulainen et al., 2011

1.3 Materials



Figure 2. Photos of raw materials, from left: Be-Wy—BT0007, Be-Wy—VT0002 and Be-Mi—BT0011.

The materials tested for the purposes of this report are listed in Table 3. The batch and shipment variability of material quality was determined by analysing multiple samples from the same batch or shipment as indicated in Table 3. Photos of raw materials are presented in Figure 2.

Table 3. Studied samples.

Original supplier	ID of the sample	Lot number	Alternative project name	Code for parallel samples	Parallel samples taken from
CETCO	Be-Wy—VT0002-BT1-Sa-R	09-175	BT1	1	Individual 25 kg bag, same batch as 2 & 3
	Be-Wy—VT0002-BT2-Sa-R	09-175	BT2	2	Individual 25 kg bag, same batch as 1 & 3
	Be-Wy—VT0002-BT3-Sa-R	09-175	BT3	3	Individual 25 kg bag, same batch as 1 & 2
IBECO	Be-Mi--BT0011-Gr-R		Ibeco 1	1	500 kg bag (upper)
			Ibeco 2	2	500 kg bag (middle)
			Ibeco 3	3	500 kg bag (lower)
?	Be-Wy—BT0007-1-Sa-R	260.08	1-1-Sa	1	Same 25 kg bag as 2
		260.08	1-2-Sa	2	Same 25 kg bag as 1

2 METHODS

2.1 Basic acceptance testing

2.1.1 Water ratio

Water ratio was measured for bulk materials by drying in a ventilated oven for 24 h at 105 °C. Water ratio (w) was calculated as:

$$w = \frac{m_w}{m_s} * 100\% \quad (1)$$

Where m_w = mass of water
 m_s = mass of dry material

2.1.2 CEC

Cation exchange capacity was measured using Cu(II)-triethylenetetramine method (Meier and Kahr, 1999; Ammann et al., 2005).

0.015 M Cu(II)-triethylenetetramine solution was prepared by dissolving 2.309 g of triethylenetetramine (purity grade ~95 %) and 2.394 g of anhydrous Cu(II) sulphate (analytical grade) in deionized water to a volume of 1000 ml. Solution had an end pH of ~8.4.

200 mg of air-dry and ground bulk sample was dispersed in 25 ml of deionized water with assistance of ultrasonic bath (45 kHz, 120 W, 10 min). 10 ml of 0.015 M Cu(II)-triethylenetetramine solution was added and allowed to react on a rocking platform for 30 minutes. The suspension was centrifuged at 3600 rpm for 15 minutes, and the supernatant collected. The water content of initial clay was determined gravimetrically by drying at 105 °C for 24 h.

The Cu(II)-triethylenetetramine concentration in the supernatant was measured spectrophotometrically. A calibration curve for the measurements was determined from a series of dilute Cu(II)-triethylenetetramine solutions (0.015 M; 0.010 M; 0.005 M; 0.0015 M; 0.00015 M). Absorptions were measured at 620 nm using Thermo Scientific Genesys 10S UV-Vis spectrophotometer and deionized water as a blank solution. 3 mL of the supernatant was pipetted into 10 mm optical glass cuvette and the absorption of the solution was measured. Cu(II)-triethylenetetramine concentration was determined by comparing the absorption of the supernatant solution to the calibration curve. CEC was calculated from the difference of Cu(II)-triethylenetetramine concentrations in initial Cu(II)-triethylenetetramine solution and sample solution. Because the extinction is shown to be pH dependent at low (< 3.5) and high pH (> 12) (Ammann et al., 2005), the pH of supernatant was measured after extraction. All extractions and determinations were done in duplicate and results reported as mean values. CEC was calculated using equation:

$$CEC = \frac{z * n_{complex}}{m_{dry}} \quad (2)$$

Where CEC = cation exchange capacity (eq/kg)
 n_{complex} = amount of adsorbed Cu(II)-complex into the sample (mol)
 m_{dry} = the dry weight of the sample (kg)
 z = the charge of the Cu(II)-complex = 2

2.1.3 Swelling index

Bulk material was ground ($< 125 \mu\text{m}$), sieved and dried in an oven for 24 h at $105 \text{ }^\circ\text{C}$. The test was performed by slowly adding 2 g of prepared bentonite material into a graduated cylinder containing deionised water (ASTM D 5890-06). The material was added approximately at a speed of 0.1 g/5 min. The sample cylinder was then covered and protected from disturbance for a period of 24 h, at which time the volume of the swelled material was determined to the nearest 0.5 ml. The free swelling index was reported as the volume of swelled material (ml/2g).

2.1.4 Liquid limit

Liquid limit (w_L) was determined with the fall-cone method (CEN ISO/TS 17892-12: 2004). Samples were prepared by mixing various volumes of water and the material of interest, which was ground to particle sizes under $500 \mu\text{m}$. The samples were isolated for a period of 24 h and after that the measurement was performed using a fall-cone apparatus (Geonor) and a $60 \text{ g}/60^\circ$ fall-cone. Before measurement, samples were not mixed, only the surfaces were leveled. After measurement, water ratios of samples were measured by drying in an oven for 24 h at $105 \text{ }^\circ\text{C}$. Liquid limit, i.e., the sample water ratio at a cone penetration depth of 10 mm, was determined from a semi-logarithmic plot of water ratio vs. cone penetration depth.

2.1.5 Granule size distribution by dry sieving

The granule size distribution of as-received bentonite materials was determined by dry sieving with test sieves of different sizes (CEN ISO/TS 17892-4: 2004). The bentonite materials were dried before sieving, at least 5 different size sieves were used and a sieve shaker (Utest) was used to facilitate sieving. The portion of material (f_n), which passed through a sieve (n) was calculated for each sieve size and the results were presented as f_n versus granule size on a graph.

2.2 Advanced quality assurance testing

2.2.1 Original exchangeable cations

Original exchangeable cations were studied using NH_4Cl in 80 % ethanol (Belyayeva 1967; Jackson 1975).

0.5 g of ground bulk material was dispersed in approximately 10 ml of 0.5 M NH_4Cl in 80% ethanol. Suspension was shaken for 30 minutes, centrifuged at 3600 rpm for 15 min, and supernatant decanted to a volumetric flask. The extraction was repeated two times with 7.5 ml of extraction solution to reach the total volume of 25 ml. The extract was filtered through $0.2 \mu\text{m}$ pore size filter, ethanol was evaporated and the extract

diluted back to 25 ml with deionized water. The amount of dissolved Ca, K, Na and Mg was determined using ICP-AES at Labtium Oy. The results were adjusted against adsorbed water content (determined gravimetrically at 105 °C) and reported as equivalent charges / kg of dry weight.

2.2.2 Chemical composition

Chemical composition was determined by analysing LOI, concentration of elements (Si, Al, Fe, Ti, Mg, Ca, Na, K), concentration of Fe²⁺, water soluble SO₄, Leco-S, and Leco-C/CO₃. The analyses were done by Labtium Oy.

The bulk materials were digested using lithium metaborate fusion and nitric acid dissolution. Concentrations of dissolved elements were determined using ICP-AES.

Concentration of Fe²⁺ was determined titrimetrically from HF decomposed samples using 0.05 N K₂CrO₇ (Saikkonen and Rautiainen 1993). The concentration of Fe³⁺ was determined by subtracting ferrous iron concentration from total concentration of Fe.

Soluble sulphate content was determined by water extraction and ion chromatography (IC). Total sulphur content was determined by combustion at 1200 °C (Leco).

The carbon content was determined with combustion (Leco). Carbon released below 550 °C was considered to be bound to organic matter, and carbon released at 550-1000 °C to be inorganic (bound to carbonates).

Adsorbed water, i.e. moisture content, was determined gravimetrically by drying approximately 10-15 g of sample in a convection oven at 105 °C for 24 h. The loss on ignition (LOI) at 1000 °C was measured gravimetrically from dry samples (105 °C).

2.2.3 Mineralogical composition

Mineralogical composition was defined by identifying minerals with x-ray diffraction (XRD) and optical microscopy, and quantifying mineralogical composition with Rietveld refinement.

Before preparing XRD mounts, a silicon standard was accurately weighed (10 wt.%) and added to the sample. Silicon was used to adjust the zero. Sample and standard was then ground in agate mortar with pestle to a particle size < 10 µm. Approximately 10 mg of ground bulk material was mixed with acetone on a glass slide. Sample mount was put into a desiccator that contained saturated Mg(NO₃)₂ solution in order to achieve standard relative humidity (54 % RH at 20 °C), and kept there at least 5 days. Sample mount was then transferred to a rotating sample holder, scanned with Philips X'Pert MPD diffractometer equipped with Cu anode tube and monochromator, a variable divergence slit, using wavelength of Kα₁ = 1.54060; Kα₂ = 1.54443; and Kβ = 1.39225; voltage of 40kV and current of 55 mA, from 2 to 70° 2θ with 0.02° counting steps and 1s/step counting time at the Geological Survey of Finland. XRD mount was analyzed in triplicate and mean pattern calculated in order to decrease the background noise for more efficient detection of accessory minerals. The low angle intensity aberrations

produced by auto-slit geometry were corrected with the HighScore Plus for the full pattern fitting with Siroquant.

Oriented mounts for XRD were prepared from purified clay fractions ($< 2 \mu\text{m}$) that had been converted to Mg-forms to identify clay minerals present. Filter-membrane peel-off technique (Drever 1973; Moore and Reynolds 1989) was used for preparation of the oriented mounts. A concentrated suspension containing approximately 600 mg of purified clay in 10 ml of deionized water was vacuum filtered onto $0.45 \mu\text{m}$ pore size cellulose filter. Sample mounts were dried in air and scanned with XRD from 2 to $35^\circ 2\theta$ with 0.02° counting steps with counting time of 1s/step. Then, oriented sample mounts were placed on a platform in a desiccator containing EG and put into an oven at 60°C for 20 h. Mounts were scanned immediately after solvation from 2 to $35^\circ 2\theta$ with 0.02° counting steps with counting time of 1s/step to identify smectites. Then, oriented mounts were placed into a furnace for 2 h at 550°C . Mounts were scanned after heating from 2 to $20^\circ 2\theta$ with 0.02° counting steps with counting time of 1s/step for distinction of kaolin minerals from chlorites.

Optical microscopy was used to identify accessory minerals in the coarse fraction ($> 2 \mu\text{m}$), which was separated from clay material by gravity sedimentation. Small amount of sample was gently ground in agate mortar, placed on a glass slide and drop of glycerol (with refractive index of 1.47) was added. Cover glass was placed on top. Sample mounts were observed with plane- and cross-polarized light. Among others, colour, pleochroism, birefringence, particle size, morphology, and isotropicity of mineral particles were examined.

Mineralogical composition was determined from randomly oriented XRD patterns of bulk samples using a full-profile Rietveld refinement by Siroquant software. First, background was subtracted. Refinement was done in several subsequent stages until no major improvement in pattern fit was achieved. Parameters like instrument zero, phase scales, half-widths, unit cell dimensions, and preferred orientation were refined. Mineralogical composition was validated with comparison to normative composition calculated from chemical composition.

2.2.4 Grain density

Empty, 50 ml volumetric flasks were weighed and filled with deionised water to the graduation mark. The exact volume of the flasks was calculated as $V=m/\rho$, where m is the mass of water in the bottles and ρ is the density of water at ambient temperature.

Bulk clay material (approximately 10-13 g) was dried at 105°C for 24 h. Immediately after removal from the oven, the sample material was placed into dry volumetric flask, sealed, and allowed to cool down. After cooling, the flask with dry sample was weighed. 1 M NaCl solution was added to completely cover the sample. The flask was agitated to facilitate the escape of air from the sample. After 24 h the flask was agitated again, filled to the graduation mark and weighed. Two reference flasks filled only with 1 M NaCl solution were used to determine the liquid density at the ambient temperature.

The grain density (D_s) was calculated as follows (Karnland et al. 2006):

$$D_s = \frac{m_s}{V_{tot} - \frac{m_{tot} - m_{s+f}}{D_l}} \quad (3)$$

Where

- m_s = mass of the solids
- V_{tot} = volume of the flask
- m_{tot} = total mass
- m_{s+f} = mass of the solids and flask
- D_l = density of the liquid

2.2.5 Swelling pressure, hydraulic conductivity, dry density and EMDD

Samples were compacted straight to 25 mm-diameter fixed-volume swelling pressure cells using hydraulic press. The samples were prepared from approximate quantities of the clay materials to achieve the density value of approximately 1.6 g/cm^3 .

Direct contact between the piston, porous frit, and compacted sample was established (Figure 3). Force transducers (Honeywell Model 53 load cells) were placed between the cell piston and top plate in order to measure axial force due to sample swelling. Pre-stress loads of approximately 10 % of expected equilibrium swelling pressure were established on each sample test cell prior to saturation. Force transducer loads were recorded every 30 minutes via data logger. De-aired 1 % salt solution (10 g/l), where the ratio of Na to Ca was 2:1 was used as the saturating solution.

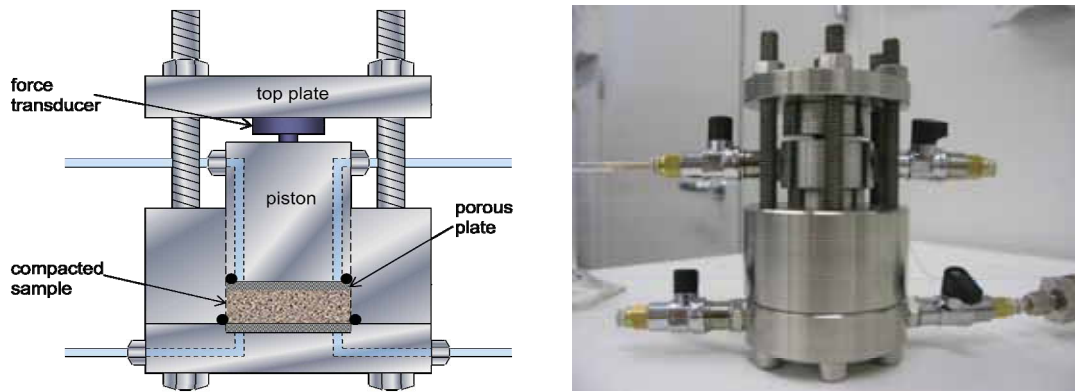


Figure 3. Schematic illustration (left) and photographic image (right) of fixed-volume swelling pressure cell (modified from Schatz and Martikainen 2010).

Saturation was provided using a peristaltic pump whereby the saturating solution was allowed to slowly flow first through the bottom circuit of the cells for 7 days and thereafter through both the top and bottom circuits of the cells for an additional 7-30 days. Such bottom-up saturation is used to allow residual air in the sample to escape through the top of the cell (Karnland et al. 2006). Flow was generally provided through the cells at intervals of 5 - 10 minutes twice per day.

Once the swelling pressure variation over three days was at maximum $\pm 0.6 \%$ and saturation had been continued at least two weeks, it was considered that equilibrium

condition was reached and hydraulic conductivity measurement was started. During hydraulic conductivity measurements, also axial force measurements were continued in order to detect any significant effect due to increased hydraulic loads. A connection was made between a pressure panel outlet and one of the cell bottom circuit ports. Additionally, one end of a clear tubing of known diameter was attached to one of the cell top circuit ports with the other end remaining open to atmosphere. Hydraulic conductivity measurements were initiated by increasing the water pressure into the cell bottom circuit to a load pressure of 500-620 kN, which does not exceed half of the measured swelling pressure in any of the samples (see Table 15), i.e., it shouldn't consolidate the samples (Karnland et al. 2006). The volume of fluid permeating through the sample and out of the cell top circuit was measured as a function of time. The composition of permeant solution was identical to that of the saturating solution for any given sample. Prior to hydraulic conductivity measurements, permeant solutions were de-aired.

After completion of all measurements, the saturated samples were removed as quickly as possible from the swelling pressure cells and immediately sectioned into two pieces. The other piece was sectioned again into two pieces, which were weighed for water content determination. After weighing, saturated sample sections were dried in a laboratory oven at 105 °C for 24 h. The sample sections were weighed again after drying to determine the mass due to water loss. Other half of the sample was used to measure bulk density of the sample (total mass divided by total volume) by immersing the sample into paraffin oil. The method applies the Archimedean principle whereby a solid immersed in a liquid is subjected to a buoyant force. In practice, an amount of solid material was weighed in air (m_{air}) and in a non-hydrating liquid of known density (m_{fluid}). As the volume of an immersed solid equals the volume of the displaced liquid (of known density), the bulk density of the solid was calculated as a function of m_{air} , m_{fluid} , and the liquid density using equation:

$$\rho_B = \frac{m_{air}}{m_{air} - m_{fluid}} * \rho_{fluid} \quad (4)$$

Where m_{air} = mass of the specimen in air.
 m_{fluid} = average mass of the specimen in fluid over 7 mass readings.
 ρ_{fluid} = density of the immersion liquid

The swelling pressure was calculated using equation (ASTM D 4546-08):

$$p_s = \frac{U}{C * A} \quad (5)$$

Where p_s = swelling pressure (kPa)
 U = measured voltage (V)
 A = area of specimen (m^2)
 C = calibration factor of force transducer (V/kN)

The sample hydraulic conductivities were determined from the measured flow rates based on a Darcy's law calculation corrected to a constant temperature of 20 °C (ASTM D 5084-03).

The quantity of flow was calculated using equation:

$$\Delta Q = \pi * r^2 * l \quad (6)$$

Where ΔQ = quantity of flow for given time interval Δt (m³)
 r = inner radius of the tubing (m)
 l = measured flow length (m)

The head loss across the specimen was calculated using equation:

$$h_{1/2} = \frac{p}{\rho * g} \quad (7)$$

Where h_1 = head loss across the specimen at t_1 (m)
 h_2 = head loss across the specimen at t_2 (m)
 p = inlet pressure (Pa)
 ρ = density of fluid (kg/m³)
 g = gravity (m/s²)

The hydraulic conductivity of the sample was calculated using equation (ASTM D 5084-03):

$$k = \frac{\Delta Q * L}{A * h * \Delta t} \quad (8)$$

Where k = hydraulic conductivity (m/s)
 L = length of specimen (m)
 A = cross-sectional area of specimen (m²)
 h = average head loss across the specimen ($(h_1 + h_2) / 2$) (m)
 Δt = interval of time, over which the flow ΔQ occurs (s)

The hydraulic conductivity was corrected to 20 °C using equation (ASTM D 5084-03):

$$k_{20} = R_T * k \quad (9)$$

Where $R_T = \frac{2.2902 * (0.9842^T)}{T^{0.1702}}$ = ratio of viscosity of water at test temperature to the viscosity of water at 20 °C
 k_{20} = hydraulic conductivity corrected to 20 °C (m/s)
 T = average test temperature during the permeation trial

The hydraulic conductivity was considered steady if four or more consecutive hydraulic conductivity determinations fell within ± 25 % or better of the mean value for $k \geq 1 \times 10^{-10}$ or within ± 50 % or better for $k < 1 \times 10^{-10}$ m/s. In addition hydraulic conductivity was not allowed to show upward or downward trend.

Dry density was determined after swelling pressure and hydraulic conductivity measurements from water ratio using equation (Karnland et al. 2006):

$$\rho_d = \frac{\rho_s * \rho_w}{\rho_s * w + \rho_w} \quad (10)$$

Where ρ_d = dry density (g/cm^3)
 ρ_s = grain density (g/cm^3)
 ρ_w = density of water (g/cm^3)
 w = water ratio

Dry density was calculated also from the bulk density determined by the paraffin oil-method using equation:

$$\rho_d = \frac{\rho_b}{1+w} \quad (11)$$

Where ρ_d = dry density (g/cm^3)
 ρ_b = bulk density (g/cm^3)
 w = water ratio

Swelling pressures and hydraulic conductivities were also plotted against effective montmorillonite dry density (EMDD) (Dixon et al. 2002). EMDD is a normalization parameter and calculated in order to compare clay materials of different densities and montmorillonite contents accordingly:

$$EMDD = (1 - f) * \left(\frac{\rho_d}{1 - \frac{f * \rho_d}{\rho_s}} \right) \quad (12)$$

Where EMDD = effective montmorillonite dry density (g/cm^3)
 ρ_d = dry density (g/cm^3)
 ρ_s = grain density (g/cm^3)
 f = fraction of non-swelling material in the sample

The swelling pressure and hydraulic conductivity results include number of uncertainties. Possible uncertainties caused by measurement equipment are e.g. different friction of the pistons in test cells and variation in force transducers. In order to minimize these effects, the measurement cells were assembled always in the same way, i.e., approximately the same amount of lubricant and similar load rings were added in every measurement, and the calibration of force transducers was performed before and after each test demonstrating less than $\pm 3\%$ variation in every case. The results were calculated using the average calibration factor.

Density determination is probably the most critical source of uncertainty in swelling pressure measurements, because the swelling pressure increases exponentially as dry density of the sample increases. The uncertainties in water ratio measurements and thereby in dry densities calculated from water ratio might be caused by water evaporation or water absorption from measurement cell and frits during sample dismantling. These uncertainties were minimized by dismantling all samples in the same way and measuring the water ratio immediately after dismantling. Bulk density determinations with paraffin oil method were used to gain supportive information of the densities.

2.3 Complementary testing

2.3.1 Specific surface area by EGME-method

100 g of dried (105 °C) anhydrous calcium chloride was mixed with 20 ml of EGME (ethylene glycol monoethyl ether), and placed in the bottom of a desiccator (Cerato and Lutenegger 2002). Sample material was ground and sieved to 500 µm. Approximately 1.1 g of prepared material was placed into an aluminous sample container, weighed and dried at 105 °C for 24 h. The samples were allowed to cool for few minutes in a desiccator, weighed and the sample material spread evenly into the bottom of the container. 3 ml of EGME was added to the sample and the mixture was swirled to ensure that the sample was fully covered with EGME. Plastic lid was added, container with lid placed into a desiccator and desiccator evacuated after 20 min equilibration period. After 20-24 h under vacuum, the samples were removed from the desiccator, weighed and placed back into the desiccator. After a subsequent 3 h under vacuum, the samples were weighed again. This process was repeated until the mass of the sample varied by only 0.001 g.

The specific surface area (SSA) was calculated as follows:

$$SSA = \frac{w_a}{0.000286 * w_s} \quad (13)$$

Where SSA = specific surface area (m²/g)
 w_a = weight of EGME retained by the sample (g)
 w_s = initial sample dry mass (g)
 0.000286 = theoretical mass of EGME required to form a monomolecular layer on one square meter of surface (g/m²)

2.3.2 Water absorption capacity by Enslin-Neff device

Approximately 0.2-0.6 g (depending on the material) of dried (105 °C ± 5 °C, 24 h), ground (to 125 µm) sample material was placed into Enslin-Neff-device, where the material was allowed to absorb de-ionized and de-aired water freely on top of a glass frit for 24 h (Deutsche norm DIN 18132, 1995; Kaufhold and Dohrmann 2008).

The water absorption capacity was calculated as follows:

$$w_a = \frac{m_w}{m_d} * 100\% = \frac{\rho_w(V_w - V_k)}{m_d} * 100\% \quad (14)$$

Where w_a = water absorption capacity (%)
 m_w = weight of absorbed water (g)
 m_d = weight of dry soil added initially (g)
 ρ_w = density of water (g/cm³)
 V_w = volume of water absorbed in 24 h (cm³)
 V_k = volume of water evaporated in 24 h (without sample) (cm³)

2.3.3 Plastic limit

Approximately 20-100 g (depending on the sample water ratio) of sample prepared for the liquid limit test was used for the plastic limit test (CEN ISO/TS 17892-12: 2004). The water content of the sample was reduced (by mixing in a beaker) to a self-consistency at which it could be rolled into a ball. The ball was remoulded by hand until it had dried to the point where small cracks appeared on the surface. The ball was divided into eight pieces. Each of these pieces was further kneaded by hand in order to spread the moisture uniformly, the piece was rolled into a thread, which had a diameter of 6 mm and the thread was then rolled between the fingers of one hand (from finger tips to the second joint) on a glass plate. Sufficient pressure was used in order to produce a thread, which had a uniform diameter of 3 mm, from 10-15 up-and-down movements of one hand at 1 s per full movement. Uniform pressure was applied at all times. The preparation of a 6 mm-thread and a 3 mm-thread was repeated until the 3 mm- thread broke into several smaller pieces along its full length. Water ratio of the broken sample piece was measured by drying in an oven for 24 h at 105 °C. The same procedure was performed on all the eight sample pieces. The average of the eight water ratios was considered to be the plastic limit (w_p) of the sample material.

The plasticity index (I_p) was calculated as the difference between the liquid limit and the plastic limit.

2.3.4 Composition of montmorillonite

Purification and homoionisation

Before particle size fractionation, the materials (Ibeco 1, BT1 and 1-1-Sa-R) were washed free from dissolvable salts (Karnland et al. 2006). Ten grams of bulk material was dropped gradually to 1 litre of deionized water in a glass beaker, which was simultaneously stirred with a magnetic stirrer. Stirring was continued overnight. Deionized water was produced with Elga Micromeg MC:DS Cartridge and had an EC < 0.5 $\mu\text{S}/\text{cm}$. Analytical grade NaCl was added to a concentration of 1 M and the mixing of the suspension was continued with a magnetic stirrer for at least 2 h. Suspension was left to settle, and the clear supernatant was removed. Addition of water and NaCl was repeated two times. Thereafter, material was washed 2-4 times by addition of deionized water and centrifugation (5-15 minutes with 2000-3600 rpm) until supernatant became slightly turbid. Sedimented slurry, except the coarsest fraction, was transferred into dialysis membranes (regenerated cellulose, 3500 MWCO) that were placed into 5 litre acrylic tubes filled with deionized water. Dialysis water outside the membranes was changed daily until the EC stabilized < 10 $\mu\text{S}/\text{cm}$ for three days. Material was taken out from dialysis membrane and suspended with 1 litre of deionized water in glass beaker. Suspension was left to settle for 48 h to remove particles > 1 μm in diameter according to Stokes' law:

$$v_s = \frac{2(\rho_s - \rho_f)}{9\mu} gR^2 \quad (15)$$

Where v_s = settling velocity of particles (m/s)
 g = gravitational acceleration (m/s^2)

μ = viscosity of fluid (kg/ms)
 R = radius of spherical particles (m)
 ρ_s = density of particles (kg/m³)
 ρ_f = density of fluid (kg/m³)

After removal, NaCl was added to a concentration of 1 M and the suspension was mixed with a magnetic stirrer for at least 2 h. The material was left to settle, supernatant removed and procedure repeated again two times. Then, material was centrifuge-washed 2-4 times with deionized water and dialysed. A third round of homoionisation, centrifuge-washing and dialysis steps were done to finalize the purification process. Initially 20 grams of each material was treated with this procedure and the final Na-exchanged clay yield was approximately 10 grams.

In addition, a carbonate removal procedure was tested on another sample of calciferous Ibeco 1. If carbonates cannot be completely removed during the normal separation of coarse fraction procedure, they will continue dissolving during dialysis. In this process divalent cations are released from remaining carbonates and they will replace the monovalent cations. Hence, the trial of removing carbonates was done by treating the material with 1 M acetate buffer with pH 5 (Newman 1987). 20.9 ml of acetic acid (100 %) and 52.065 grams of sodium acetate were dissolved to deionized water and the solution was diluted to 1 litre. 10 grams of sample material was added to the solution and the mixture was stirred with a magnetic stirrer for 48 h. Suspension was left to settle, and the clear supernatant was removed. The suspension was treated three times with analytical grade NaCl, centrifuge-washed, dialysed and the coarse fraction was removed, as above. However, despite of carbonate removal with acetic acid, large carbonate granules were identified using optical microscope from the coarse fraction. Hence, the clay fraction suspension was treated with 1 M acetate buffer with pH 5 again in order to ensure that the carbonates were removed completely from the clay fraction. The rest of the homoionisation and purification procedure was performed as above.

After purification procedures, clay material was dried at 60 °C and ground gently in agate mortar or in oscillating mill.

CEC, chemical composition and CBD-extraction

CEC and chemical composition of Na-exchanged clay fractions (< 1 μ m) were determined as presented in sections 2.1.2 and 2.2.2, respectively.

Citrate-bicarbonate-dithionite (CBD) extraction (Mehra and Jackson, 1960) was used for quantification of poorly crystalline Fe oxides. 0.5 g of Na-exchanged clay fraction was placed in a 50 ml polypropene (PP) centrifuge tube together with 20 ml of 0.3 M Na-citrate solution and 2.5 ml of 1 M NaHCO₃. The tube was placed in a water bath and heated to 80 °C. Then, one third of 0.5 g of Na₂S₂O₄ was added, the mixture stirred constantly for one minute and then occasionally for 5 minutes. Addition of sodium dithionite and mixing was repeated twice until there was no reddish colour visible in the clay. The mixture was allowed to cool down. Then 5 mL of saturated NaCl solution was added to induce flocculation. The mixture was centrifuged at 3600 rpm for 15 min, supernatant collected, the residue washed with 35 mL of deionized water and 5 mL of

saturated NaCl solution, recentrifuged, added to the previous supernatant, filtered through 0.45 μm and diluted to 100 mL with deionized water in a volumetric flask. Concentration of Fe of the extract was studied with ICP-AES at Labtium Oy. The results were adjusted against adsorbed water content (determined gravimetrically at 105 °C).

Structural calculations

Before calculation of structural formula for smectite, the chemical composition of purified clay fraction was adjusted according to Karnland et al. (2006) by subtracting still remaining mineral impurities from clay fraction (illite, poorly crystalline Fe and Si phases, calcite, gypsum and pyrite), in order to get chemical composition of pure smectite phase. Amount of illite was calculated from the K^+ -content in the clay fraction using the ideal formula $\text{K}_{1.5}(\text{Si}_7\text{Al})(\text{Al}_{3.5}\text{Mg}_{0.5})\text{O}_{20}(\text{OH})_4$ for illite. Poorly crystalline Fe and Si phases were determined with CBD-extraction. The amounts of calcite, gypsum and pyrite were calculated from the amounts of carbonate, sulphate and sulphidic sulphur in the clay fraction. The Al, C, Ca, Fe, K, Mg, S and Si contents were adjusted accordingly. TiO_2 was considered as separate mineral phase in the calculations, not a constituent of the montmorillonite structure as in Karnland et al. (2006).

Calculations were done according to Newman (1987) assuming that structural units contained 24 anions ($\text{O}_{20}(\text{OH})_4$), but that unit cell and density were unknown.

2.3.5 Grain size distribution by laser diffraction

Bulk samples (Ibeco 2 and BT1) were dispersed in water and stirred overnight. Clay fractions were sedimented for 24 or 48 h after first dialysis (see section 2.3.4). Volumetric grain size distribution was determined with laser diffraction technique using Mastersizer 2000 at the Aalto University. During measurements, samples were stirred at least at 2000 rpm and treated with ultrasonicator. Mie theory, refractive index of 1.55 and adsorption of 0.1 were used in calculations.

2.3.6 FTIR, Greene-Kelly test and the amount of illite

Validity of the analysis of mineralogical composition was further improved with additional information from FTIR-measurements, Greene-Kelly test and the chemical composition of the purified, homoionised clay fractions. FTIR spectra were measured in order to detect accessory kaolin minerals and amorphous accessory minerals; Greene-Kelly test was performed to identify and quantify beidellite from montmorillonite; and the amount of illite, which was done by determining the K^+ -content in purified clay fraction (see section 2.3.4 Composition of montmorillonite; structural calculations) to correct the montmorillonite and illite contents achieved by Siroquant.

FTIR

Na-exchanged clay fractions were ground in agate mortar with few drops of pure ethanol. Excess ethanol was evaporated in 60 °C oven. 2 mg of dry and ground sample material was mixed with 200 mg of KBr powder in vibratory grinder and pressed to 13

mm diameter discs. The spectrum was recorded immediately after preparation and after drying the KBr discs at 150 °C for 20 h to remove adsorbed water. Infrared spectrum was recorded in triplicate using transmission mode in a range from 4000 to 200 cm^{-1} with Perkin Elmer Spectrum One FTIR spectrometer at the Department of Geology, University of Helsinki. Resolution of scans was 4 cm^{-1} .

Greene-Kelly test

Greene-Kelly test (Greene-Kelly 1953; Lim and Jackson 1986) was used to identify the charge location in smectite structure, i.e. to differentiate montmorillonite (octahedral charge > tetrahedral charge) from beidellite, nontronite or saponite (octahedral charge < tetrahedral charge). The technique is based on saturation of clay with LiCl and heating to 250 °C, which results into permanent collapse of the montmorillonite basal spacing to 9.5 Å and further, decrease in CEC (Lim and Jackson 1986).

Only one sample of each material was selected to be tested, namely BT1, Ibeco1 and 1-1-Sa-R. Purified and homoionised clay was dispersed in deionized water, treated three times with 3 M LiCl solution and thereafter washed three times with 0.01 M LiCl in 90 % ethanol. Oriented mounts were prepared by smearing a thick paste of Li-clay on a silica slide. Oriented clay mounts were dried in air and heated at 250 °C overnight. After cooling, the mounts were placed in a desiccator containing glycerol and heated at 90 °C for 18 h. Sample mounts were dried in air and scanned with XRD from 2 to 15° 2 θ with 0.02° counting steps.

Loss of CEC due to Li uptake was also tested. The bulk sample was dispersed in 3 M LiCl, stirred at least for 2 h with magnetic stirrer, washed with deionized water and the clay fraction (<1 μm in diameter according to Stokes' law) was separated by sedimentation. The clay fraction was treated once with 3 M LiCl solution in the same way and washed with deionized water until incipient dispersion. The sample was dried at 60 °C and placed into a porcelain crucible and heated at 250 °C for 24 h. The samples were ground using oscillating mill and agate mortar before CEC determination with Cu(II)-triethylenetetramine-method (see section 2.1.2). The results were adjusted against adsorbed water content.

3 RESULTS

3.1 Basic acceptance testing

3.1.1 Water ratio, CEC, swelling index, liquid limit and granule size distribution by dry sieving

The water ratios, cation exchange capacities, swelling indexes and liquid limits of bulk materials are presented in Table 4. The results for CEC, swelling index, and liquid limit of Ibeco 1, 2 and 3 are similar as Ca-bentonites in Ahonen et al. (2008) and Kumpulainen and Kiviranta (2010), and the results of BT1, BT2, BT3, 1-1-Sa and 1-2-Sa are similar as Na-bentonites in Ahonen et al. (2008) and Kumpulainen and Kiviranta (2010).

The variation in results from the same 25 kg bag (1-1-Sa and 1-2-Sa) was similar to the variation from different 25 kg bags (BT1, BT2 and BT3) of the same lot (Table 4). Larger variation was seen in Ibeco samples, which were taken from top, middle and bottom parts of a 500 kg bag. The first swelling index measured for Ibeco 1 was anomalously high (20 ml/2g) compared to Ibeco 2 and 3, but upon re-measurement the value was in line with the results of Ibeco 2 and 3. Ibeco 1 had also higher CEC than other Ibeco batches.

Table 4. Water ratios, cation exchange capacities, swelling indexes and liquid limits of bulk materials.

Material	Water ratio (%)	CEC (eq/kg)	Swelling index (ml/2g)	Liquid limit (%)
BT1	12.4	0.861	22.0	490
BT2	12.2	0.861	22.3	480
BT3	12.3	0.866	21.8	480
Mean	12.3	0.863	22.0	483
Std	±0.1	±0.003	±0.3	±6
Ibeco 1	17.1	0.948	12.0	220
Ibeco 2	16.9	0.889	9.5	240
Ibeco 3	17.1	0.891	11.3	240
Mean	17.0	0.909	10.9	233
Std	±0.1	±0.03	±1.3	±12
1-1-Sa	6.4	0.835	24.8	500
1-2-Sa	6.6	0.832	24.8	520
Mean	6.5	0.834	24.8	510
Std	±0.1	±0.002	±0	±14

The granule size distributions of all materials are presented in Figures 4-6 and Table 5. The granule size distributions in 1-1-Sa and 1-2-Sa (Figure 5) and also in all BT samples (Figure 6) were almost identical among themselves (Table 5). The amount of larger granules was slightly higher in Ibeco 3 than in other Ibeco samples (Figure 4, Table 5). Ibeco 3 was taken from the bottom part of a 500kg bag and Ibeco 1 and 2 from the top and middle parts, respectively.

Table 5. Percentages of different granule sizes.

Granule size	Ibeco 1 (%)	Ibeco 2 (%)	Ibeco 3 (%)	1-1-Sa (%)	1-2-Sa (%)	BT1 (%)	BT2 (%)	BT3 (%)
> 4 mm	0.1	0.0	0.0	0.0	0.0	0.0	0.0	0.0
2-4 mm	20.6	20.9	26.3	0.9	0.9	0.0	0.1	0.0
1-2 mm	46.4	45.1	47.1	4.5	5.0	0.3	0.2	0.6
0.5-1 mm	23.3	22.9	18.8	21.3	23.6	33.6	29.8	31.2
0.25-0.5 mm	6.0	6.6	4.7	37.9	39.3	34.0	33.2	33.1
0.125-0.25 mm	2.4	3.1	2.0	20.7	18.7	19.2	21.0	20.1
0.063-0.125 mm	0.9	1.2	0.9	9.3	7.6	9.7	11.9	11.0
< 0.63 mm	0.3	0.3	0.2	5.3	4.9	3.2	3.8	4.0

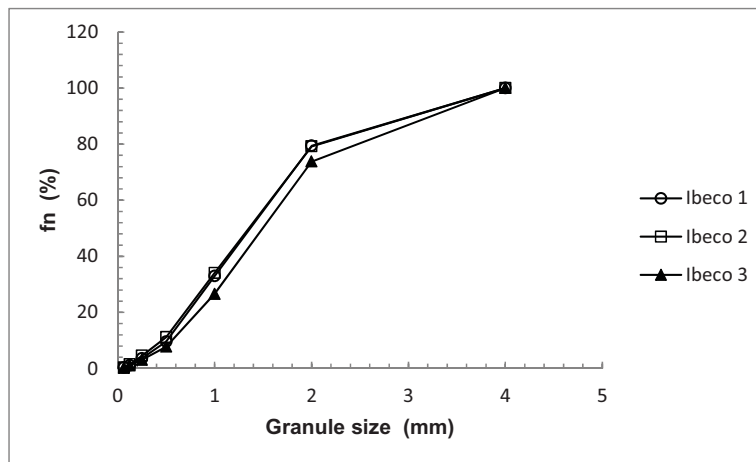


Figure 4. Plot of granule size vs. percent passing different size sieves for three batches of Ibeco.

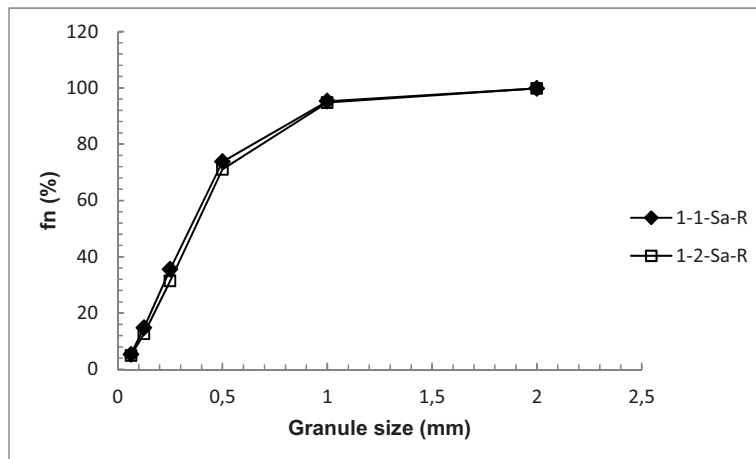


Figure 5. Plot of granule size vs. percent passing different size sieves for two batches of Wy--BT0007.

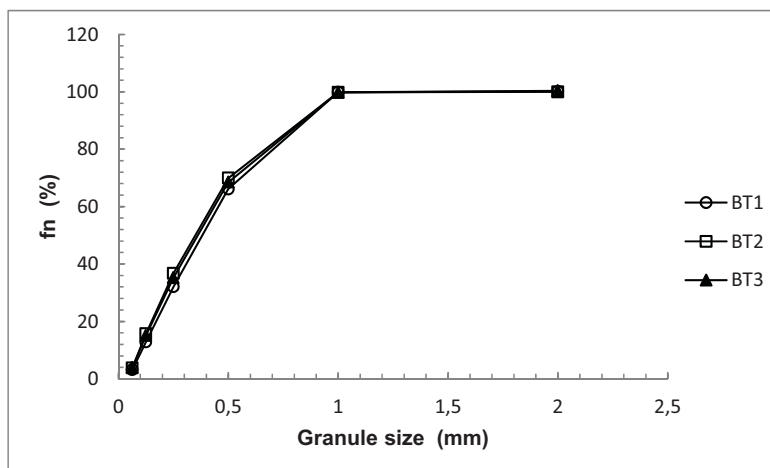


Figure 6. Plot of granule size vs. percent passing different size sieves for three batches of Wy--VT0002.

3.1.2 Comparison to acceptance requirements

The quality requirements for acceptance of the material concerning water ratio, swelling index, liquid limit and CEC (Table 1) were fulfilled for the Wyoming bentonite materials. The Ibeco material, on the other hand, was deficient with respect to both swelling index (-27 % on average) and water ratio (+31 % on average) criteria.

3.2 Further quality assurance testing

3.2.1 Original exchangeable cations

Based on the analyses of exchangeable cations, all the Wyoming-bentonite samples (BT1, BT2, BT3, 1-1-Sa and 1-2-Sa) were predominantly Na-bentonites (Table 6). They also contained some amount of exchangeable Ca and Mg as well. Exchangeable cations in Ibeco samples were more clearly mixtures of Na, Ca and Mg.

The sum of cations in NH_4Cl -extraction was in general slightly higher than the CEC measured with Cu(II)-triethylenetetramine-method, indicating that a small amount of soluble accessory minerals may have dissolved during the extraction.

The results of parallel samples (denoted with r) were almost identical. The saturation of exchangeable sites was almost identical in all Ibeco samples, but the results presented as eq/kg were smaller in Ibeco 1 for each exchangeable cation in a same proportion.

Table 6. Exchangeable cations and CEC of bulk materials measured with NH_4Cl - and $Cu(II)$ -triethylenetetramine-methods.

Sample	Saturation of exchangeable sites				Exchangeable cations (in dry (105°C) weight)					CEC
	Ca (%)	K (%)	Mg (%)	Na (%)	Ca (eq/kg)	K (eq/kg)	Mg (eq/kg)	Na (eq/kg)	Sum (eq/kg)	Cu-trien (eq/kg)
BT1	26	2	9	62	0.24	0.02	0.09	0.58	0.93	0.86
BT1r	27	2	9	62	0.25	0.02	0.09	0.59	0.95	0.86
Ibeco 1	43	2	31	23	0.39	0.02	0.29	0.21	0.91	0.95
Ibeco 2	42	2	32	24	0.41	0.02	0.31	0.24	0.97	0.89
Ibeco 3	43	2	32	24	0.40	0.02	0.30	0.22	0.95	0.89
1-1-Sa	27	2	9	62	0.25	0.02	0.08	0.58	0.93	0.84
1-1-Sar	27	2	9	62	0.25	0.02	0.08	0.58	0.93	0.84

3.2.2 Chemical composition

Chemical analyses showed (Table 7) that Ibeco samples contained significant amount of inorganic carbon, approximately 1.2 wt.%. The amount of organic carbon was low in all samples, ranging between 0.1 and 0.3 wt.%. The amount of total iron was ranging between 2.9-3.9 wt.%. Iron was mostly in ferric form in all samples (Tables 7 and 8). All samples contained small amounts of soluble sulphate (< 1 wt.%). Also the amount of sulphur bound to sulphides was low in all samples (< 0.5 wt.%). Ibeco samples contained more sulphidic sulphur (0.5 wt.%) than other samples. Sulphides (pyrite) were also identified in mineralogical analysis (see 3.2.3, Table 10) in all Ibeco samples using XRD, but in other samples it was detected only in sample 1-2-Sa.

Table 7. Total chemical composition of bulk materials, mean and standard deviation (std) of parallel samples. All results are in wt.% and normalized to 100 %.

Sample	SiO ₂	Al ₂ O ₃	Fe ₂ O ₃	FeO	TiO ₂	MgO	CaO	Na ₂ O	K ₂ O	Inorg. C	Org. C	Sulphate S	Sulphide S	LOI
BT1	61.85	20.28	3.85	0.55	0.17	2.52	1.30	2.42	0.80	0.17	0.14	0.13	0.16	6.26
BT2	61.54	20.62	3.90	0.51	0.17	2.54	1.28	2.41	0.77	0.14	0.14	0.12	0.16	6.27
BT3	61.27	20.76	3.93	0.52	0.17	2.53	1.38	2.42	0.76	0.15	0.17	0.12	0.14	6.26
Mean	61.55	20.55	3.89	0.53	0.17	2.53	1.32	2.41	0.78	0.15	0.15	0.12	0.15	6.26
Std	±0.29	±0.25	±0.04	±0.02	±0.00	±0.01	±0.05	±0.01	±0.02	±0.02	±0.02	±0.01	±0.01	±0.01
Ibeco 1	53.37	16.30	4.67	0.78	0.70	5.10	5.79	0.80	0.40	1.15	0.12	0.06	0.51	12.08
Ibeco 2	54.42	16.80	5.05	0.63	0.72	4.90	5.14	0.89	0.56	1.31	<0.05	0.04	0.49	10.90
Ibeco 3	54.88	16.92	4.65	0.69	0.72	4.86	4.82	0.91	0.65	1.25	<0.05	0.04	0.45	10.89
Mean	54.22	16.67	4.79	0.70	0.71	4.95	5.25	0.87	0.54	1.24	0.07	0.05	0.48	11.29
Std	±0.78	±0.33	±0.22	±0.08	±0.01	±0.13	±0.50	±0.06	±0.13	±0.08	±0.04	±0.01	±0.03	±0.68
1-1-Sa	59.72	21.42	3.60	0.50	0.15	2.78	1.50	2.83	0.47	0.21	0.28	0.12	0.15	7.03
1-2-Sa	59.92	21.13	3.64	0.48	0.15	2.76	1.48	2.89	0.64	0.31	0.28	0.12	0.15	6.92
Mean	59.82	21.27	3.62	0.49	0.15	2.77	1.49	2.86	0.55	0.26	0.28	0.12	0.15	6.98
Std	±0.14	±0.20	±0.03	±0.02	±0.00	±0.02	±0.01	±0.04	±0.12	±0.07	±0.00	±0.00	±0.00	±0.08

No significant differences were seen in samples taken from same 25 kg bag (1-1-Sa and 1-2-Sa), only the amount of inorganic carbon was smaller in 1-1-Sa (Table 7). Also no significant differences were seen in different 25 kg bags (BT1, BT2 and BT3) of a same lot. Larger variation was seen in Ibeco samples, which were taken from top, middle and bottom parts of a 500 kg bag. The amount of organic carbon in Ibeco samples exceeded

detection limit of the method only in Ibeco 1. Also LOI was slightly higher in Ibeco 1 than in other Ibeco samples despite its lower inorganic carbon content.

Differences of parallel samples of at least Wyoming bentonites are very small and thus probably within the analysis errors.

Table 8. *The ratio of Fe^{2+} and Fe^{3+} in bulk materials and clay fractions (see section 3.3.2).*

Sample	Fe^{2+}/Fe^{3+} (Bulk)	Fe^{2+}/Fe^{3+} ($< 1 \mu m$ Na-exchanged)
BT1	0.160	0.070
BT2	0.145	-
BT3	0.148	-
Ibeco 1	0.185	0.029
Ibeco 2	0.138	-
Ibeco 3	0.164	-
1-1-Sa	0.155	0.060
1-2-Sa	0.146	-

3.2.3 Mineralogical composition

XRD

Analysis of randomly oriented bulk material

The XRD patterns and interpreted minerals are presented in Appendix 1. In addition to overall mineralogy, the position of d(060) lines were assessed (Table 9). All studied samples showed presence of dioctahedral clay mineral, which had the d(060) line located in 1.495-1.498 Å, which is typical for montmorillonite. Some samples showed also small additional peaks at 1.529 Å (BT1), 1.566 Å (Ibeco 1) and 1.520 Å (Ibeco 3), which may indicate the presence of other, trioctahedral clay minerals. The d(060) lines presented in Table 9 are mean values of three subsequent runs. The compilation of identified minerals in bulk and clay fractions using XRD is presented in Table 10.

Analysis of oriented clay fractions

The compilation of line positions of clay minerals and identified minerals in clay fractions are presented in Table 9. The XRD patterns are presented in Appendix 2. All samples contained mainly swelling clay mineral smectite (illite–smectite I/S). In addition, samples contained small amounts of non-swelling clay minerals (illite, possibly chlorite) as well as some silica impurities (quartz, possibly cristobalite). The oriented samples were prepared from $< 2 \mu m$ Mg-exchanged clay fractions, hence quartz and cristobalite impurities are observed.

Table 9. Most important line positions of clay minerals (in Å), and interpreted clay mineralogy.

Fraction	Bulk		Clay						Identified clay minerals and impurities
	Treatment		Oriented	EG			550°C		
Line/interpretation	d(060) (Intensity)	Dioc./Trioc.	d(001)	d(001)	d(002)	d(003)	I % in I/S	d(001)	
Be-Wy—VT0002-									
BT1	1.496 (35), 1.529 (2)	Di, Tri?	14.62	16.55	8.41	5.60	0.6	9.81	I/S, Cr?
BT2	1.496 (25)	Di	14.30	16.41	8.35	5.57	0.2	9.54	I/S, Cr?
BT3	1.497 (27)	Di	13.83	16.44	8.36	5.57	0.4	9.51	I/S, Cr?
Be-Mi--BT0011-Gr-R									
Ibeco 1	1.498 (26), 1.566 (4)	Di, Tri?	14.38	16.40	8.34	5.54	3.8	9.80	I/S, I, Cl?
Ibeco 2	1,496 (26)	Di	14.87	16.85	8.44	5.58	4.1	9.83	I/S, I, Cl?
Ibeco 3	1,495 (44), 1.520 (3)	Di, Tri?	13.90	17.05	8.51	5.64	0.9	9.75	I/S, I, Cl?
Be-Wy--BT0007-1-Sa-R									
1-1-Sa	1.497 (29)	Di	13.99	16.41	8.35	5.57	0.9	9.56	I/S, Q, Cl, Cr?
1-2-Sa	1.498 (32)	Di	14.30	17.05	8.51	5.64	0.2	9.76	I/S, Q, Cl, Cr?

Notices: Di=diocahedral, Tri=trioctahedral, I/S=illite/smectite, Q=quartz, Cl=Chlorite, Cr=Cristobalite, I=Illite

Compilation of minerals identified with XRD is presented in Table 10. In addition to minerals identified with XRD also minerals identified with optical microscopy (next section) were included in quantification.

Table 10. Compilations of minerals identified with XRD.

	Be-Wy--BT0007-		Be-Mi--BT0011-			Be-Wy--VT0002-		
	1-1-Sa	1-2-Sa-	Ibeco 1	Ibeco 2	Ibeco 3	BT1	BT2	BT3
Smectite	x	x	x	x	x	x	x	x
Quartz	x	x	x	x	x	x	x	x
Plagioclase	x	x	x	x	x	x	x	x
Cristobalite	x?	x?				x?	x?	x?
Calcite			x	x	x	x	x	
Dolomite			x	x	x			
Illite			x	x		x	x	
Chlorite	x	x	x?	x?	x?			
Pyrite		x	x	x	x			

Optical microscopy

Accessory minerals identified by optical microscopy are listed in Table 11. In BT samples a microcline grid structure was observed in some of the particles indicating the presence of K-feldspar (Figure 7b). BT1, BT2 and BT3 samples contained opaque minerals. Some of the round opaque mineral grains consisted of aggregates of smaller round opaque grains, and were assumed to be framboidal pyrite (Figure 7c). Additionally, some of the opaque minerals were thought to be magnetite since small, black mineral particles were found attached to the magnetic stirrer.

Table 11. Accessory minerals identified by optical microscopy.

	Be-Wy--BT0007-		Be-Mi--BT0011-			Be-Wy--VT0002-		
	1-1-Sa	1-2-Sa	Ibeco 1	Ibeco 2	Ibeco 3	BT1	BT2	BT3
Quartz	x	x	x	x	x	x	x	x
Plagioclase	x	x	x	x	x	x	x	x
Carbonate	x	x	x	x	x	x	x	x
K-feldspar			x	x				x
Biotite	x	x	x	x	x	x	x	x
Muscovite			x	x	x			
Chlorite			x	x	x	x		x
Hornblende			x					
Zircon	x	x	x		x	x	x	x
Apatite		x	x	x	x	x	x	x
Hematite	x	x	x	x	x	x	x	x
Goethite			x	x	x			
Opaque	x	x	x	x	x	x	x	x
Opal-A			x	x	x			x

Both 1-1-Sa and 1-2-Sa samples contained some black mineral grains that were found attached to the magnetic stirrer, indicating presence of magnetic minerals, presumably magnetite. The extinction angles of plagioclase grains were used to determine the composition of plagioclase which turned out to be oligoclase.

All Ibeco samples contained cubic opaque minerals, presumably pyrite or magnetite. Some of the black mineral particles were observed to be magnetic. All Ibeco samples contained opal –A (biogenic amorphous silica), which formed circular structures and was colourless in plane polarized light (Figure 8b), and grey in cross-polarized light. The presence of opal-A was further confirmed on the basis of movement of Becke's line indicating that the refractive index of the particle (opal) was < 1.47 (Figure 8c-d).

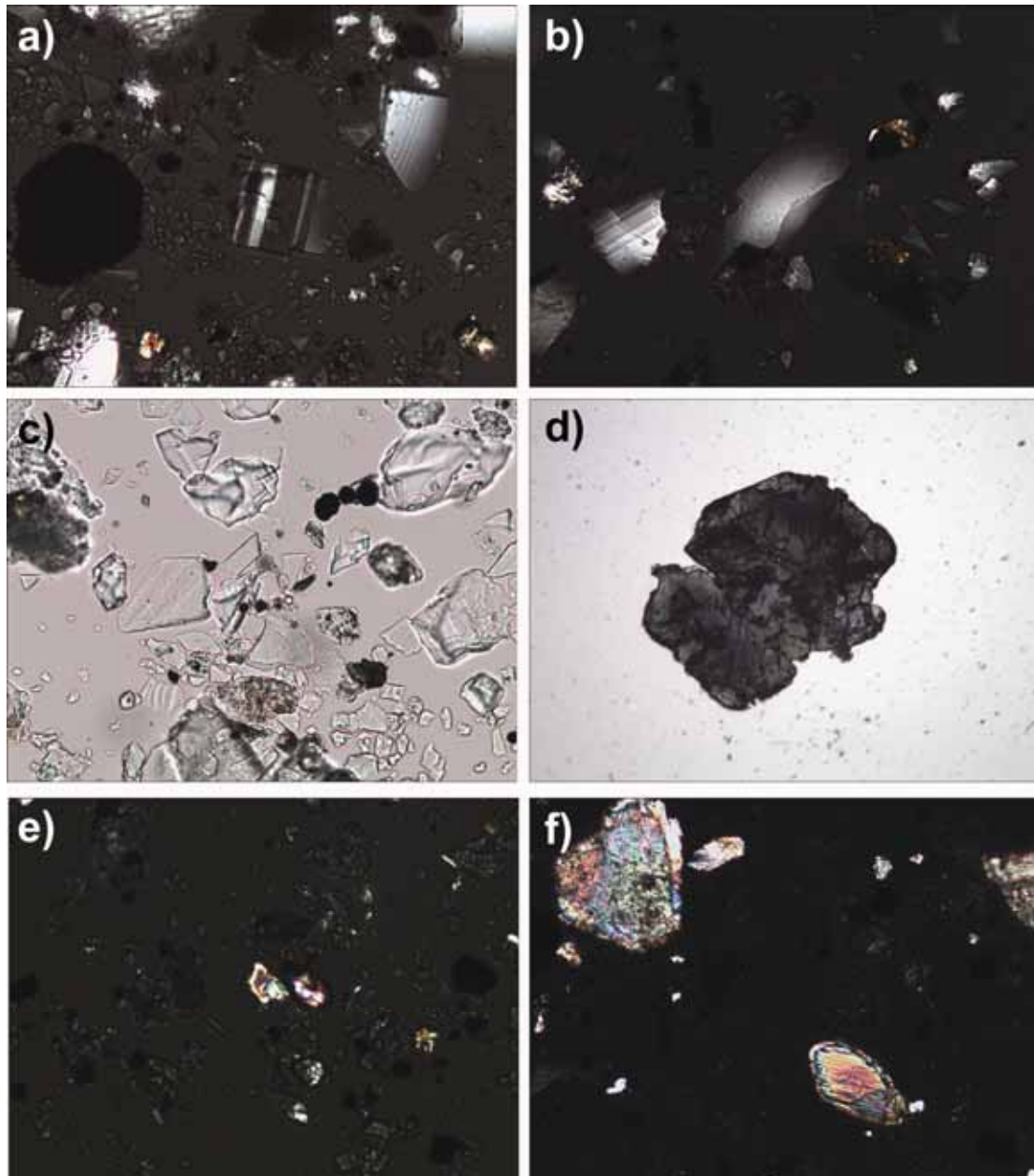


Figure 7. Optical microscopy images. a) Plagioclase in sample 1-1-Sa in cross-polarized light with x20 magnification b) Microcline in sample BT3 in cross-polarized light with x20 magnification c) Framboidal pyrite in sample BT3 in plane-polarized light with x20 magnification d) Hornblende in sample Ibeco 1 in cross-polarized light with x4 magnification e) Muscovite and zircon in sample Ibeco 1 in cross-polarized light with x20 magnification f) Carbonates in sample Ibeco 2 in cross-polarized light with x20 magnification.

Dissolution of unconditioned raw materials of Ibeco was also performed in an attempt to remove carbonates (see section 2.3.4). After the extraction, it was noticed that coarse grained material remained in the bottom of the beaker of which rounded white grains were thought to be undissolved carbonate (Figure 8a). These single grains were crushed gently in an agate mortar and examined under the microscope. Only quartz and

hornblende (in Figure 7d) were observed to exist as single mineral particles, other particles were agglomerates of several minerals. The white agglomerates consisted mostly of clay, but also some carbonates. The reddish grains contained predominantly hematite and opaque minerals, dark greyish grains of mica and chlorite, and greenish grains of opal-A.

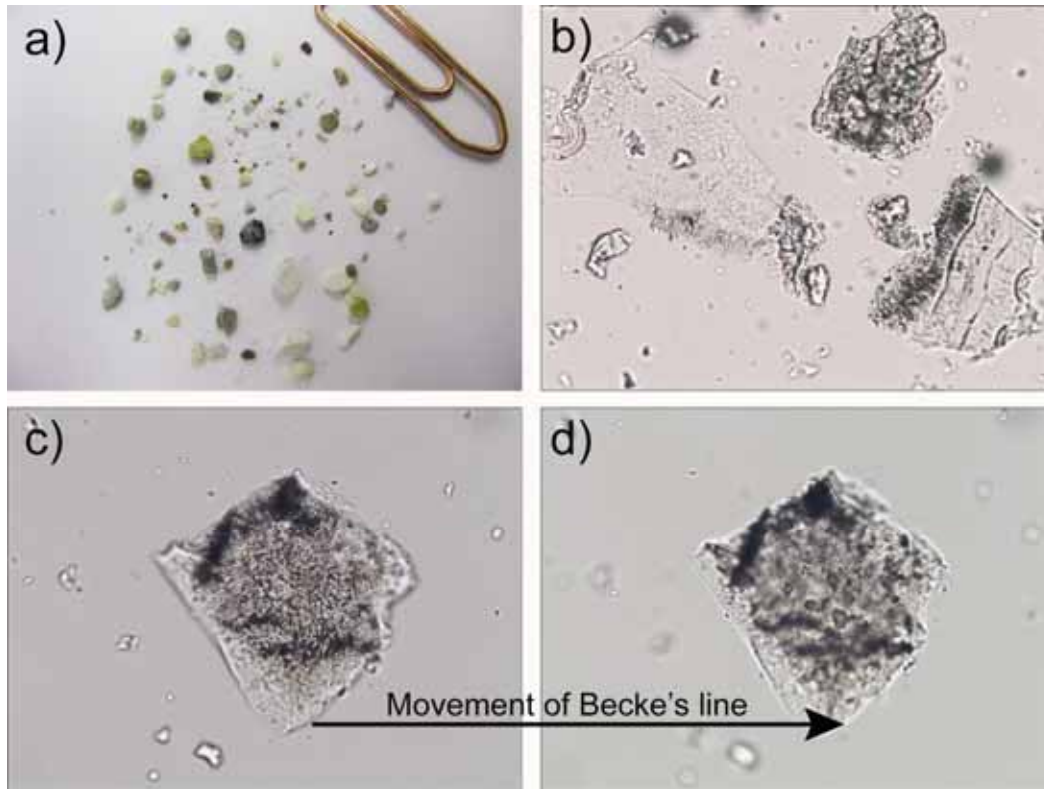


Figure 8. a) Agglomerates and some accessory mineral grains in coarse fraction of Ibeco 1. b-d) optical microscopy pictures (plane polarized light, x20 magnification) from Opal-A showing c-d) movement of Becke's line towards material of higher refractive index.

Although there were some differences between the accessory minerals identified with optical microscopy of parallel samples, it cannot be stated that such differences are truly characteristic since the objective was to identify presence of minerals. The analyzed samples were not fully representative as only one grain mount was analyzed and the identification was largely based on only one or two mineral grains. Furthermore, some minerals are hard to distinguish from each other due to their small grain size in smear slides, e.g. feldspars from quartz. Additional accessory minerals may be present that were not identified with the 'fast and easy' microscopy studies described here. For quantification purposes, minerals that were detected in any of the parallel samples were taken into account.

Quantification

Mineralogical compositions are presented in Table 12. In order to estimate the precision of analyses and compare the differences in compositions of parallel samples and

compositions of similar type of materials, also mean values and standard deviations are shown (Table 12).

In general, Wyoming bentonite samples 1-1-Sa and 1-2-Sa, and BT1, BT2 and BT3 had very similar mineralogical compositions with a mean smectite content of 88 wt.%. BT1, BT2 and BT3 samples had less quartz, plagioclase and calcite, but more other polymorphs of silica (cristobalite, opal), K-feldspar, biotite and chlorite than BT0007 samples (Table 12). However, it should be noted that most of the compositional differences between materials 1-1-Sa and 1-2-Sa, and BT1, BT2 and BT3 were within the variability of the parallel samples.

Mean smectite content of Ibeco samples was 79 wt.% and mean illite content 3 wt.%.

Table 12. Mineralogical composition (in wt.%) determined with Siroquant.

	Be-Wy--BT0007-			Be-Mi--BT0011-				Be-Wy--VT0002-			
	1-1-Sa	1-2-Sa	Mean±Std	Ibeco 1	Ibeco 2	Ibeco 3	Mean±Std	BT1	BT2	BT3	Mean±Std
Smectite	88.5	86.7	87.6±1.3	77.5	80.3	80.4	79.4±1.6	90.6	89.4	84.6	88.2±3.2
Illite	<i>0.1</i>	<i>0.1</i>	<i>0.1±0</i>	2.7	2.8	4.0	3.2±0.7	0.1	0.1	<i>0.1</i>	0.1±0
Quartz	4.0	4.3	4.1±0.2	2.5	0.3	tr	1.0±1.3	3.5	3.4	3.5	3.5±0.1
Cristobalite	<i>tr?</i>	<i>tr?</i>	<i>tr?</i>					0.1	0.2	<i>tr?</i>	0.1±0.1
Plagioclase	4.2	4.2	4.2±0	3.0	0.8	1.7	1.8±1.1	2.5	2.4	3.7	2.9±0.7
Calcite	0.5	0.6	0.6±0.1	3.0	3.8	6.0	4.3±1.5	0.4	0.1	0.1	0.2±0.2
Dolomite				7.2	6.4	3.4	5.7±2.0				
K-feldspar	<i>1.5</i>	<i>2.1</i>	<i>1.8±0.5</i>	<i>tr</i>	0.9	0.7	0.6±0.4	<i>1.4</i>	<i>1.7</i>	4.1	2.4±1.5
Biotite	<i>tr</i>	<i>tr</i>	<i>tr</i>	<i>tr</i>	<i>tr</i>	<i>tr</i>	<i>tr</i>	0.3	0.4	<i>tr</i>	0.3±0.2
Chlorite				0.9	1.4	0.4	0.9±0.5	<i>tr</i>		1.1	0.4±0.6
Hornblende				<i>tr</i>			<i>tr</i>				
Zircon	<i>tr</i>	<i>tr</i>	<i>tr</i>	<i>tr</i>		<i>tr</i>	<i>tr</i>	<i>tr</i>	<i>tr</i>	<i>tr</i>	<i>tr</i>
Apatite		<i>tr</i>	<i>tr</i>	<i>tr</i>	<i>tr</i>	<i>tr</i>	<i>tr</i>	<i>tr</i>	<i>tr</i>	<i>tr</i>	<i>tr</i>
Hematite	0.1	<i>tr</i>	<i>tr</i>	0.7	0.7	0.7	0.7±0.1	<i>tr</i>	<i>tr</i>	0.1	0.1±0
Goethite				<i>tr</i>	<i>tr</i>	<i>tr</i>	<i>tr</i>				
Pyrite	0.4	0.8	0.6±0.3	1.6	1.4	1.6	1.5±0.1	0.6	1.0	1.0	0.8±0.2
Magnetite	<i>tr</i>	<i>tr</i>	<i>tr</i>	<i>tr</i>	<i>tr</i>	<i>tr</i>	<i>tr</i>	<i>tr</i>	<i>tr</i>	<i>tr</i>	<i>tr</i>
Opal-A				<i>tr</i>	0.5	0.5	0.4±0.3			0.8	0.3±0.5
Rutile	<i>0.7</i>	<i>1.0</i>	<i>0.9±0.2</i>	<i>0.4</i>	<i>0.5</i>	<i>0.2</i>	0.4±0.2	<i>0.3</i>	<i>0.2</i>	<i>1.0</i>	0.5±0.4
Gypsum									<i>1.1</i>		0.4±0.6

Notices: Phases added in quantification phase are marked in cursive. Phases observed with XRD or optical microscopy but not given quantified values were considered to be present only as traces (*tr*).

Assuming that there were no compositional variations between parallel samples, precision of the mineralogical quantification could be estimated. For smectite content, the average standard deviation was ±2 %. For accessory minerals, errors were much larger, on average 40-50 % from total content of the accessory mineral.

The accuracy of mineralogical quantification was estimated by comparing measured chemical compositions to those calculated (Table 13) by converting quantified mineralogical compositions to chemical compositions using an ideal formula for illite and a calculated structural formula for montmorillonite (Table 19). Such comparisons indicated that for 1-1-Sa and 1-2-Sa samples mineralogical quantification underestimated Na-bearing mineral phases (e.g. montmorillonite, plagioclase) and carbonates and overestimated silica (e.g. quartz) and Ti-bearing phases (e.g. rutile). For the Ibeco samples mineralogical quantification underestimated silica (e.g. quartz, opal)

and overestimated S-bearing phases (e.g. pyrite), carbonates and Mg-bearing phases (e.g. dolomite). For the BT1, BT2 and BT3 samples mineralogical analysis underestimated Na-bearing phases (e.g. montmorillonite, plagioclase) and carbonates, and overestimated S-bearing phases (e.g. pyrite, gypsum).

Table 13. Accuracy of mineralogical quantifications. Observed vs. calculated chemical composition (in wt.%).

	Be-Wy--BT0007-				Be-Mi--BT0011-						Be-Wy--VT0002-					
	1-1-Sa		1-2-Sa		Ibeco 1		Ibeco 2		Ibeco 3		BT1		BT2		BT3	
	Obs.	Calc.	Obs.	Calc.	Obs.	Calc.	Obs.	Calc.	Obs.	Calc.	Obs.	Calc.	Obs.	Calc.	Obs.	Calc.
Na ₂ O	2.9	2.1	2.9	2.1	0.8	0.9	0.9	0.7	0.9	0.8	2.4	2.0	2.4	2.0	2.4	2.0
MgO	2.8	2.5	2.8	2.5	5.2	5.9	5.0	6.1	4.9	5.1	2.5	2.7	2.6	2.7	2.6	2.8
CaO	1.5	1.6	1.5	1.6	5.9	6.0	5.2	6.2	4.9	6.5	1.3	1.5	1.3	1.7	1.4	1.3
Fe ₂ O ₃	4.2	3.8	4.2	3.9	5.6	6.0	5.8	5.6	5.5	6.0	4.5	4.0	4.5	4.2	4.5	4.1
Al ₂ O ₃	21.6	20.0	21.3	19.7	16.5	16.7	17.0	17.0	17.1	17.4	20.4	20.4	20.8	20.1	20.9	19.9
SiO ₂	60.1	63.9	60.3	63.3	54.1	53.2	55.1	52.9	55.5	53.3	62.3	63.5	61.9	62.6	61.6	62.8
H ₂ O	4.7	4.2	4.5	4.1	6.8	3.8	5.7	4.0	6.0	4.0	4.3	4.3	4.4	4.5	4.3	4.2
CO ₂	1.0	0.2	1.2	0.3	2.6	4.6	2.7	4.7	2.5	4.2	0.6	0.2	0.6	0.1	0.7	0.1
K ₂ O	0.5	0.3	0.6	0.4	0.4	0.3	0.6	0.5	0.7	0.6	0.8	0.3	0.8	0.3	0.8	0.7
SO ₃	0.7	0.6	0.7	1.1	1.5	2.1	1.3	1.9	1.2	2.1	0.7	0.7	0.7	1.8	0.7	1.3
TiO ₂	0.2	0.7	0.2	1.0	0.7	0.4	0.7	0.5	0.7	0.2	0.2	0.3	0.2	0.2	0.2	0.9

3.2.4 Grain density

Table 14. Grain densities of bulk materials in 1 M NaCl solution.

Sample	Grain density (g/cm ³)
BT1	2.781 ± 0.001
BT2	2.779 ± 0.004
BT3	2.781 ± 0.012
Ibeco 1	2.810 ± 0.026
Ibeco 2	2.814 ± 0.004
Ibeco 3	2.804 ± 0.021
1-1-Sa	2.780 ± 0.007
1-2-Sa	2.775 ± 0.003

The grain densities measured for BT1, BT2, BT3, 1-1-Sa and 1-2-Sa samples (Table 14) are typical for Wyoming bentonites (Kumpulainen and Kiviranta 2011; Karnland et al. 2006). Measurement precision was estimated by performing three parallel measurements for each sample and calculating standard deviations for them (Table 14). The results of parallel samples taken from the same lot are generally within the calculated standard deviations, but distinct variations in precision were observed.

3.2.5 Swelling pressure, hydraulic conductivity, dry density and EMDD

A systematic difference between dry densities calculated from water ratio and measured bulk density was observed (Table 15, Figure 9), as expected (when sample is dismantled, the stress on the sample is liberated and it enlarges slightly). The dry density that was calculated from water ratio was approximately 1-3 % higher than what was measured with paraffin oil method in all samples.

Table 15. Swelling pressure, hydraulic conductivity, dry density and bulk density of bulk materials.

Sample	SP (MPa)	HC at 20 °C (m/s)	Ratio of non-swelling material	w (%)	Calculated from w			Immersion method		
					ρ_d (g/cm ³)	ρ_b (g/cm ³)	EMDD (g/cm ³)	ρ_d (g/cm ³)	ρ_b (g/cm ³)	EMDD (g/cm ³)
BT1	13.56	$3.27 \cdot 10^{-14}$	0.094	24.50	1.654	2.059	1.587	1.631	2.031	1.564
BT2	10.83	$2.92 \cdot 10^{-14}$	0.106	25.00	1.640	2.050	1.564	1.611	2.013	1.535
BT3	10.90	$3.02 \cdot 10^{-14}$	0.154	25.22	1.634	2.046	1.520	1.617	2.025	1.503
Ibeco 1	11.47	$9.25 \cdot 10^{-14}$	0.225	29.27	1.542	1.993	1.363	1.506	1.947	1.327
Ibeco 2	9.66	$9.84 \cdot 10^{-14}$	0.197	29.54	1.536	1.989	1.382	1.489	1.929	1.335
Ibeco 3	10.76	$8.84 \cdot 10^{-14}$	0.196	29.31	1.541	1.993	1.389	1.496	1.934	1.343
l-1-Sa	8.44	$3.00 \cdot 10^{-14}$	0.115	25.12	1.637	2.048	1.554	1.608	2.012	1.524
l-1-Sar	10.49	-	0.115	24.39	1.657	2.061	1.574	1.638	2.038	1.555
l-2-Sa	5.31	$4.78 \cdot 10^{-14}$	0.133	28.30	1.556	1.996	1.458	1.543	1.980	1.445

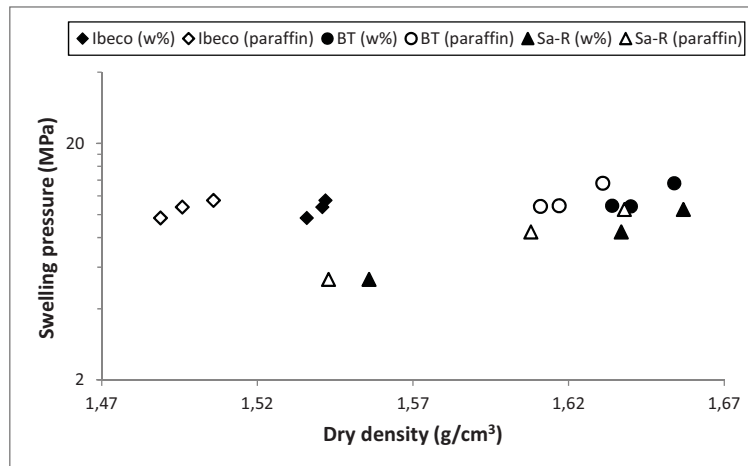


Figure 9. Swelling pressure vs. dry density (determined with two different methods, i.e., water ratio and immersion methods).

In general, relative to density, the swelling pressures of the Ibeco samples were larger than the swelling pressures of the Wyoming samples (Table 15; Figure 9). This variation could not be explained on the basis of smectite content alone (see Figure 10), assuming that the mineralogical composition reported in section 3.2.3 was considered to be valid. As such, some other chemical or physical material parameter may have caused the observed difference in the swelling pressure of Wyoming and Ibeco samples. The hydraulic conductivity was similar for all materials (Figures 11 and 12).

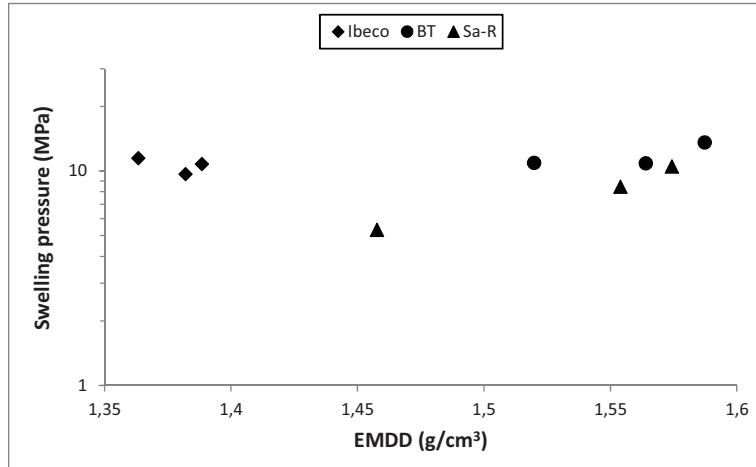


Figure 10. Swelling pressure vs. EMDD (calculated using dry density calculated from water ratio).

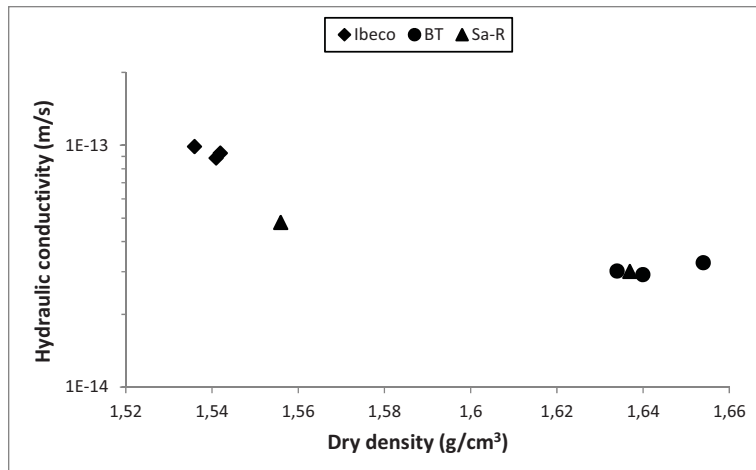


Figure 11. Hydraulic conductivity vs. dry density determined from water ratio.

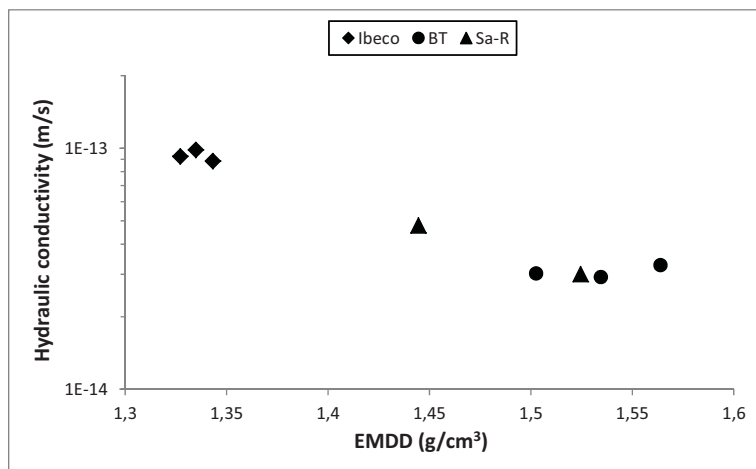


Figure 12. Hydraulic conductivity vs. EMDD (calculated using dry density calculated from water ratio).

3.2.6 Comparison to acceptance requirements

The quality requirements/minimum performance requirements (Table 1) concerning swelling pressure, hydraulic conductivity and smectite content were fulfilled for all materials.

3.3 Complementary testing

3.3.1 Specific surface area, water absorption capacity and plastic limit

The results for specific surface areas, water absorption capacities, plastic limits and plasticity indexes of bulk materials are presented in Table 16. Plasticity index and water absorption capacity of Ibeco 1 are smaller than for Wyoming bentonites, because the amount of exchangeable sodium was lower than in Wyoming bentonites. Water absorption capacities and specific surface areas correlate with smectite contents (see Figures 19 and 20).

Table 16. Plastic limits, plasticity indexes, water absorption capacities (Enslin-Neff) and specific surface areas (EGME).

Sample	Plastic limit (%)	Plasticity index (%)	Water absorption capacity (%)	Specific surface area (m ² /g)
BT1	50	440	630 ± 9	624 ± 7
Ibeco 1	50	170	253 ± 2	566 ± 6
1-1-Sa	40	460	587 ± 2	632 ± 7

3.3.2 Composition of montmorillonite

Chemical analyses of purified and Na-exchanged clay fractions (< 1 µm) showed that they still contained small amounts of Ca and K, as well as carbonates and organic matter (Table 17). Ibeco 1 sample that was treated with acid in order to remove carbonates also contained carbonates due to improper sample preparation, i.e., samples were not ground before suspending to acid solution (see additionally optical microscopy observations in section 3.2.3). Sulphates and sulphides were removed.

Table 17. Chemical composition of purified Na-exchanged clay fractions. All results are in wt.% and normalized to 100 %.

	SiO ₂	Al ₂ O ₃	Fe ₂ O ₃	FeO	TiO ₂	MgO	CaO	Na ₂ O	K ₂ O	Inorg. C	Org. C	Sulphate S	Sulphide S	LOI
IBECO1	60.41	18.97	4.85	0.13	0.75	3.66	0.03	3.17	0.28	0.03	0.03	0.00	0.00	7.75
IBECO1 CO ₃ - removed	60.68	19.00	4.84	0.11	0.74	3.68	0.02	3.14	0.33	0.07	0.03	0.00	0.00	7.47
1-1-Sa	62.79	20.96	3.81	0.20	0.14	2.44	0.01	2.84	0.06	0.10	0.19	0.00	0.00	6.74
BT1	62.54	21.33	3.82	0.24	0.13	2.44	0.01	2.89	0.06	0.07	0.03	0.00	0.00	6.52

Table 18. Structural composition of montmorillonite.

	Wyoming, USA BT1	Wyoming, USA 1-1-Sa	Milos, Greece Ibeco1	Milos, Greece Ibeco1, CO3-removed
Tetrahedral positions				
-Si ⁴⁺	7.909	7.949	7.900	7.912
-Al ³⁺	0.091	0.051	0.100	0.088
-Sum	8.000	8.000	8.000	8.000
Octahedral positions				
-Al ³⁺	3.114	3.106	2.800	2.806
-Fe ³⁺	0.349	0.348	0.461	0.451
-Fe ²⁺	0.025	0.022	0.014	0.012
-Mg ²⁺	0.465	0.466	0.727	0.731
-Sum	3.953	3.943	4.002	3.999
Interlayer positions				
-Ca ²⁺	0.000	0.000	0.000	0.000
-Mg ²⁺	0.000	0.000	0.000	0.000
-K ⁺	0.000	0.000	0.000	0.000
-Na ⁺	0.722	0.711	0.836	0.833
-Sum	0.722	0.711	0.836	0.833
O	24	24	24	24
H	4	4	4	4
Unit cell weight	745	745	752	751
Charges				
-Tetrahedral charge	-0.091	-0.051	-0.100	-0.088
-Octahedral charge	-0.631	-0.660	-0.736	-0.745
-Total charge	-0.722	-0.711	-0.836	-0.833
-Beidellite content (%)	13	7	12	11
CEC (for smectite) calculated from structural composition (eq/kg)	0.97	0.95	1.11	1.11
CEC (for clay fraction) measured (eq/kg)	0.90	0.89	1.07	1.07
CEC (for clay fraction) calculated from mineralogical composition (eq/kg)	0.95	0.94	1.18	-

The extended sedimentation time used in the purification procedure (48 h, see section 2.3.4) resulted in more effective removal of accessory quartz, cristobalite and poorly crystalline Si phases (e.g. opal) from purified clay fractions than the shorter time (24 h) used in Kumpulainen and Kiviranta (2010). Hence, chemical composition of purified fraction in this study is closer to the composition of pure smectite, and similar problems in composition calculations as in Kumpulainen and Kiviranta (2010) with impurities were not encountered. The calculated structural compositions of montmorillonites are presented in Table 18. The results indicated that all of the studied materials were beidellitic montmorillonites (octahedral charge > tetrahedral charge). The results are similar to those reported by Karnland et al. (2006) for similar materials.

The calculated cation exchange capacities for smectites were approximately 0.05 eq/kg higher than CEC values measured for clay fractions. This difference may be related to the fact that clay fraction includes in addition to smectite also minor or trace amounts of other clay minerals like illite, which have lower cation exchange capacity than the smectite. Additionally, mineralogical composition determined in section 3.2.3 was used to calculate the CEC of clay fraction (Table 18). These values were very close to the CEC values calculated from structural composition at least for Wyoming bentonites (Table 18).

The calculated structural formulas for smectites are presented in Table 19. The occupation of exchangeable cation sites is adjusted according to measured original exchangeable cation distribution in bulk materials excluding potassium.

Table 19. Structural formulas of smectites. Exchangeable cations are adjusted according to original exchangeable cation distribution in bulk material excluding potassium.

Sample	Structural formula of smectite			
	Exchangeable cation sites	Octahedral sites	Tetrahedral sites	
Ibeco 1	$\text{Na}_{0.20}\text{Ca}_{0.37}\text{Mg}_{0.27}$	$\text{Al}_{2.80}\text{Fe}^{3+}_{0.46}\text{Fe}^{2+}_{0.01}\text{Mg}_{0.73}$	$\text{Si}_{7.90}\text{Al}_{0.10}$	$\text{O}_{20}(\text{OH})_4$
Ibeco 1, CO_3 -removed	$\text{Na}_{0.20}\text{Ca}_{0.37}\text{Mg}_{0.27}$	$\text{Al}_{2.81}\text{Fe}^{3+}_{0.45}\text{Fe}^{2+}_{0.01}\text{Mg}_{0.73}$	$\text{Si}_{7.91}\text{Al}_{0.09}$	$\text{O}_{20}(\text{OH})_4$
BT1	$\text{Na}_{0.46}\text{Ca}_{0.19}\text{Mg}_{0.07}$	$\text{Al}_{3.11}\text{Fe}^{3+}_{0.35}\text{Fe}^{2+}_{0.03}\text{Mg}_{0.47}$	$\text{Si}_{7.91}\text{Al}_{0.09}$	$\text{O}_{20}(\text{OH})_4$
1-1-Sa	$\text{Na}_{0.45}\text{Ca}_{0.20}\text{Mg}_{0.06}$	$\text{Al}_{3.11}\text{Fe}^{3+}_{0.35}\text{Fe}^{2+}_{0.02}\text{Mg}_{0.47}$	$\text{Si}_{7.95}\text{Al}_{0.05}$	$\text{O}_{20}(\text{OH})_4$

3.3.3 Grain size distribution

Grain size distributions of bulk samples are shown for BT1 and Ibeco 2 materials in Figure 13. Based on these results, it can be observed that Ibeco 2 consisted of larger grains than BT1.

Grain size distributions of purified clay fractions are presented in Figure 14 showing that increasing the sedimentation time to 48 h resulted in a fractionation of smaller particles than 24 h settlement (Table 20). It should be noted that compared to the traditional methods (e.g. pipette), laser diffraction often underestimates the amount of clay sized particles (Eshel et al. 2004), because the laser diffraction method is designed for optical detection of sphere shapes, and other methods are based on different parameters, e.g. in this study Stokes' law of gravitation of sphere-shaped particles in viscous fluids was used to calculate the sedimentation time needed to separate clay particles with a certain size. Especially for optical detection of clay minerals the sphere shape assumption causes a challenge, because instead of spheres the clay minerals form elongated flakes. The particle size estimated by calculation using Stokes' law and particle sizes measured by laser diffraction therefore do not give the same values (Table 20). The determination of particle size that can be considered clay in laser diffraction is therefore higher, for most samples $<8 \mu\text{m}$, compared to the conventional methods such as pipette or sieving (Konert and Vandenberghe 1997).

Table 20. Calculated diameters of grains by sedimentation (Stokes' law) and by laser diffraction (Mie equation).

Sample	Sedimentation time	Sedimentation	Laser diffraction	
		Stokes' diameter (μm)	Measured mean (μm)	Measured max (μm)
Ibeco 2	24h	1.14	2.03	15.14
Ibeco 2	48h	0.80	1.25	3.80
BT1	24h	1.15	2.59	15.14
BT1	48h	0.81	1.70	5.01

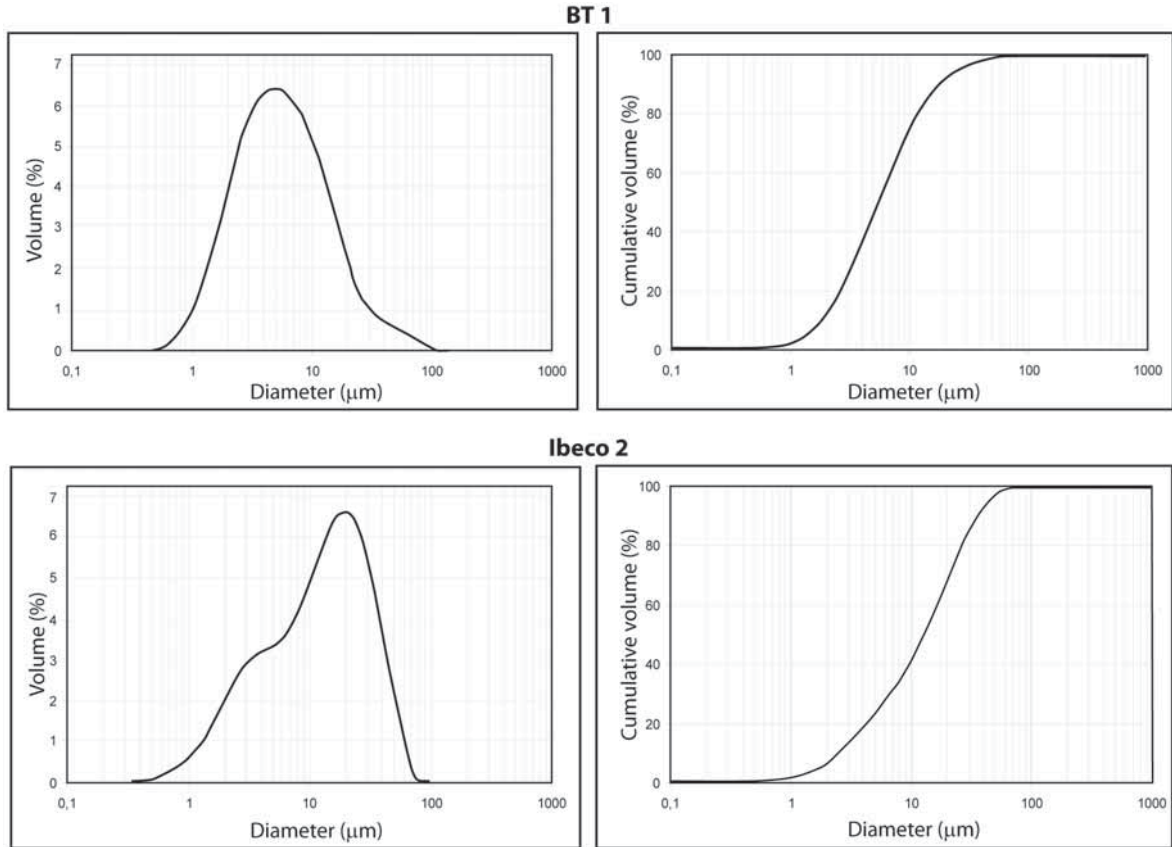


Figure 13. Volumetric particle size distribution of bulk samples of BT 1 and Ibeco2.

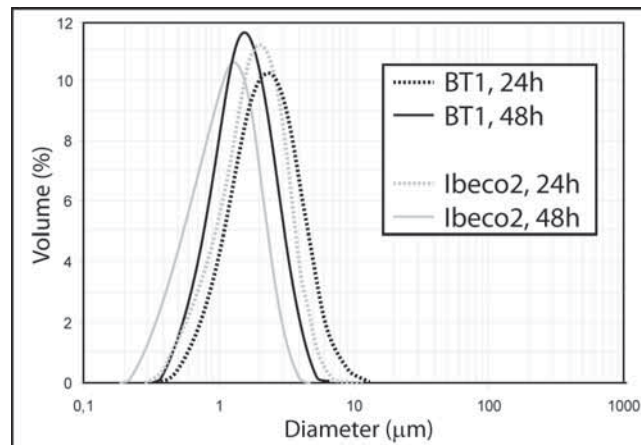
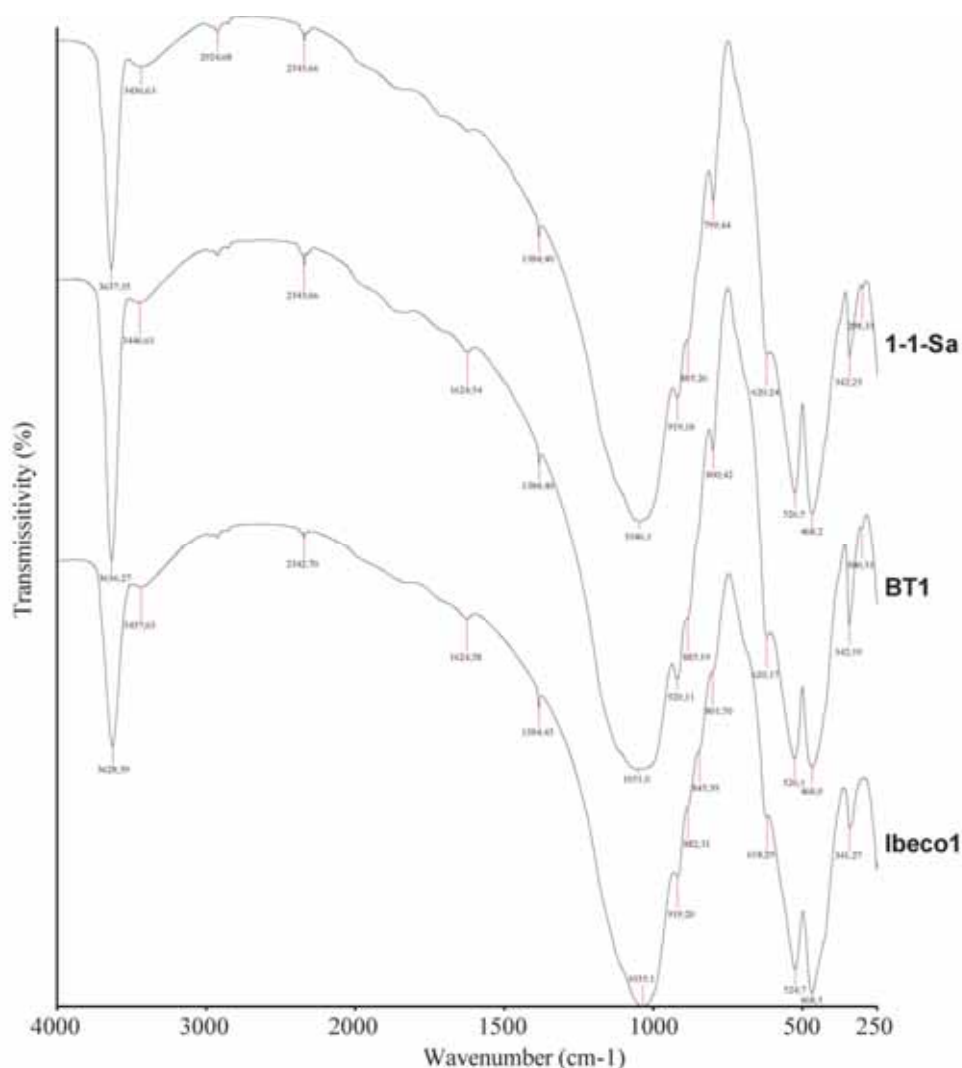


Figure 14. Volumetric particle size distributions of BT1 and Ibeco2 clay fractions after particle size fractionation by 24h or 48h sedimentation.

3.3.4 FTIR, Greene-Kelly test and amount of illite

FTIR

Purified clay fractions showed OH stretching and bending bands typical for smectites (see e.g. Kumpulainen and Kiviranta 2010) appearing at wavenumbers ~ 3630 , 1040 , 919 , and 884 cm^{-1} . FTIR patterns of samples 1-1-Sa and BT1 were almost identical. In addition to bands seen in samples 1-1-Sa and BT1, sample Ibeco1 showed also AlMgOH bending at 845 cm^{-1} .



Greene-Kelly test

All tested samples showed permanent loss of swelling ability after Li saturation and heating demonstrating that the identified smectite was montmorillonite (Table 21).

The loss in CEC for the studied materials was somewhat smaller than in Kumpulainen and Kiviranta (2010) for similar materials, but still in same range as reported by Karnland et al. (2006). The loss in CEC was used to quantify the percentage of montmorillonitic layers in smectite, which varied from 67 to 78 %. The remaining fractions (33-22 %) were assumed to consist of beidellite and/or accessory clay minerals, namely illite (see next paragraph). However, structural calculations (Table 18) of purified clay fractions indicated that the amount of beidellitic layers in smectite was much smaller, only 7-13 %.

Table 21. Results from Greene-Kelly test.

Sample	XRD		CEC		
	Li-sat.	Li-sat. + 250°C+G	Initial	After Li-sat.+250°C	Loss in CEC
	d(001) in Å	d(001) in Å	eq/kg	eq/kg	%
1-1-Sa	12.42	9.76	0.89	0.22	75
BT1	12.38	9.80	0.90	0.20	78
Ibeco 1	12.28	9.81	1.07	0.36	67

Amount of illite

The Moore and Reynolds (1989) method and Rietveld analysis, which both are based on XRD, but analysed from different material fractions, gave similar illite contents as the illite content calculated from the potassium content in clay fraction (Table 22). The illite content from Rietveld analysis (Table 12) was converted to the illite content in clay fraction (Table 22) assuming that all quantified clay minerals (Table 12) were in the clay fraction.

Table 22. Illite contents of clay fractions (wt.%) estimated with three different methods.

Sample	XRD: Moore and Reynolds (1989)	Chemical composition (K+)	Rietveld
Ibeco 1	3.8	3.1	3.3
Ibeco 1, CO ₃ -removed	-	3.6	-
Ibeco 2	4.1	-	3.3
Ibeco 3	0.9	-	4.7
BT1	0.6	0.7	0.1
BT2	0.2	-	0.1
BT3	0.4	-	0.1
1-1-Sa	0.9	0.7	0.1
1-2-Sa	0.2	-	0.1

4 DISCUSSION

4.1 Index tests to determine smectite content

The idea of basic acceptance testing is to assure the quality of bentonite with relative fast and inexpensive tests. The QA –tests suggested (per material lot) by Ahonen et al. (2008) and Laaksonen (2010) include water content, swelling index, smectite content, liquid limit and cation exchange capacity. All of these except determination of smectite content are also included in the basic acceptance testing of this study. Smectite content cannot be determined quantitatively with any above mentioned tests, but requires complicated and time-consuming determination with XRD, of total chemical composition and full pattern fitting with Rietveld (see sections 2.2.2 and 2.2.3).

However, some of the basic acceptance test parameters such as swelling index, liquid limit and cation exchange capacity do correlate with the smectite content. Furthermore, some of the complementary acceptance tests done in this study, such as specific surface area and water absorption capacity, also correlate with the smectite content. However, many of above listed methods are influenced by other factors such as type of exchangeable cations and other clay minerals than just the amount of smectites present.

One of the objectives of this study was to compare different basic acceptance test results with smectite content determined with XRD and full-pattern refinement in order to give recommendations for the use of such tests in estimating the smectite content. In addition to materials studied in this report, also results of ABM reference materials (Kumpulainen et al. 2011; Kumpulainen and Kiviranta 2011), results from analyses of potential backfill materials (Appendix 5) and results from other previous studies (Appendices 3 and 4) were considered.

Swelling index and liquid limit

The exchangeable cation population of smectite determines the degree of hydration and the rheological properties (e.g. Pusch 2001). Hence also swelling index and liquid limit are affected by the type of exchangeable cations. Better correlation between swelling index or liquid limit and smectite content is obtained after multiplying smectite content by the exchangeable Na^+ content (eq/kg) (Figures 16 and 17).

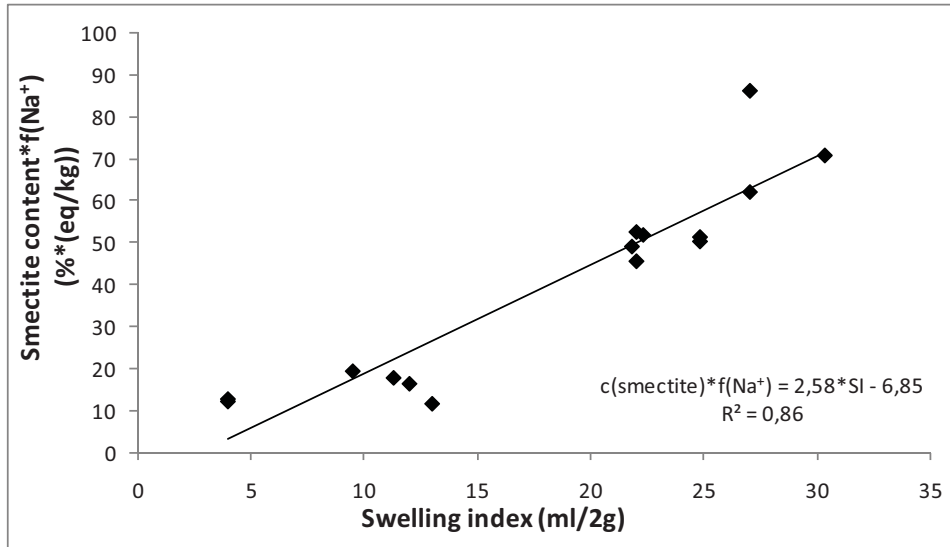


Figure 16. Dependency of swelling index on smectite content (%) multiplied by the content of exchangeable Na^+ . AC200, Friedland clay, Milos B, Milos granules and Milos pellets are included in the analysis (Data from Appendices 3, 4 and 5 and Kumpulainen et al. (2011)).

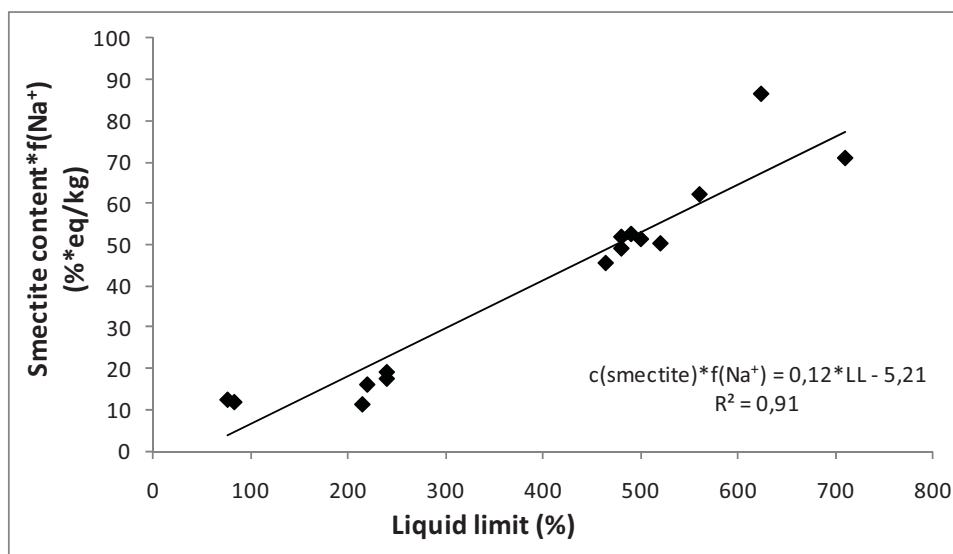


Figure 17. Dependency of liquid limit on smectite content (%) multiplied by the content of exchangeable Na^+ . AC200, Friedland clay, Milos B, Milos granules and Milos pellets are included in the analysis (Data from Appendices 3, 4 and 5 and Kumpulainen et al. (2011)).

CEC

In addition to smectite, other clay minerals, poorly crystalline aluminosilicates, oxides, hydroxides and organic matter, affect the measured CEC. CEC of montmorillonite varies typically between 80-120 meq/100g, kaolinite 3-15 meq/100g, illite 20-50 meq/100g, vermiculite 100-200 meq/100g (Appelo and Postma 1999). The dependency of CEC on smectite content is presented in Figure 18.

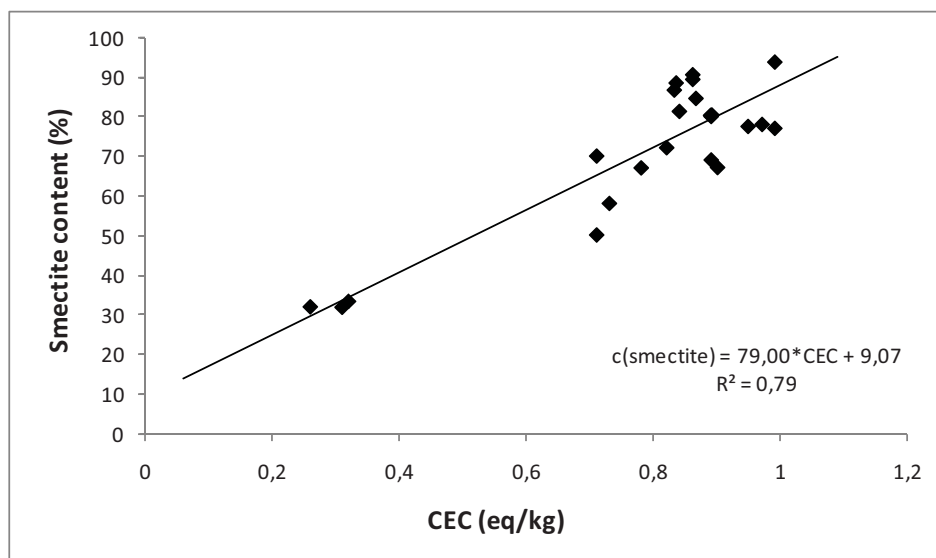


Figure 18. Dependency of cation exchange capacity (CEC) on smectite content. ABM reference materials, Milos B, Milos granules and Milos pellets are included in the analysis (Data from Kumpulainen et al. (2011) and Appendix 5).

EGME-SSA

The specific surface areas of clay materials correlate with smectite contents of the materials, i.e., higher surface areas were measured for samples with larger smectite content (Figure 19).

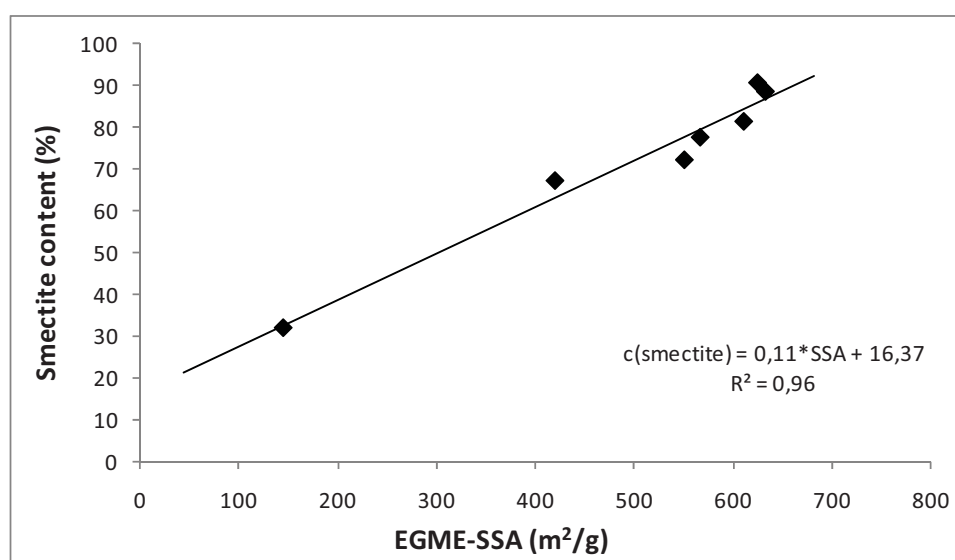


Figure 19. Dependency of EGME-SSA on smectite content. ABM reference materials are included in the analysis (Data from Kumpulainen and Kiviranta (2011) and Kumpulainen et al. (2011)).

WAC

The water absorption capacity results are influenced by the amount of swelling clay minerals in the material, and especially the type of exchangeable cations (Neff 1959; Kaufhold et al. 2010) (Figure 20).

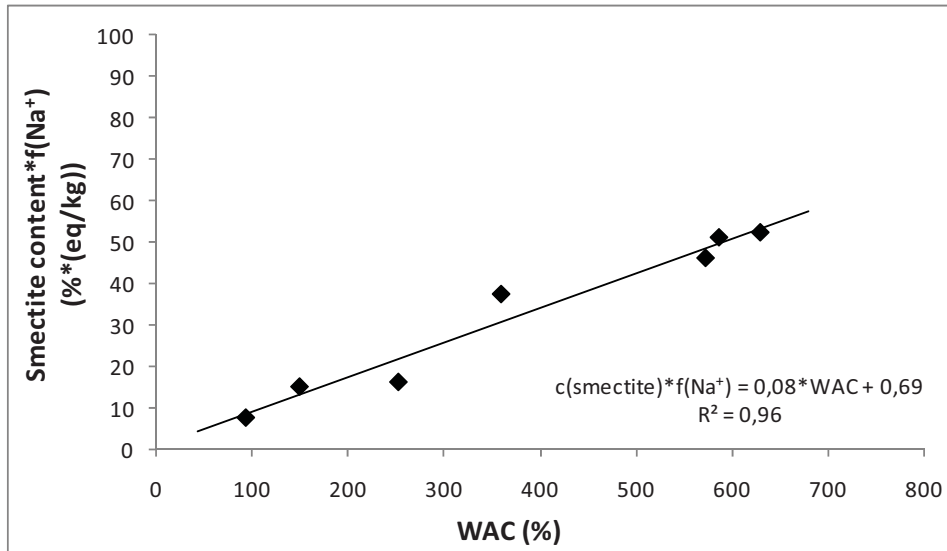


Figure 20. Dependency of water absorption capacity on smectite content (%) multiplied by the content of exchangeable Na^+ . ABM reference materials are included in the analysis (Data from Kumpulainen and Kiviranta 2011 and Kumpulainen et al. 2011).

All tested index tests correlated with the smectite content, but only EGME-SSA and CEC didn't require additional information of the exchangeable cation population in the sample (Table 23). However, results from CEC and SSA may be affected by other minerals and organic matter in the sample. For example, vermiculite may produce high CECs even if there is no smectite in the sample, and specific surface area may turn to be high due to high content of organic matter. Hence, results from all index tests need to be assessed carefully and additional information is needed when using some of the tests. It should also be noted that number of data points, and the composition and type of smectite-rich materials explored in this study was low, which brings uncertainty in the validity of indexing smectite content of other type of materials than tested here.

Table 23. Comparison of index tests for determining smectite content.

Index test	Main factors that also affect the result	Other tests that are needed for index determination of smectite content
Swelling index	Exchangeable cations	Exchangeable cation extraction
Liquid limit	Exchangeable cations	Exchangeable cation extraction
CEC	Other clay minerals, iron oxides, aluminium oxides and organic matter	
EGME-SSA	Other clay minerals, iron oxides, aluminium oxides and organic matter	
WAC	Exchangeable cations	Exchangeable cation extraction

To conclude, index tests provide a simple and considerably rapid way to test the smectite content of a material on a rough scale, meaning the errors in smectite content of typically 5-10 wt.%, but up to 25 wt.%. The index tests do not require highly sophisticated equipment or expertise, and are therefore suitable for quality control purposes of materials of trusted source. However, as many other factors than the smectite content affect the results of these index tests, they are not enough for determination of smectite content even on a rough scale, or indicate the presence of smectite in an unknown materials. In such cases, thorough chemical, mineralogical and physical characterization is required.

4.2 Index testing requirement limits

Based on the results in this study, the preliminary required values for certain tests (Table 1) should be updated. In particular, the relevance of water ratio as a material requirement is questionable because it is sensitive to environmental conditions and thus adjustable. Currently, the requirement for water ratio for all materials is set to 13 %. The idea of setting this requirement has been that increase in water ratio can be used to verify possible disturbances of the material during the transport or storage. However, as the water ratio is in reality dependent on purchased product, the requirement should be set for each purchased batch separately.

The preliminary required values for Ca-bentonites should be updated. The water absorption capacity of Ca-bentonites is limited and according to this study, the requirement of a swelling index over 15 ml/2g cannot be met as all Ca-bentonite samples tested in this study were below this value (except one, but after re-test, it was also below the required value). On the contrary, the liquid limit requirement limit could be raised, because all the liquid limits measured in this study were well above the required values (including those for Na-bentonites).

It is also uncertain when material can be considered as a Ca-bentonite and when a Na-bentonite. Natural materials such as bentonites contain always more or less mixtures of mono- and divalent cations on their exchangeable cation surfaces. Further, the preliminary required values for CEC of Na- and Ca- bentonites are specified separately (Table 1), even though there are no such differences in this property which would require such distinction. It may be that certain CEC test methods are sensitive to exchangeable cation content (e.g. MBI method), but the strict use of the well-documented, Cu(II)-triethylenetetramine-method would eliminate such concerns. If this CEC test is used to ensure smectite content at ≥ 75 %, in average a value of 0.83 eq/kg is required (see Figure 18). By taking into account the relatively high variation in the CEC results, a minimum value for CEC should also be defined, but in order to do this, more samples of variable compositions should be studied, and more knowledge on other material parameters affecting the CEC should be included in the analysis. Additionally, there should be an upper limit for CEC since high charged smectites or vermiculites contain non-swellable layers and thus do not necessarily fulfil the swelling requirements shown in Table 1.

Requirement limits can be evaluated also for the other index tests used in this study using equations presented in Figures 16-20. However, the dependence on exchangeable cation composition makes the evaluation more complex for swelling index, liquid limit and water absorption capacity tests. Thus, the need for the additional exchangeable cation content information renders the effectiveness of these methods as index tests for smectite content.

4.3 Determination of trace mineral contents

Rietveld refinement is based on randomly oriented XRD patterns. The detection limit of mineral contents with XRD is typically 1 %, but it is dependent on, e.g., instrumental and statistical factors, crystallinity of the mineral and peak overlap. For many of the minerals indicated by Siroquant to be present in low amounts (<1 %), the estimated analytical error is of the same magnitude or even greater than the actual determined value for the mineral amount (Ward et al. 1999).

Accessory minerals, which are important for pH buffering reactions (e.g. carbonates), Eh (e.g. pyrite) or buffer pore water composition (e.g. gypsum) are usually present in bentonite only in trace amounts. Relatively high detection limits of XRD technique and uncertainty in Rietveld refinement combined mean that the analytical error for the amounts of these mineral constituents is high in mineralogical analysis. To demonstrate the accuracy of determination of trace mineral content, comparison between calculated normative mineral concentrations (based on chemical composition) and determined mineralogical composition (Table 12) was done for all materials quantified in this study, and materials from earlier studies of Kumpulainen and Kiviranta (Appendix 5) and Kumpulainen et al. (2011) (Table 24).

The comparison (Table 24) shows that the amount of gypsum was overestimated on average 0.8 wt.% when included in the refinement or underestimated on average 0.5 wt.% when left out from the refinement. Also the amount of pyrite was either overestimated on average 0.3 wt.% when included in the refinement or underestimated on average 0.2 wt.% when left out from the refinement. On the other hand, when carbonates were present only in trace amounts, they were underestimated on average 0.9 wt.% (carbonates were included in the refinement in all materials).

As the accuracy of quantitative mineralogical analyses for trace minerals such as gypsum, pyrite or carbonates was shown to be low, chemical composition based normative amounts are recommended to be used for these minerals instead. On the other hand, mineralogical quantification procedures could be improved by determining the quality of important mineral phases better e.g. by microscopic methods, determining the quantity of the reactive trace mineral phases with other methods e.g. by chemical extractions, and assessing types of errors in quantification procedure step by step.

Table 24. Comparison of chemically and mineralogically determined contents (wt.%) of gypsum, pyrite and carbonates.

Sample	Reference	Gypsum (CaSO ₄ *2H ₂ O)		Pyrite (FeS ₂)		Carbonates	
		Chemical analysis	Mineralog. analysis	Chemical analysis	Mineralog. analysis	Chemical analysis	Mineralog. analysis
		Assuming all water soluble SO ₄ bound to gypsum		Assuming all sulphuric S bound to pyrite		Assuming only calcite, except in Friedland clay only siderite	Calcite+ Dolomite+ Siderite
ABM MX80	Kumpulainen et al. (2011)	0.24	0.70	0.37	0.70	1.31	0.50
Volclay MX80	Kumpulainen et al. (2011)	0.15	1.20	0.34	0.80	1.65	0.70
WyMX80	Kumpulainen et al. (2011)	0.12	1.20	0.42	0.80	1.03	0.70
ABM Friedland c.	Kumpulainen et al. (2011)	0.95	1.20	0.73	0.70	4.63	2.70
SH Friedland c.	Kumpulainen et al. (2011)	1.26	2.00	0.88	0.80	3.92	1.60
ABM DepCaN	Kumpulainen et al. (2011)	0.62	1.60	1.15	0.90	8.55	8.30
SH AC200	Kumpulainen et al. (2011)	0.36	1.20	0.73	1.40	9.33	6.20
ABM Asha	Kumpulainen et al. (2011)	0.02	0.90	0.04	0.00	0.60	0.70
Basic-Starbent	Kumpulainen et al. (2011)	0.43	1.50	0.30	0.00	1.13	1.90
Ca-Starbent	Kumpulainen et al. (2011)	0.44	1.20	0.31	0.00	0.54	1.10
HLM-Starbent	Kumpulainen et al. (2011)	0.07	1.60	0.05	0.00	1.62	0.90
I-1-Sa	This study	0.65	0.00	0.28	0.40	1.74	0.50
I-2-Sa	This study	0.64	0.00	0.27	0.80	2.60	0.60
Ibeco1	This study	0.32	0.00	0.96	1.60	9.60	10.20
Ibeco2	This study	0.22	0.00	0.91	1.40	10.92	10.20
Ibeco3	This study	0.21	0.00	0.84	1.60	10.39	9.40
BT1	This study	0.68	0.00	0.30	0.60	1.38	0.40
BT2	This study	0.62	1.10	0.29	1.00	1.13	0.10
BT3	This study	0.65	0.00	0.27	1.00	1.28	0.10
Milos granules	Appendix 5	0.39	0.00	0.55	0.70	19.52	18.70
Milos pellets	Appendix 5	0.66	0.00	1.00	1.30	17.26	17.40
Milos B	Appendix 5	0.08	0.00	0.19	0.50	31.41	31.30

5 CONCLUSIONS

All three of the bentonite materials met the preliminary required values/minimum performance requirements for CEC, smectite content, swelling pressure, and hydraulic conductivity. Wyoming bentonites contained approximately 88 wt.% of smectite, and Milos bentonites 79 wt.% of smectite and 3 wt.% of illite. Precision of smectite analyses was 2 %, and variances in composition of parallel samples within analytical errors, at least for Wyoming bentonites. For accessory minerals, precision was much lower, in average 40-50 % from the total content of the accessory mineral. Comparison of normative and mineralogically determined trace mineral contents showed that the accuracy of quantitative analyses for trace minerals such as gypsum, pyrite or carbonates, was also low. As the concentrations of these minerals are important for Eh or pH buffering reactions or development of bentonite pore water composition, normative concentrations are recommended to be used instead of mineralogically determined concentrations.

The swelling pressures and hydraulic conductivities of different materials were compared using EMDD. Swelling pressure was relatively higher for the studied Ca-bentonite than for the studied Na-bentonites and the small difference could not be explained with different smectite contents, but was considered to be caused by some other chemical or physical material parameter. Hydraulic conductivities seemed to be similar for all materials.

The changes made in experimental procedures of separation of clay fraction improved the reliability of the calculations of montmorillonite composition, which further brought reliability to the results of other analyses e.g. experimental CEC, beidellite content and overall mineralogical quantification.

The index tests (CEC, SSA, LL, SI, WAC) correlated with the smectite content. Thus, index tests can be used to determine the smectite content semiquantitatively for quality control purposes for materials of known sources.

The preliminary required values (Table 1) should be updated at least for Ca-bentonites. Ibeco samples had very high smectite contents, but still the swelling index requirement wasn't fulfilled. In addition, the previously set CEC requirement value was defined separately for Na- and Ca- bentonites even though there are no such differences in their CEC's, that would require this, and there are methods, which work for bentonites regardless of their exchangeable cation population. Thus CEC requirement limits should also be updated.

REFERENCES

- Ahonen L., Korkeakoski P., Tiljander M., Kivikoski H., Laaksonen R. 2008. Quality assurance of the bentonite material. Posiva WR 2008-33. Posiva Oy, Olkiluoto, Finland.
- ASTM D 4546-08. Standard Test Methods for One-Dimensional Swell or Collapse of Cohesive Soils.
- ASTM D 5890-06. Standard Test Method for Swell Index of Clay Mineral Component of Geosynthetic Clay Liners.
- ASTM D 5084-03. Standard Test Methods for Measurement of Hydraulic Conductivity of Saturated Porous Materials Using a Flexible Wall Permeameter.
- Ammann L., Bergaya F., Lagaly G. 2005. Determination of the cation exchange capacity of clays with copper complexes revisited. *Clay Minerals*, 40, 441-453.
- Appelo C.A.J., Postma D. 1999. *Geochemistry, groundwater and pollution*. A.A. Balkema, Rotterdam, The Netherlands. 479p.
- Belyayeva N.I., 1967. Rapid method for the simultaneous determination of the exchange capacity and content of exchangeable cations in solonchic soils. *Soviet Soil Science*, 1409-1413.
- Eshel, G., Levy, G.J., Mingelgrin, U., Singer, M.J. 2004. Critical evaluation of the laser diffraction for particle-size distribution analysis. *Science Society of America Journal*, 68, 736-743.
- Finnish standard CEN ISO/TS 17892-4: 2004. Geotechnical investigation and testing. Laboratory testing of soil. Part 4: Determination of particle size distribution.
- Finnish standard CEN ISO/TS 17892-12: 2004. Geotechnical investigation and testing. Laboratory testing of soil. Part 12: Determination of Atterberg limits.
- Cerato A. B., Lutenecker A. J. 2002, Determination of surface area of fine-grained soils by the ethylene glycol monoethyl ether (EGME) method, *Geotechnical Testing Journal*, 25, 3.
- Deutsche norm DIN 18132, december 1995. Soil, testing procedures and testing equipment – Determination of water absorption.
- Dixon D.A., Chandler N.A., Baumgartner P. 2002. The influence of groundwater salinity and interfaces on the performance of potential backfilling materials. *In Proceedings of the 6th International Workshop on design and Construction of Final Repositories, Backfilling in Radioactive Waste Disposal*, Brussels, 11–13 March 2002. ONDRAF/NIRAS, Brussels, Belgium. Transactions, Session IV, Paper 9.

- Drever J.I. 1973. The preparation of oriented clay mineral specimen for x-ray diffraction analysis by a filter-membrane peel technique. *American Mineralogist*, 58, 553-554.
- Greene-Kelly R. 1953. The identification of montmorillonoids in clays. *Journal of Soil Science*, 4, 233-237.
- Jackson M.L. 1975. *Soil chemical analysis – advanced course*. Second edition. Madison, Wisconsin. 991p.
- Karnland O., Olsson S., Nilsson U. 2006. Mineralogy and sealing properties of various bentonites and smectite-rich clay materials. SKB TR-06-30. Swedish Nuclear Fuel and Waste Management Company (SKB), Stockholm, Sweden.
- Kaufhold S., Dohrmann R. 2008. Comparison of the Traditional Enslin-Neff Method and the Modified Dieng Method for Measuring Water-Uptake Capacity, *Clays and Clay Minerals*, 56, 686-692.
- Kaufhold S., Dohrmann R., Klinkenberg M. 2010. Water-uptake capacity of bentonites. *Clays and Clay Minerals*, 58, 37-43.
- Konert M., Vandenberghe J. 1997. Comparison of laser grain size analysis with pipette and sieve analysis: a solution for the underestimation of the clay fraction. *Sedimentology* 44, 523-535.
- Kumpulainen S., Kiviranta L. 2010. Mineralogical and chemical characterization of various bentonite and smectite-rich clay materials. Posiva WR 2010-52. Posiva Oy, Olkiluoto, Finland.
- Kumpulainen S., Kiviranta L. 2011. Mineralogical, chemical and physical study of potential buffer and backfill materials from ABM test package 1. Posiva WR 2011-41. Posiva Oy, Olkiluoto, Finland.
- Kumpulainen S., Kiviranta L., Korkeakoski P. 2011. Mineralogical and chemical characterization of various bentonite rocks and smectite-rich clay materials. *Physics and Chemistry of the Earth*, (accepted).
- Laaksonen R. 2010. MANU - Purchase of bentonite -Process description. Posiva WR 2009-64. Posiva Oy, Olkiluoto, Finland.
- Lim C.H., Jackson M.L. 1986. Expandable phyllosilicate reactions with lithium on heating. *Clays and Clay Minerals*, 34, 346-352.
- Mehra O.P., Jackson M.L. 1960. Iron oxide removal from soils and clays by a dithionite-citrate system buffered with sodium bicarbonate. 7th National Conference on Clays and Clay Minerals, 317-327.

Moore D.M., Reynolds R.C. 1989. X-ray diffraction and the identification and analysis of clay minerals. Oxford University Press, Inc.

Meier L.P., Kahr G. 1999. Determination of the cation exchange capacity (CEC) of clay minerals using the complexes of copper(II) ion with triethylenetetramine and tetraethylenepentamine. *Clays and Clay Minerals*, 47, 386-388.

Neff K.H. 1959. Über die messung der wasseraufnahme ungleichförmiger bindiger anorganischer bodenarten in einer neuen ausführung des Enslingerätes. *Die Bautechnik*, 39, 415-421.

Newman A.C.D. (Ed.) 1987. Chemistry of clays and clay minerals. Mineralogical Society, Monograph No. 6.

Posiva 2010. TKS-2009 Nuclear Waste Management at Olkiluoto and Loviisa Power Plants, Review of Current Status and Future Plans for 2010-2012. Posiva Oy, Olkiluoto, Finland.

Pusch R. 2001. The buffer and backfill handbook, Part 2: Materials and techniques. SKB TR-02-12. Swedish Nuclear Fuel and Waste Management Company (SKB), Stockholm, Sweden.

Saikkonen R.J., Rautiainen I.A. 1993. Determination of ferrous iron in rock and mineral samples by three volumetric methods. *Bulletin of the Geological Society of Finland*, 65, 59-63.

Schatz T., Martikainen J. 2010. Laboratory studies on the effect of freezing and thawing exposure on bentonite buffer performance: closed-system tests. Posiva report 2010-06. Posiva Oy, Olkiluoto, Finland.

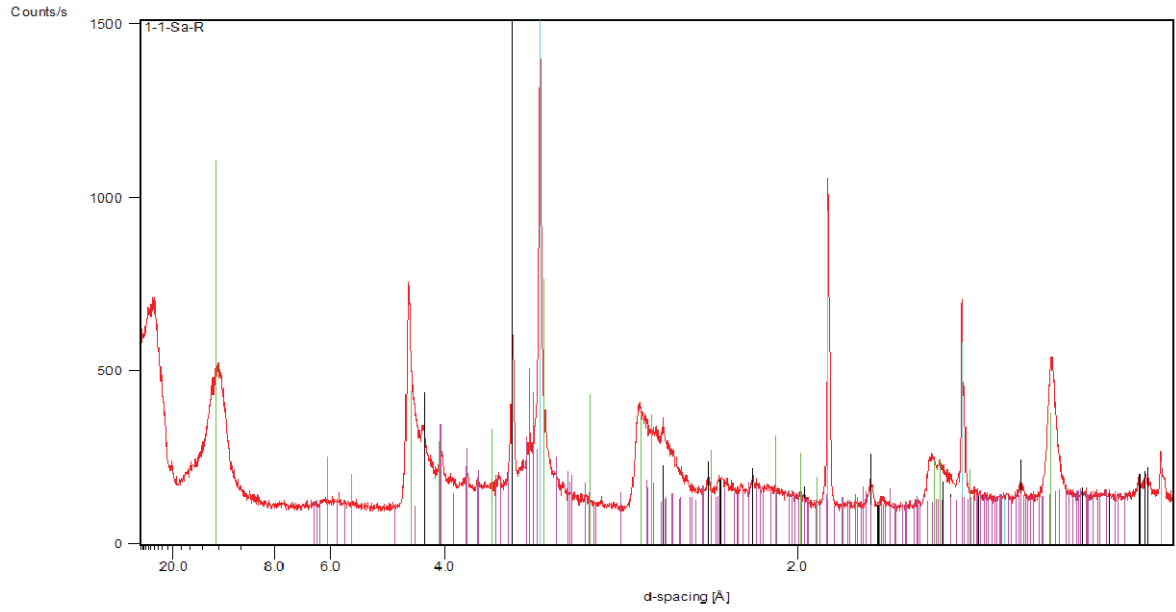
SKB 2009. Design premises for a KBS-3V repository based on results from the safety assessment SR-Can and some subsequent analyses. SKB Technical report TR-09-22. Swedish Nuclear Fuel and Waste Management Company (SKB), Stockholm, Sweden.

Ward C.R., Taylor J.C., Cohen D.R. 1999. Quantitative mineralogy of sandstones by x-ray diffractometry and normative analysis. *Sedimentary Research* 69, 1050-1062.

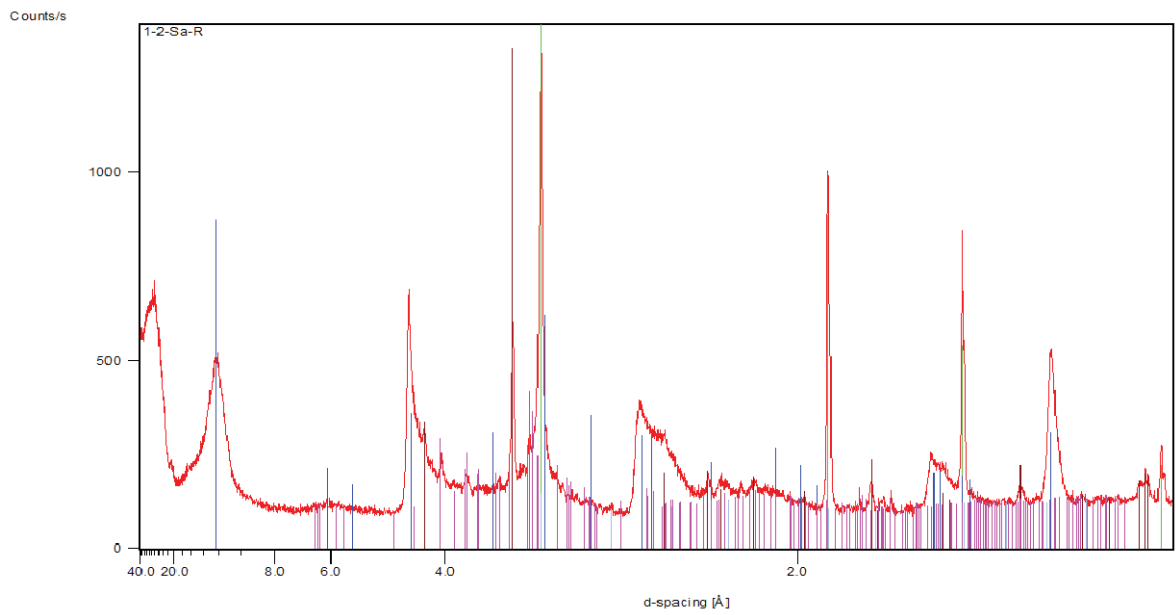
LIST OF APPENDICES

- Appendix 1** XRD patterns of randomly oriented bulk samples and identified minerals
- Appendix 2** Compilation of XRD patterns (bulk, oriented, EG treated, heated)
- Appendix 3** Basic and further quality control type analyses of two backfill materials (B+Tech memo 5.7.2010)
- Appendix 4** Characterization analyses of backfill materials (B+Tech memo 18.3.2011)
- Appendix 5** Composition and properties of Milos B, Milos granules and Milos pellets (B+Tech memo 2.11.2011)

XRD patterns of randomly oriented bulk samples and identified minerals.

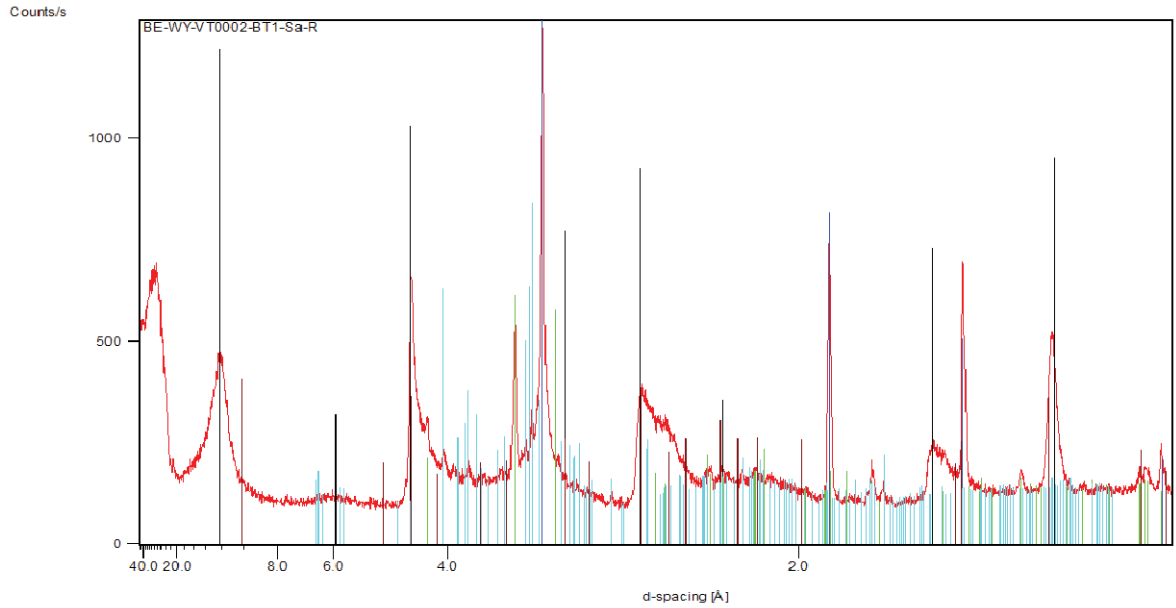


Peak List
01-079-1906; Quartz, syn: Si O ₂
00-058-2010; Montmorillonite, Na _{0.3} (Al, Mg) ₂ Si ₄ O ₁₀ (OH) ₂ · x H ₂ O
04-001-7247; Silicon, syn: Si
04-007-9875; Anorthite, sodian, Na _{0.4} Ca _{0.6} Al _{1.6} Si _{2.4} O ₈



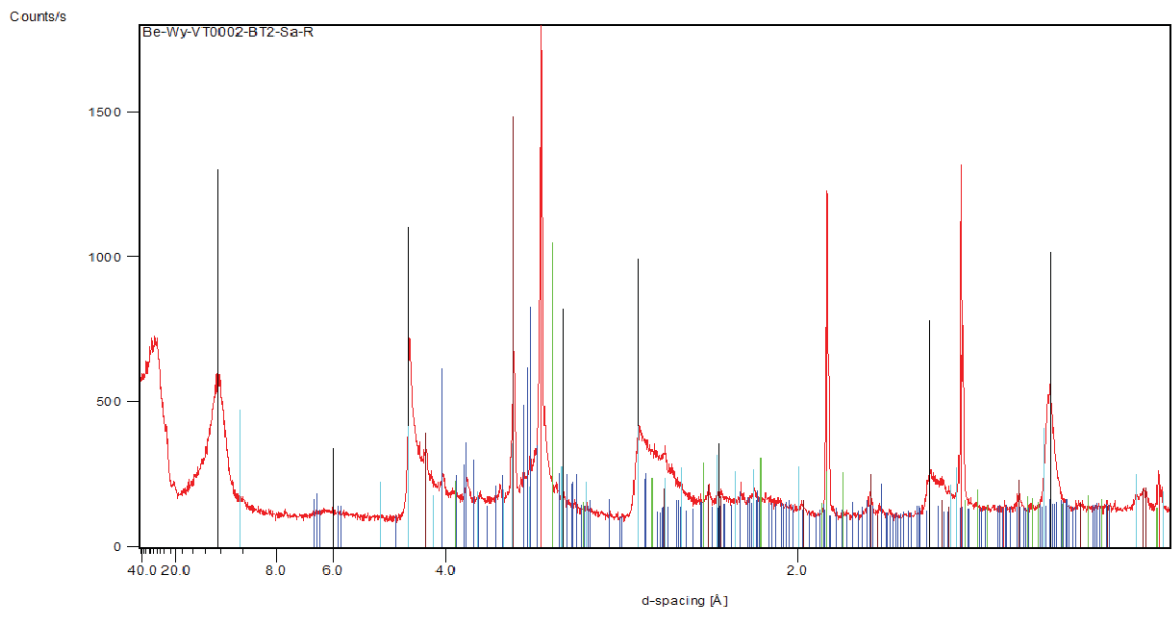
Peak List
04-001-7247; Silicon, syn: Si
01-070-7344; Quartz, Si O ₂
00-058-2010; Montmorillonite, Na _{0.3} (Al, Mg) ₂ Si ₄ O ₁₀ (OH) ₂ · x H ₂ O
04-007-9875; Anorthite, sodian, Na _{0.4} Ca _{0.6} Al _{1.6} Si _{2.4} O ₈
00-042-1340; Pyrite, Fe S ₂

XRD patterns of randomly oriented bulk samples and identified minerals.



Peak List

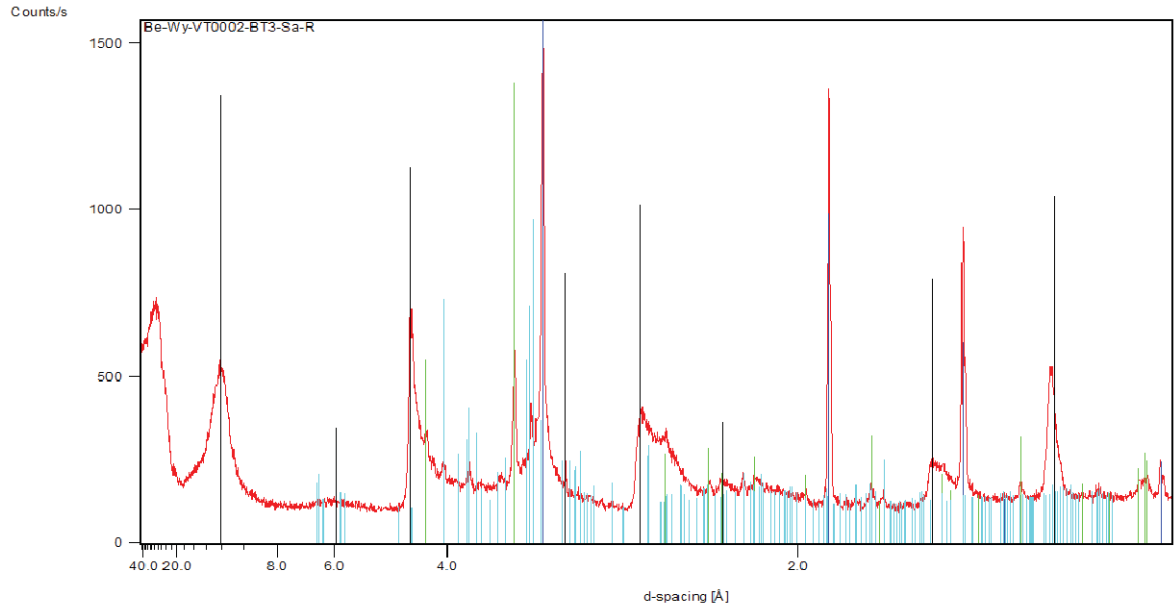
00-002-0037	Montmorillonite	Al ₂ Si ₂ O ₆ (OH) ₂
00-002-0050	Illite	2 K ₂ O · 3 MgO · Al ₂ O ₃ · 24 SiO ₂ · 12 H ₂ O
00-005-0586	Calcite, syn.	Ca C O ₃
01-075-6978	Silicon, syn.	Si
01-075-8322	Quartz	Si O ₂
04-011-6768	albite high P	Na _{0.22} Na _{0.78} Al ₂ Si ₃ O ₈



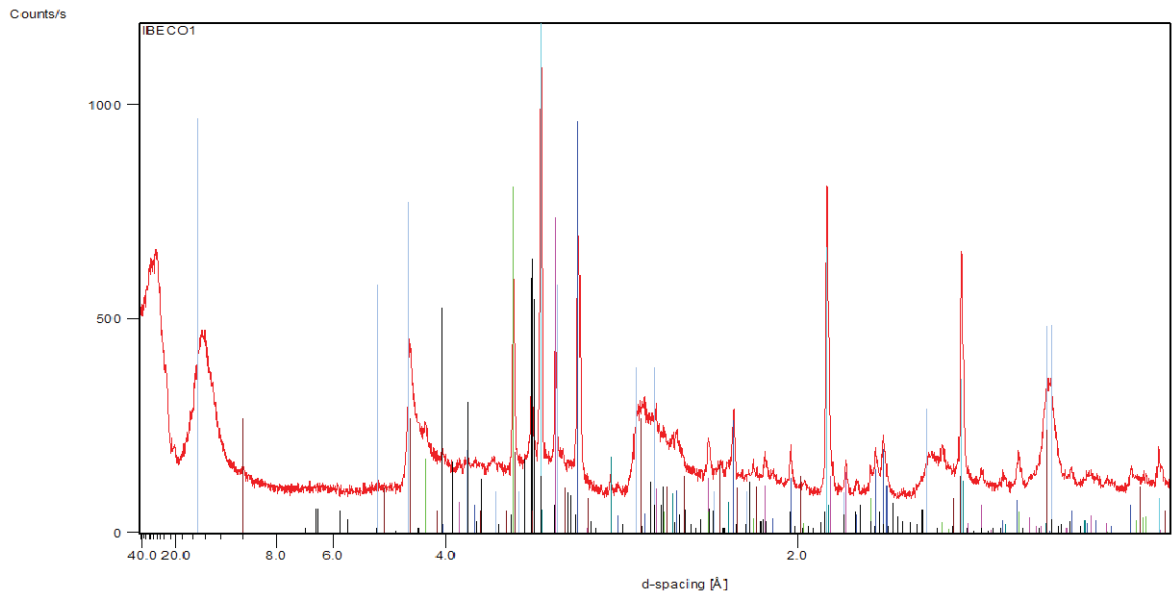
Peak List

01-075-6978	Silicon, syn.	Si
01-075-8322	Quartz	Si O ₂
00-002-0037	Montmorillonite	Al ₂ Si ₂ O ₆ (OH) ₂
04-011-6768	albite high P	Na _{0.22} Na _{0.78} Al ₂ Si ₃ O ₈
00-005-0586	Calcite, syn.	Ca C O ₃
00-002-0050	Illite	2 K ₂ O · 3 MgO · Al ₂ O ₃ · 24 SiO ₂ · 12 H ₂ O

XRD patterns of randomly oriented bulk samples and identified minerals.

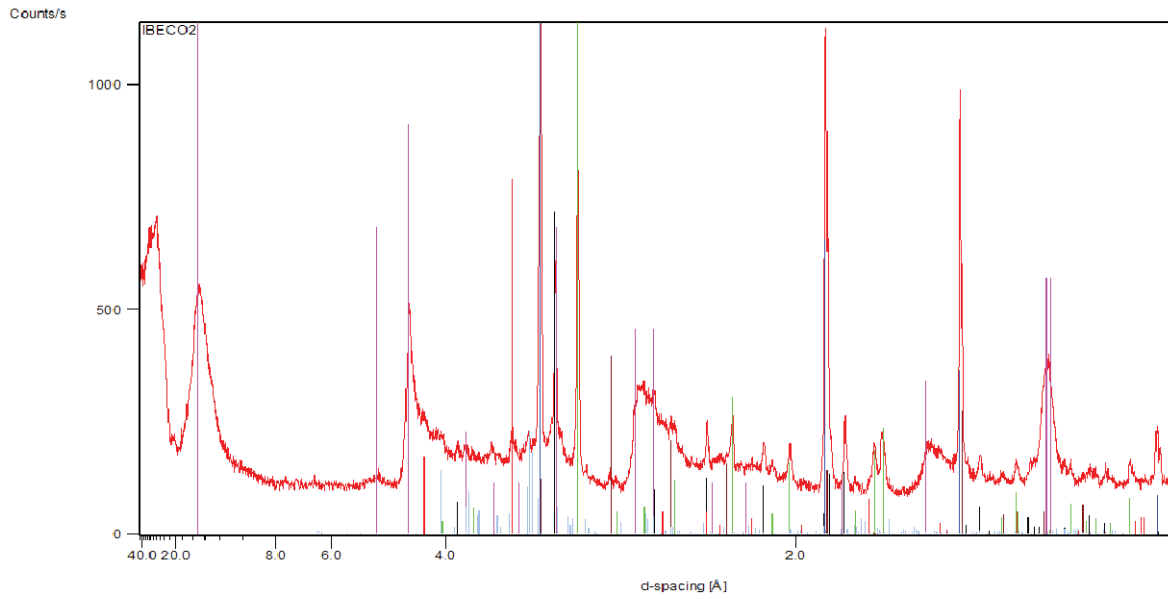


Peak List
04-005-9699: Silicon, syn: Si
00-005-0490: Quartz, low: SiO ₂
00-002-0037: Montmorillonite [Al ₃ Si ₂ O ₆ (OH) ₂]
04-011-6768: albite high, K _{0.22} Na _{0.78} Al ₁ Si ₃ O ₈

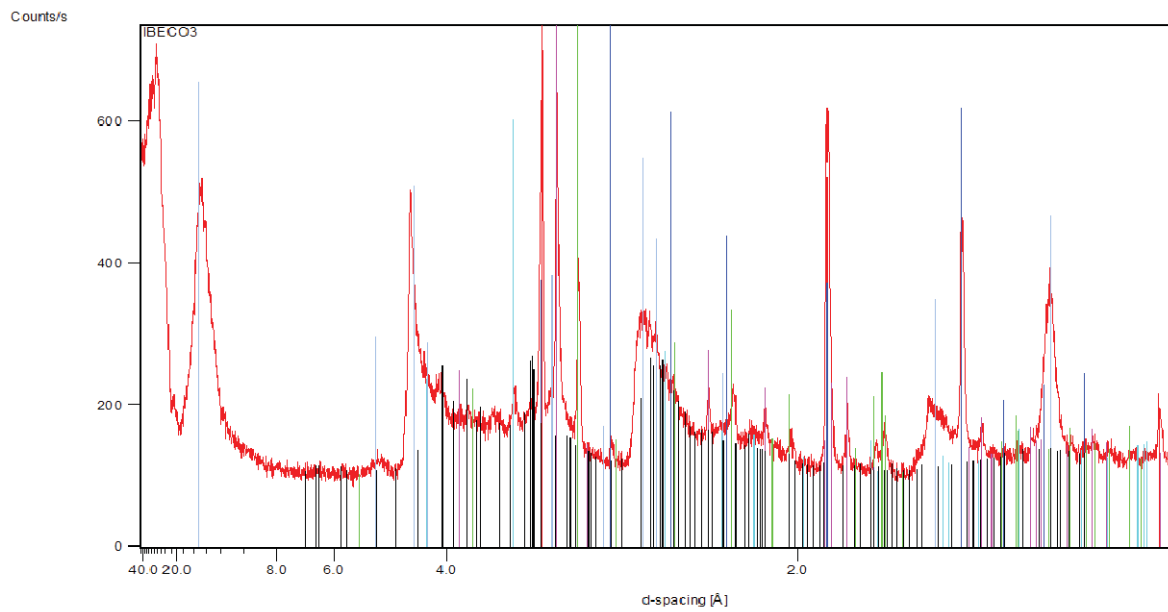


04-011-9828: Dolomite, Ca ₁ Mg _{0.92} (C ₂ O ₄) ₂
01-082-0577: Calcite, Ca(CO ₃)
01-070-3756: Quartz, SiO ₂
04-001-7247: Silicon, syn: Si
00-014-0135: Montmorillonite-15A, Ca _{0.2} (Al, Mg) ₂ Si ₄ O ₁₀ (OH) ₂ ·4H ₂ O
00-020-0528: Anorthite, CaAl ₂ (OH)F ₂ (Al ₁ Si ₂ Si ₂ O ₈)
00-042-1340: Pyrite, FeS ₂
00-002-0050: Ilite, 2K ₂ O·3MgO·4H ₂ O·24SiO ₂ ·12H ₂ O

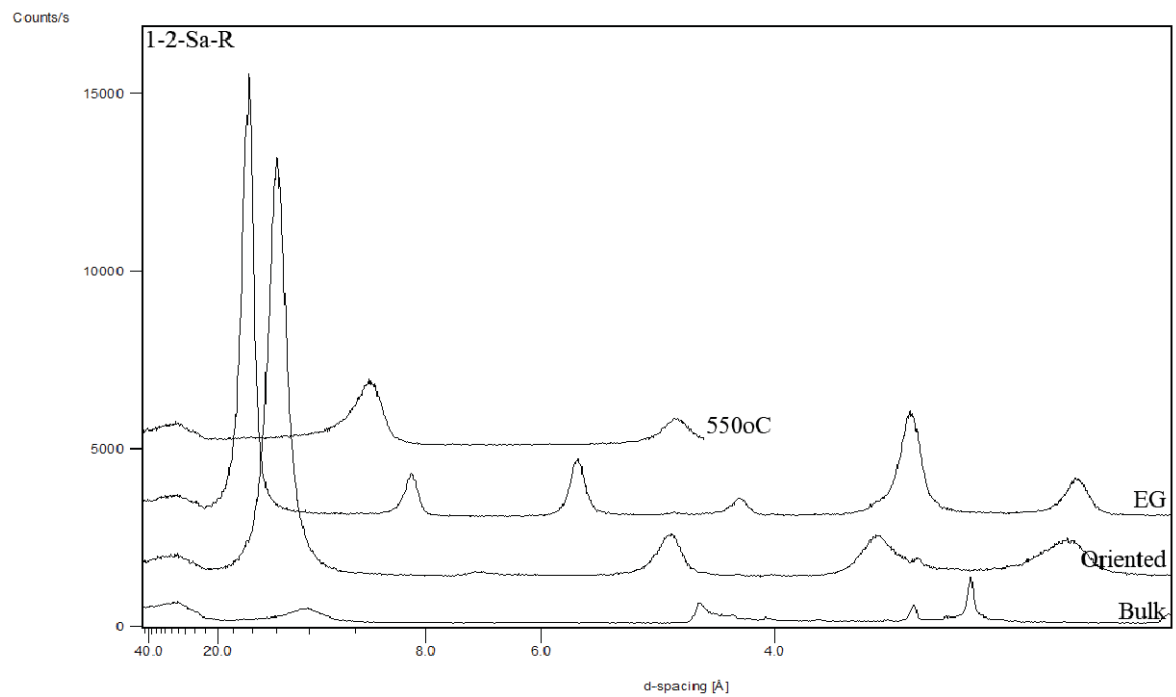
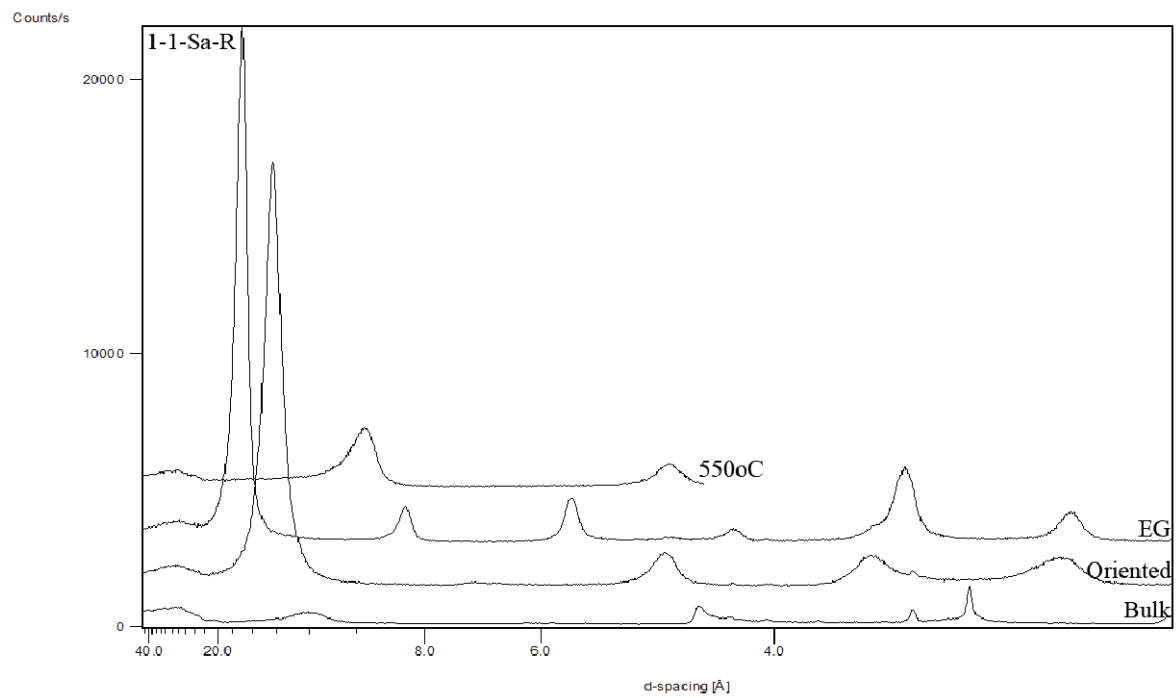
XRD patterns of randomly oriented bulk samples and identified minerals.



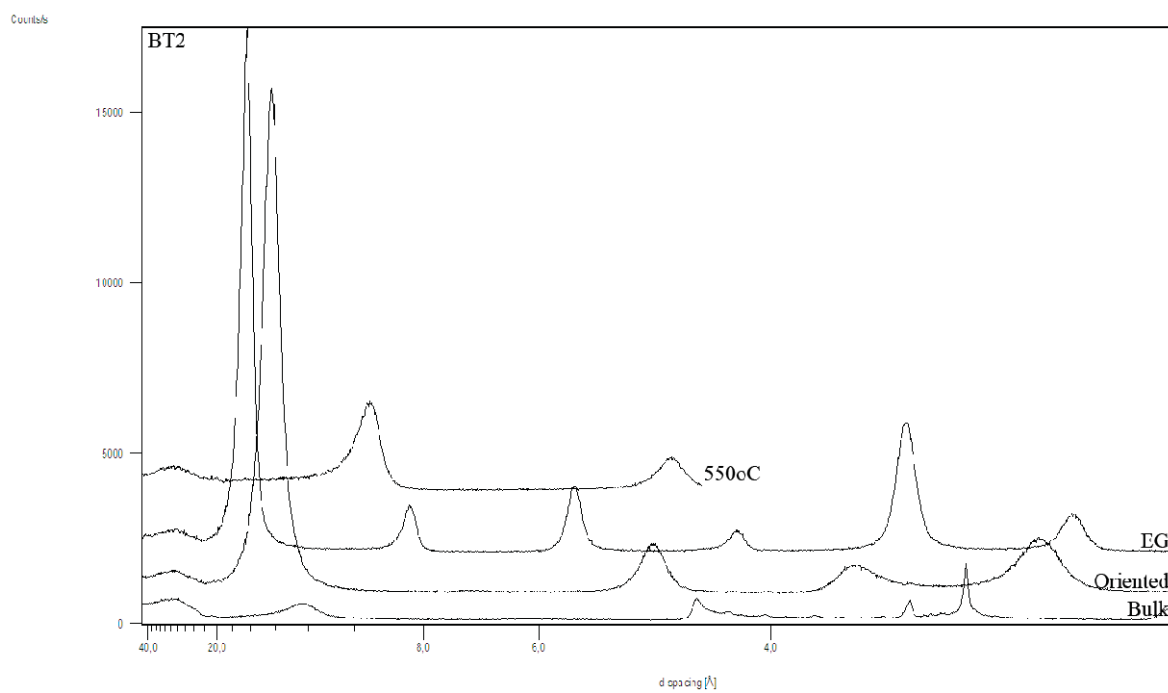
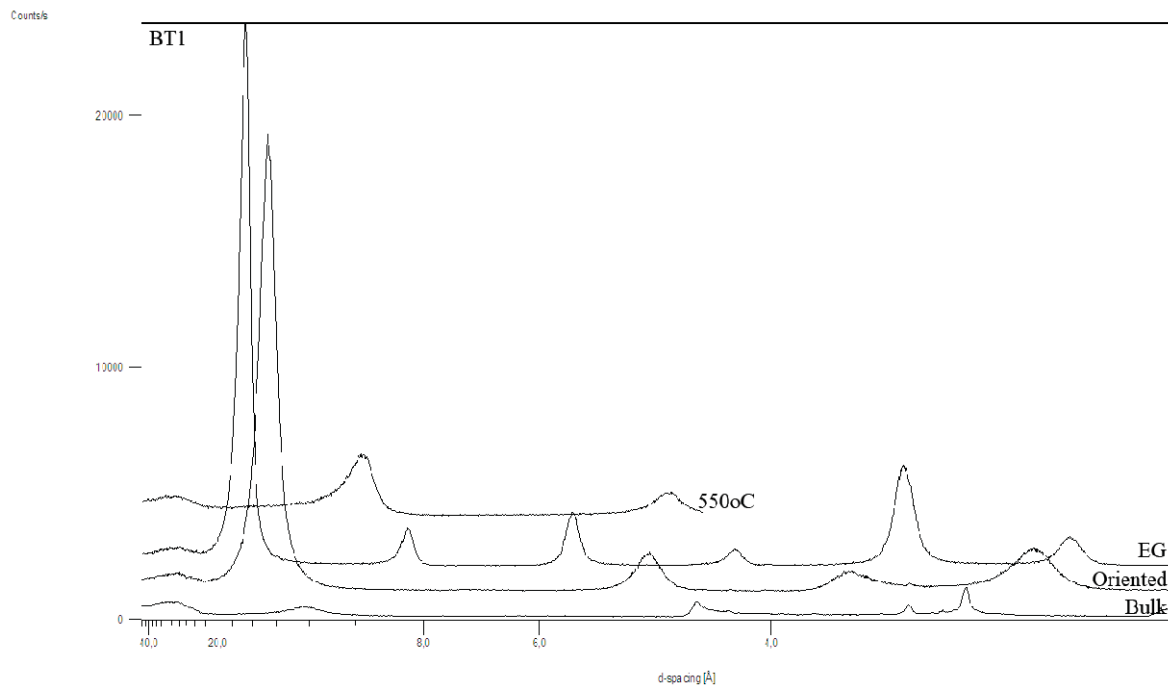
01-070-5680	Silicon, syn. Si
01-083-0577	Calcite, Ca (C O3)
01-083-1530	Dolomite, Ca Mg (C O3)2
00-013-0135	Montmorillonite-15A, Ca0.2 (Al, Mg)2 Si4 O10 (OH)2 · 4H2O
01-070-3750	Quartz, Si O2
00-042-1340	Pyrite, Fe S2
04-007-9875	Anorthite, sodium, Na0.4 Ca0.6 Al1.6 Si2.4 O8

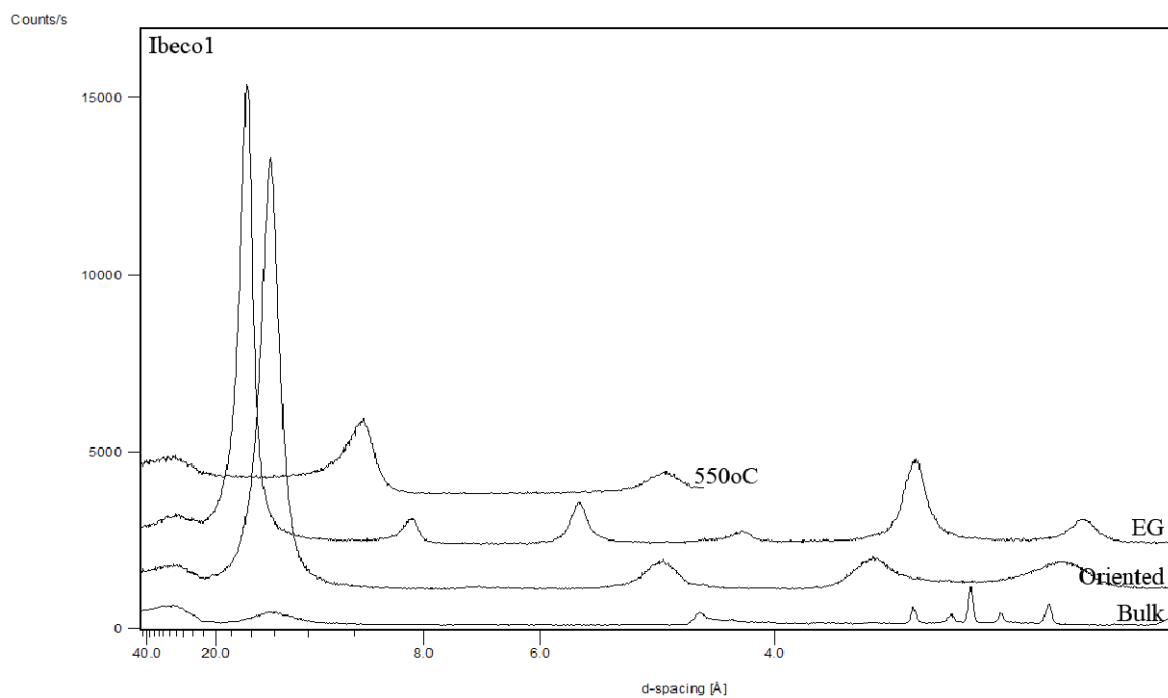
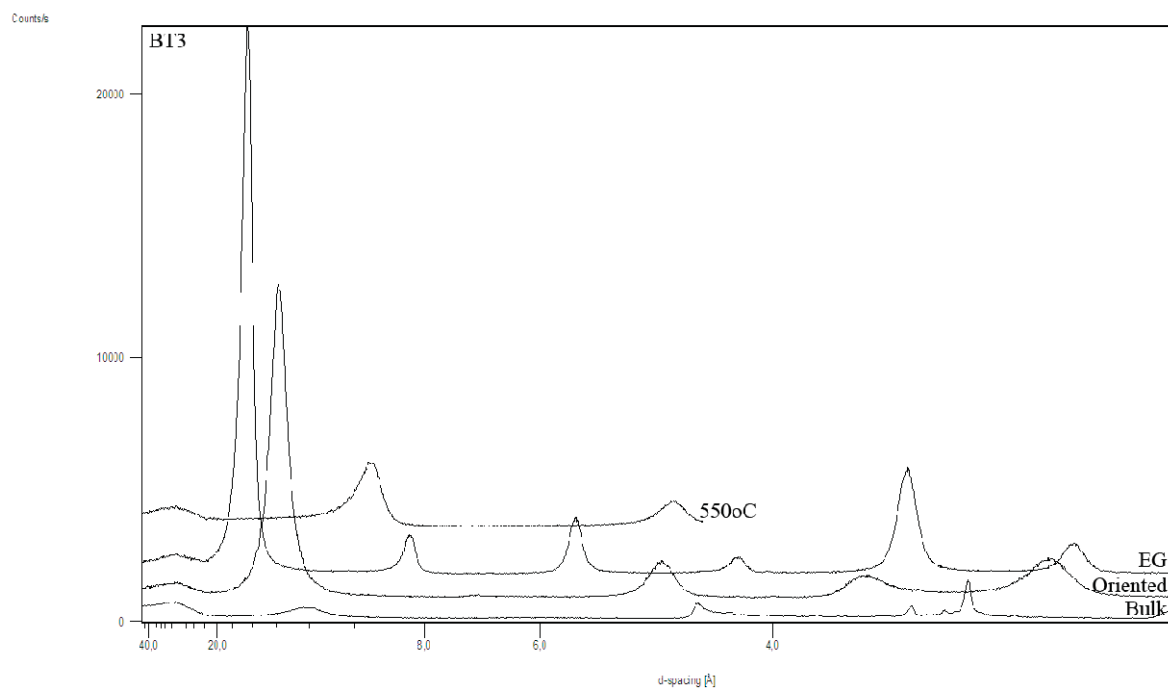


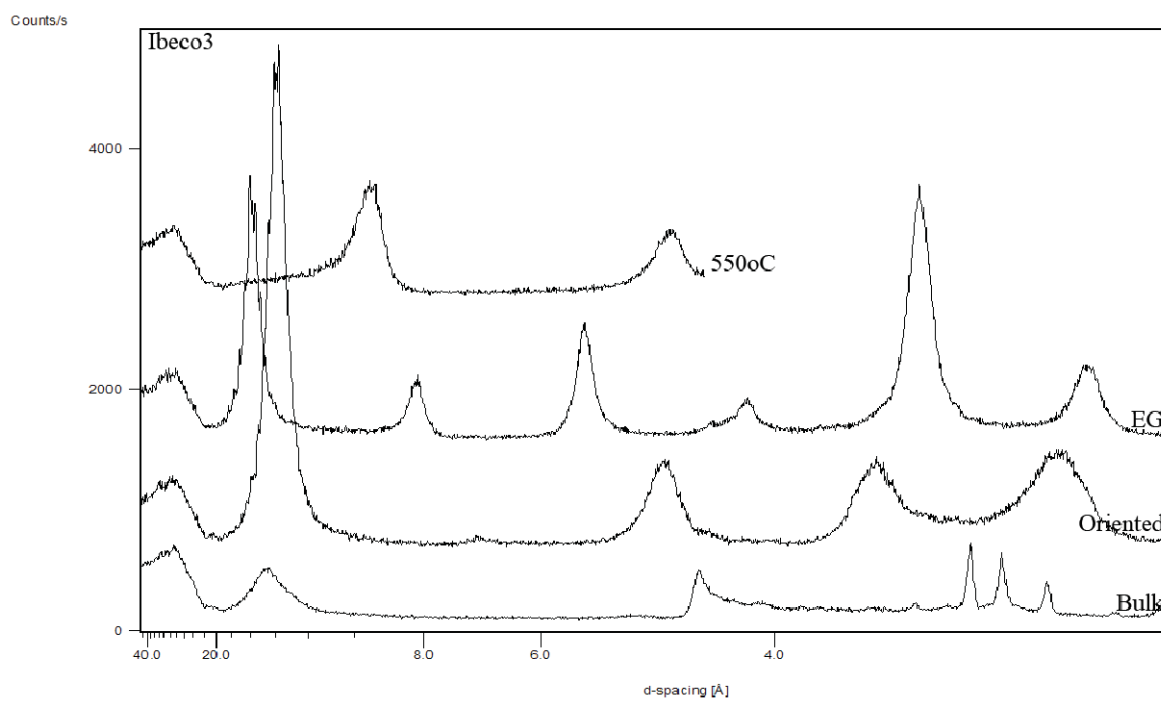
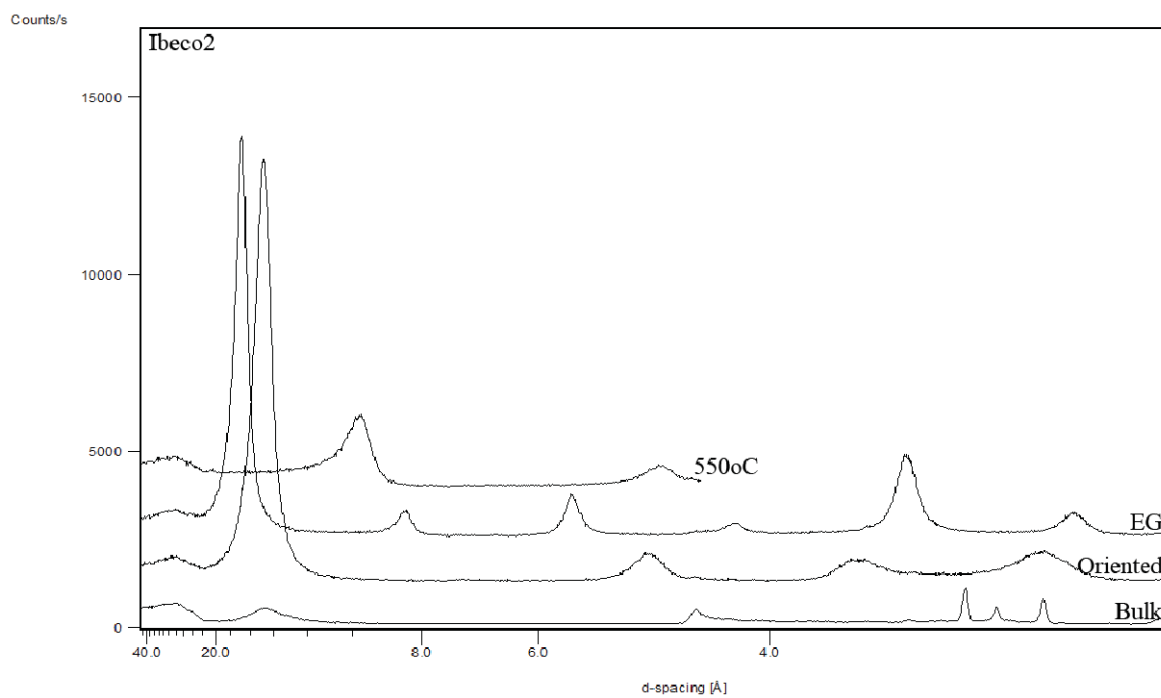
01-070-5680	Silicon, syn. Si
04-011-9828	Dolomite, Ca1.08 Mg0.92 (C O3)2
01-070-1906	Quartz, syn. Si O2
04-007-4388	calcite, Ca (C O3)
00-005-0010	Montmorillonite, (Na, Ca)0.3 (Al, Mg)2 Si4 O10 (OH)2 · xH2O
00-042-1340	Pyrite, Fe S2
00-021-0528	Anorthite, schmalzschneider, (Ca1.14 Na) Al1.8 Si2.8 O8

Compilation of XRD patterns (bulk, oriented, EG treated, heated).

Compilation of XRD patterns (bulk, oriented, EG treated, heated).



Compilation of XRD patterns (bulk, oriented, EG treated, heated).

Compilation of XRD patterns (bulk, oriented, EG treated, heated).

Basic and further quality control type analyses of two backfill materials (B+Tech memo 5.7.2010).

Author Leena Kiviranta	Reviewed by Timothy Schatz	Approved by Jorma Autio
date 08.01.2010	date 05.07.2010	date 08.01.2010

BASIC AND FURTHER QUALITY CONTROL TYPE ANALYSES OF TWO BACKFILL MATERIALS

1 BASIC ACCEPTANCE TESTING

Basic acceptance testing was performed on material batches (approximately 1.5 kg each), which were received at B+Tech on 3.11.2009 (batch 1 of both AC200 and Friedland clay, B+Tech-codes: Mi0010s1 and Fr0003s1). Basic acceptance testing was performed on these material batches. Water ratio was also measured for the second batches, which were received on 10.11.2009 (batch 2 of both AC200 and Friedland clay). The results of basic testing are presented in Table 1 and Figure 1. All presented values in Table 1 are average values of 2-3 measurements, except liquid limit, which is interpolated from a linear fit to measurement data. All measurements were performed according to B+Tech standard operating procedures (SOPs).

Table 1. Results of basic acceptance testing of backfill-materials AC200 and Friedland clay.

Measurement	Method	AC200	Friedland clay
Water ratio (batch 1)	Oven drying 105°C 24h	9.9 %	6.8 %
Water ratio (batch 2)	Oven drying 105°C 24h	9.9 %	10.3 %
CEC (batch 1)	Cu(II)-triethylenetetramine-exchange	0.99 meq/g	0.32 meq/g
Liquid limit (batch 1)	Fall-cone	709 %	77 %
Swelling index (batch 1)	Based on ASTM D 5890-06	30.3 ml/2 g	4.0 ml/2 g

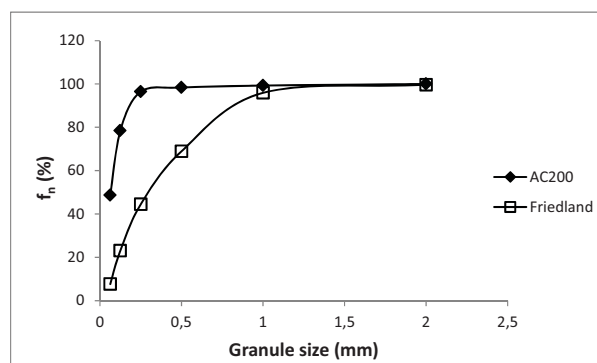


Figure 1. Plot of granule size vs. percent passing for AC200 and Friedland clay. Determined by dry sieving.

2 FURTHER QUALITY ASSURANCE TESTING

Grain density and XRD-measurements were made for batch 1 of both materials.

2.1 Grain Density

Grain density measurements were performed according to B+Tech standard operating procedures (SOPs). The measured grain densities are presented in Table 2. The presented values are mean values of three measurements.

Table 2. Grain densities of backfill materials.

Material	Grain density (g/cm ³)	Standard deviation (g/cm ³)
AC200 (batch1)	2.781	0.039
Friedland clay (batch 1)	2.832	0.001

2.2 XRD-measurements

XRD-bulk sample preparations, XRD-measurements and mineral identifications were provided by the Geological Survey of Finland.

2.2.1 XRD-Analysis of bulk samples

Randomly oriented bulk samples were prepared by grinding a small amount of bulk material in agate mortar with pestle to a particle size < 10 µm. Approximately 10 mg of ground clay was mixed with acetone on a glass slide. Samples were scanned with Philips X'Pert MPD diffractometer equipped with Cu anode tube and monochromator, a variable divergence slit, using wavelength of $K\alpha_1 = 1.54060$; $K\alpha_2 = 1.54443$; and $K\beta = 1.39225$; voltage of 40kV and current of 55 mA, from 2 to 70° 2θ with 0.02° counting steps and 1 s/step counting time at the Geological Survey of Finland.

XRD-patterns of bulk samples are presented in Figures 2 and 3 and in Appendix 1, which also includes a list of identified minerals.

Diocahedral and trioctahedral clay minerals were identified using positioning of d(060) reflections (Brindley & Brown 1980). The position of d(060) line for AC200 was at 1,497 Å (Table 3) indicating the presence of dioctahedral smectite, such as montmorillonite. For Friedland clay the position of d(060)-lines was at 1,501 and at 1,542 Å. The possible presence of trioctahedral clay minerals in Friedland clays can't be discounted, due to strong reflection of quartz at the same d-value (1.542 Å).

2.2.2 XRD-Analysis of clay fraction

Oriented mounts were prepared from purified clay fractions (< 2 µm fraction of the material) that had been converted to Mg-forms. The filter-membrane peel-off technique (Drever, 1973; Moore & Reynolds, 1989) was used for preparation of the oriented mounts. A concentrated suspension containing approximately 600 mg of purified clay in 10 mL of deionized water was vacuum filtered onto 0.45 µm pore size cellulose filter.

Sample mounts were dried in air and scanned with XRD from 2 to 35° 2 θ with 0.02° counting steps with counting time of 1s/step.

Oriented sample mounts were placed on a platform in a desiccator containing EG and put into an oven at 60°C for 20 h. Mounts were scanned immediately after solvation from 2 to 35° 2 θ with 0.02° counting steps with counting time of 1s/step.

After EG-solvation, oriented mounts were placed in a furnace for 2 h at 550°C. Mounts were scanned after heating from 2 to 20° 2 θ with 0.02° counting steps with counting time of 1s/step.

The diffraction patterns of bulk, oriented, EG-solvated and heated AC200 and Friedland clay samples are presented in Figures 2 and 3, respectively. AC200 showed a strong d(001) reflection in oriented sample at approximately 14 Å, which shifted fully to 15.6 Å after EG solvation, indicating the presence of smectite (Moore & Reynolds, 1989). The d(001) reflection of Friedland clay shifted only partly from 13.6 Å to 16.5 Å indicating the presence of mixed-layer smectite-illite (Moore & Reynolds, 1989). After heating at 550°C, the d(001) line in both samples collapsed to 9.8 Å (Figures 2 and 3, Table 3). Based on this behavior, it can be concluded that the swelling clay mineral in both materials is smectite (Moore & Reynolds, 1989).

Friedland clay sample showed a peak at 7 Å, which disappeared after heating in 550°C indicating the presence of kaolin minerals (Figure 3) (Moore & Reynolds 1989).

The peak angle difference of the composite peaks at 10 °2 θ and at ~15-16 °2 θ in EG-solvated samples was used to determine the percentage of illite layers in illite/smectite mixed-layer minerals for AC200 and Friedland clay (Moore & Reynolds, 1989) (Table 3). For Friedland clay, the illite content in mixed-layers was also estimated by using the 002/003 peak position because of the peak interferences at 001/002. With both methods the result was over 100 %, which can be considered indicative of the material containing a relatively large amount of illite.

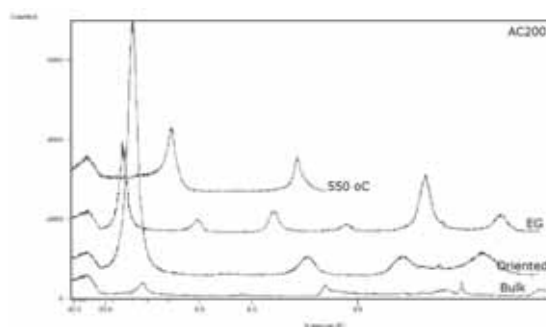


Figure 2. X-ray diffraction patterns of AC200. From bottom to top: randomly oriented bulk sample, oriented clay fraction, ethylene glycol (EG) solvated oriented and heated (550 °C) mounts.

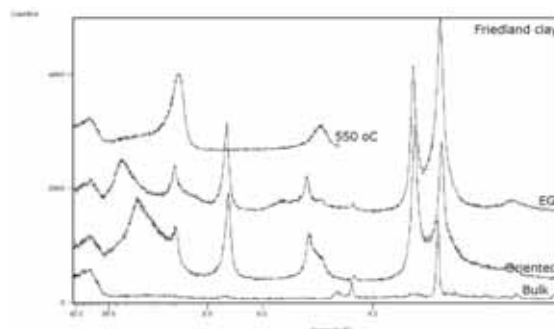


Figure 3. X-ray diffraction patterns of Friedland clay. From bottom to top: randomly oriented bulk sample, oriented clay fraction, ethylene glycol (EG) solvated oriented and heated (550 °C) mounts.

Table 3. Position of important lines (in Å) used in identification of illite/smectite (I/S). The amount of illite (I) interlayers in I/S was calculated based on Moore and Reynolds (1989). The illite content for Friedland clay is not reliable.

Fraction	Bulk		Clay					Identified clay minerals and impurities	
	Treatment		Oriented	EG			550°C		
Line/interpretation	d(060)	Dioc./Trioc.	d(001)	d(001)	d(002)	d(003)	I % in I/S	d(001)	
AC200	1.497	Dioc.	13.95	15.63	8.12	5.42	8	9.77	I/S
Friedland clay	1.501; 1.542	Dioc.(+ Trioc.?)	13.62	16.54	9.96	4.99	>100	9.75	I/S, K

Abbreviations: I/S=illite/smectite, K=kaolin

2.2.3 Mineralogical composition

Table 4. Mineralogical composition determined with Rietveld-method for Friedland clay and with RIR-method for AC200. The results are mean values from analyses of three diffractograms.

Mineral	AC200 (RIR)	Friedland clay (Rietveld)
Montmorillonite (smectite)	77	33.2
Illite		31.1
Kaolin		7.9
Calcite	8	0.1
Muscovite		5.0
Dolomite	1	
Quartz	4	14.9
Siderite		2.0
Gypsum		0.2
Goethite		0.2
Pyrite	5	1.7
Albite	5	1.5
Orthoclase		1.4
Rutile		0.6

The total mineralogical composition of the studied materials is presented in Table 4. For Friedland clay, the results are average values of Rietveld quantifications of three diffractograms. The variation in mineralogical composition results are presented in Appendix 2. The same mineral phases as Karnland et al. (2006) used, were utilized in these calculations. For AC200, the results are average values of RIR (Relative Intensity Ratio) determinations of three diffractograms.

3 CONCLUSIONS

The results are typical for the materials studied. The Rietveld analysis wasn't performed for AC200, but previous results for same material type can be found in Kumpulainen & Kiviranta (2010). The RIR-method provides only the amounts of minerals, which can be identified explicitly with XRD, i.e. the indicative peak of minerals must be distinct and interference with other peaks should not occur. Hence, for example illite was not identified in AC200 with RIR-method, even though it was detected previously with Rietveld-method (Kumpulainen & Kiviranta, 2010). In addition, the amount of illite in illite/smectite mixed-layers determined using the Moore & Reynolds (1989) method indicate, that AC200 contains a small amount of illite (Table 3).

4 REFERENCES

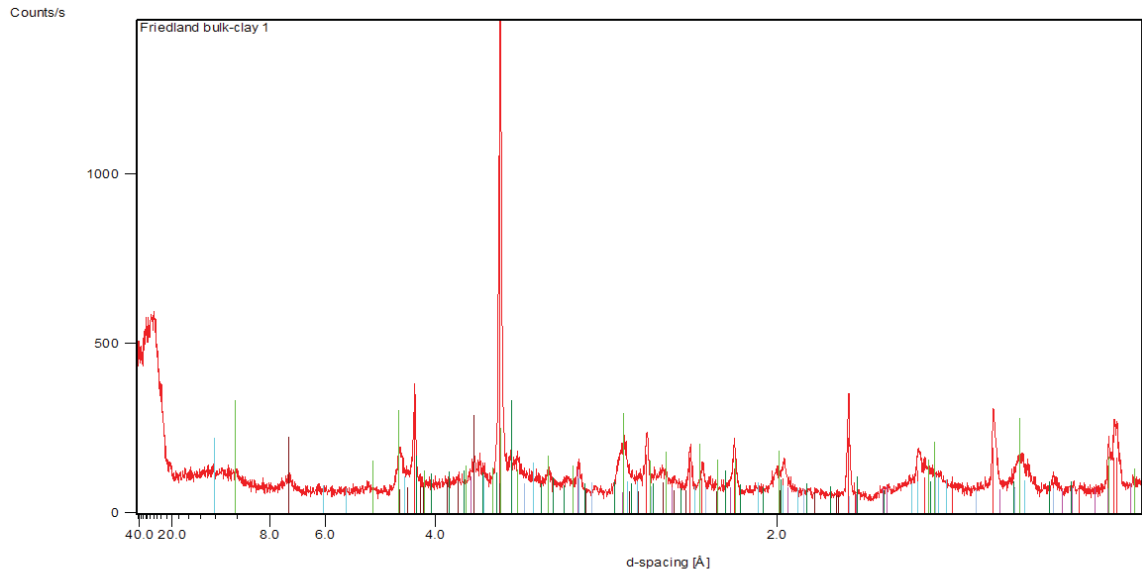
- Brindley G.W., Brown G. (Eds.) 1980. Crystal structures of clay minerals and their x-ray identification. Mineralogical Society, Monograph 5. 495p.
- Drever J.I. 1973. The preparation of oriented clay mineral specimen for x-ray diffraction analysis by a filter-membrane peel technique. *American Mineralogist* 58, 553-554.
- Moore D.M., Reynolds R.C. 1989. X-ray diffraction and the identification and analysis of clay minerals. Oxford University Press, Inc.
- Karnland O., Olsson S., Nilsson U. 2006. Mineralogy and sealing properties of various bentonites and smectite-rich clay materials. SKB TR-06-30. Swedish Nuclear Fuel and Waste Management Company (SKB), Stockholm, Sweden.
- Kumpulainen S., Kiviranta L. 2010. Mineralogical and chemical characterization of various bentonite and smectite-rich clay materials. Posiva WR-2010-xx. (in press)

5 LIST OF APPENDICES

- Appendix 1.** X-ray diffraction patterns of randomly oriented bulk fractions
- Appendix 2.** Variations in mineralogical compositions determined from three diffractograms using Rietveld refinement for Friedland clay and RIR-method for AC200.

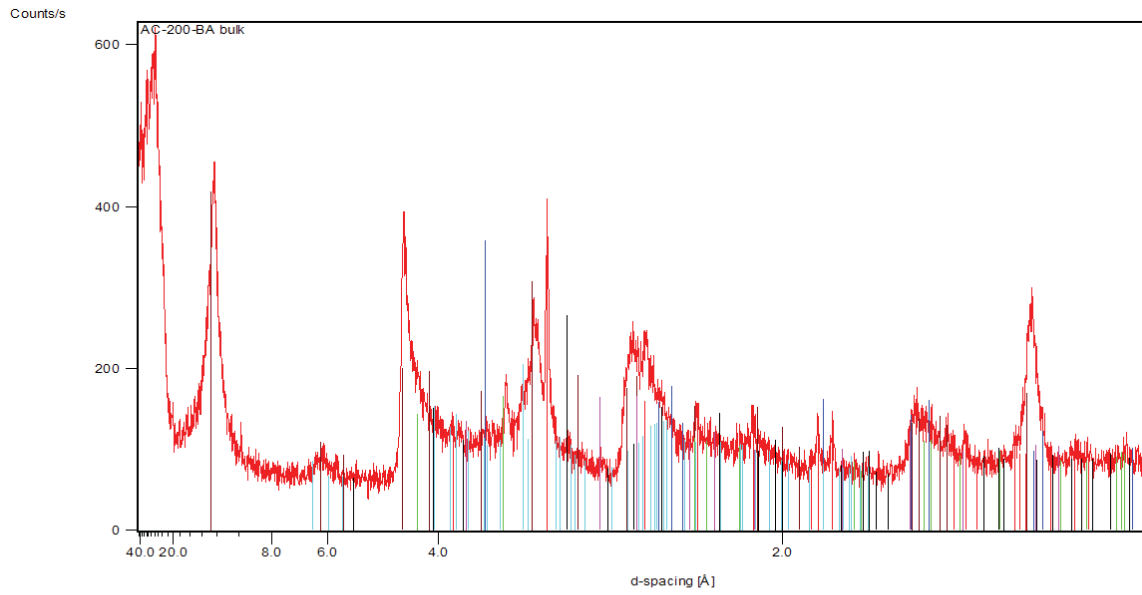
Appendix 1: X-ray diffraction patterns of randomly oriented bulk fractions.

Friedland clay



Peak List
01-070-7345: Quartz, SiO ₂
00-058-2028: Kaolinite, Al ₂ Si ₂ O ₅ (OH) ₄
00-002-0050: Illite, 2 K ₂ O · 3 MgO · Al ₂ O ₃ · 24 SiO ₂ · 12 H ₂ O
00-058-2010: Montmorillonite, Na _{0.3} (Al, Mg) ₂ Si ₄ O ₁₀ (OH) ₂ · x H ₂ O
00-029-0696: Siderite, FeCO ₃
00-042-1340: Pyrite, FeS ₂
00-003-0471: Microcline, K ₂ O · Al ₂ O ₃ · 6 SiO ₂

AC200



Peak List
01-072-4582: Calcite, Ca(CO ₃)
00-058-2010: Montmorillonite, Na _{0.3} (Al, Mg) ₂ Si ₄ O ₁₀ (OH) ₂ · x H ₂ O
00-021-1972: Anataase, syn. TiO ₂
00-005-0490: Quartz, low SiO ₂
00-009-0466: Albite, ordered, NaAlSi ₃ O ₈
00-024-0172: Hematite, Fe ₂ O ₃
01-071-4892: Dolomite, CaMg(CO ₃) ₂

Appendix 2. Variations in mineralogical compositions determined from three diffractograms using Rietveld refinement for Friedland clay and RIR-method for AC200.

Table 1.

Mineral	AC200 1	AC200 2	AC200 3	AC200 average
Montmorillonite (smectite)	83	75	74	77
Calcite	6	7	10	8
Dolomite	1	1	1	1
Quartz	2	7	2	4
Pyrite	3	5	7	5
Albite	5	5	6	5

Table 2.

Mineral	Friedland clay 1	Friedland clay 2	Friedland clay 3	Friedland clay average
Montmorillonite (smectite)	29.7	38	32	33.2
Illite	33.1	33.3	27	31.1
Kaolin	8.4	7	8.2	7.9
Calcite	0.2	0.1	0.1	0.1
Muscovite	5.5	3.5	6	5.0
Quartz	15	11.2	18.6	14.9
Siderite	2.3	1.4	2.3	2.0
Gypsum	0.4	0	0.3	0.2
Goethite	0.3	0	0.2	0.2
Pyrite	1.1	3.2	0.8	1.7
Albite	1.5	0.9	2	1.5
Orthoclase	1.6	0.6	2	1.4
Rutile	0.6	0.6	0.5	0.6
Anatase	0.1	0	0	0
Lepidocrocite	0.1	0	0	0

Characterization analyses of backfill materials (B+Tech memo 18.3.2011)

Author Leena Kiviranta, Sirpa Kumpulainen	Reviewed by Timothy Schatz	Approved by Jorma Autio
date 18.3.2011	date 28.4.2011	date 9.5.2011

CHARACTERIZATION ANALYSES OF BACKFILL MATERIALS**1 BASIC ACCEPTANCE TESTING**

Basic acceptance testing was performed on material batches (approximately 2.5 kg each), which were received at B+Tech on 23.9.2010. The received material and analyses performed are presented in Table 1.

Table 1. Analysed materials.

Received material	Sample code (other name used in this report)	Measurements
AC200	Be-Mi-NaA-BT0012-Po-R (AC200)	Water ratio, CEC, granule size distribution, swelling index, liquid limit, bulk XRD & quantification
FC1	CL-Fr—BT0004-Sa-R (Friedland clay)	Water ratio, CEC, granule size distribution, swelling index, liquid limit, bulk XRD & quantification
Granule size 2	CL-Fr—BT0005-Cr-R	granule size distribution
Granule size 3	CL-Fr—BT0006-Sa-R	granule size distribution

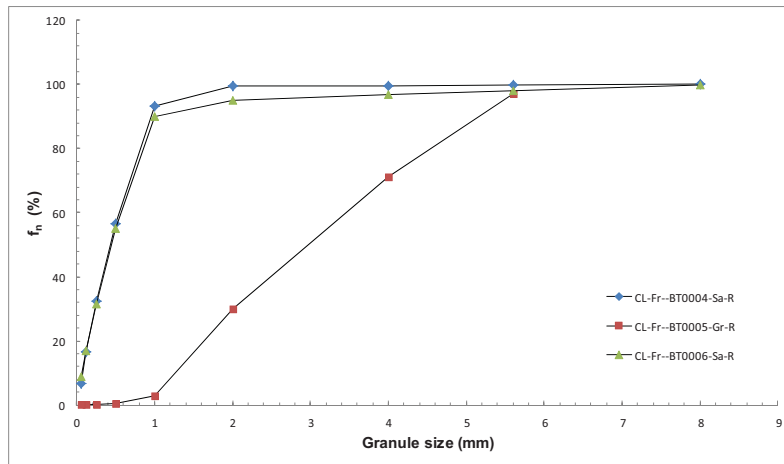
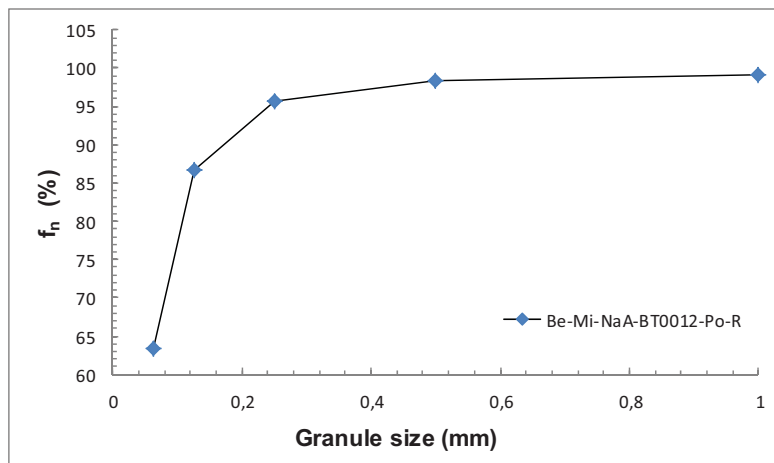
The results of basic testing are presented in Tables 2 and 3 and in Figures 1 and 2. All presented values in Table 2 are average values of 2-3 measurements, except liquid limit, which is interpolated from a linear fit to measurement data. All measurements were performed according to B+Tech standard operating procedures (SOPs).

Table 2. Results of basic acceptance testing of backfill-materials AC200 and Friedland clay.

Measurement	Method	AC200	Friedland clay
Water ratio	Oven drying 105°C 24h	10.5 %	6.1 %
CEC	Cu(II)-triethylenetetramine-exchange	0.99 meq/g	0.31 meq/g
Liquid limit	Fall-cone	623%	84 %
Swelling index	Based on ASTM D 5890-06	27 ml/2g of dry material	4 ml/2g of dry material

Table 3. Cumulative granule size distributions (mass %) for all materials.

Granule size (mm)	f_n (CL-Fr--BT0004-Sa-R)	f_n (CL-Fr--BT0005-Gr-R)	f_n (CL-Fr--BT0006-Sa-R)	f_n (Be-Mi-NaA-BT0012-Po-R)
8.000	100.1	-	99.7	-
5.600	99.8	97.2	97.9	-
4.000	99.7	71.3	96.8	-
2.000	99.4	30.0	95.1	-
1.000	93.1	2.8	89.9	99.0
0.500	56.5	0.6	55.1	98.3
0.250	32.5	0.3	31.4	95.7
0.125	16.6	0.3	16.9	86.7
0.063	6.8	0.1	8.8	63.3

**Figure 1.** Plot of granule size vs. percent passing (f_n) for Friedland clay samples. Determined by dry sieving.**Figure 2.** Plot of granule size vs. percent passing (f_n) for AC200. Determined by dry sieving.

2 FURTHER QUALITY ASSURANCE TESTING

2.1 XRD-measurements

XRD-bulk sample preparations and XRD-measurements were provided by the Geological Survey of Finland.

2.1.1 XRD-Analysis of bulk samples

Randomly oriented bulk samples were prepared by grinding a small amount of bulk material in agate mortar with pestle to a particle size $< 10 \mu\text{m}$. Approximately 10 mg of ground clay was mixed with acetone on a glass slide. Samples were scanned with Philips X'Pert MPD diffractometer equipped with Cu anode tube and monochromator, a variable divergence slit, using wavelength of $K\alpha_1 = 1.54060$; $K\alpha_2 = 1.54443$; and $K\beta = 1.39225$; voltage of 40kV and current of 55 mA, from 2 to $70^\circ 2\theta$ with 0.02° counting steps and 1 s/step counting time at the Geological Survey of Finland.

The XRD-patterns that were used to identify the minerals are shown in Figures 3-4 and minerals listed Table 4. Identified minerals were used as starting parameters for quantification.

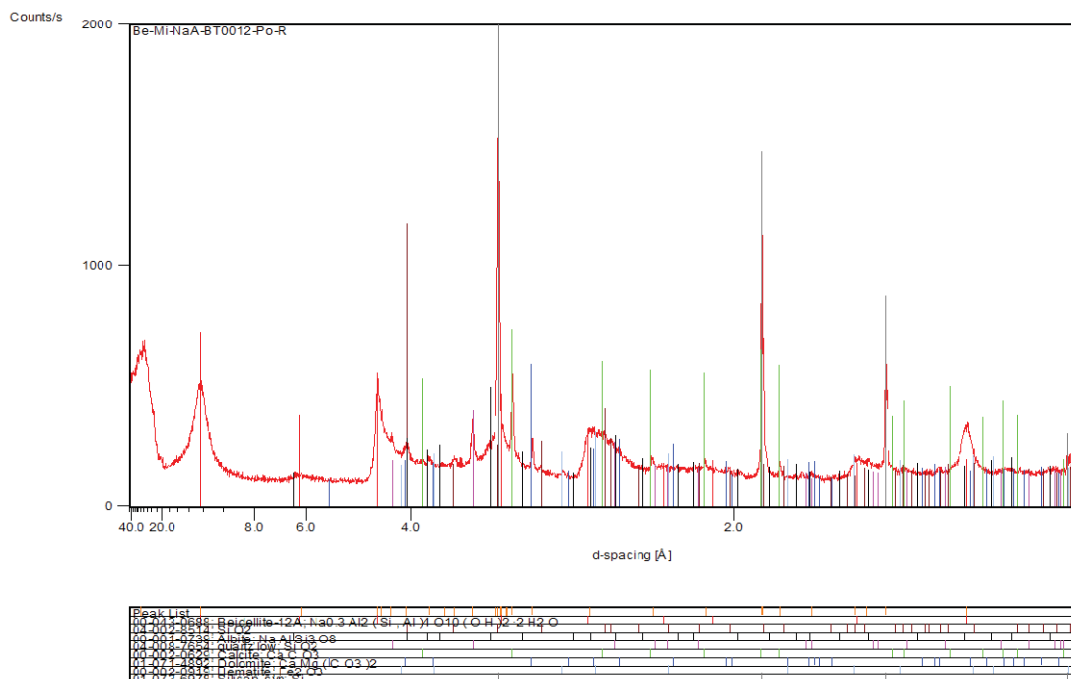


Figure 3. XRD-pattern of bulk AC-200.

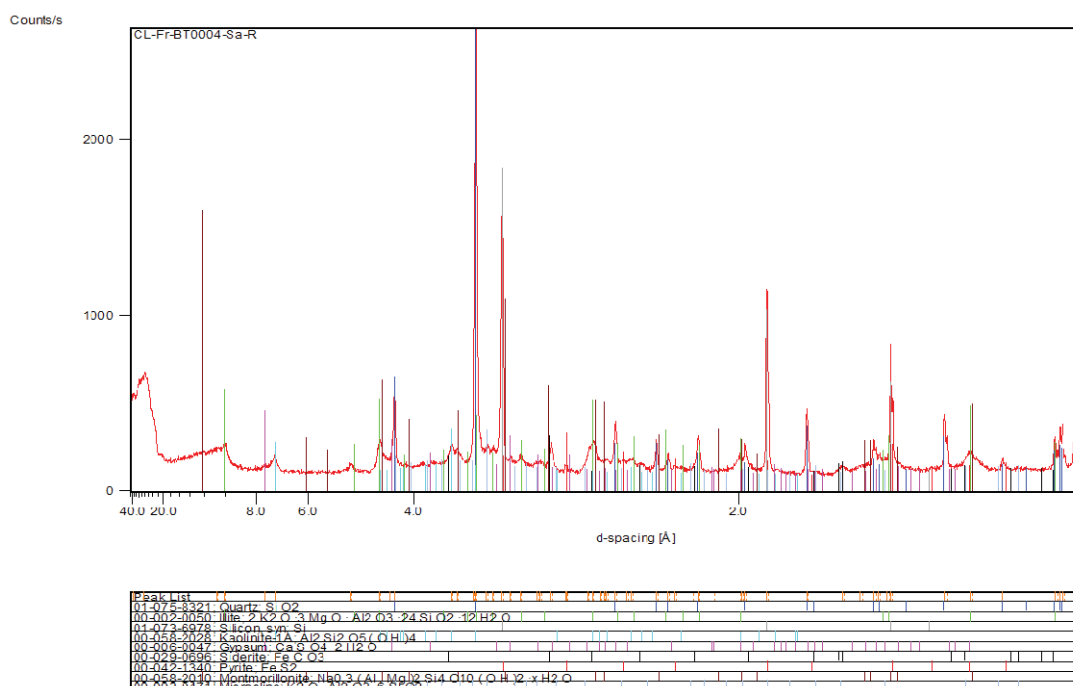


Figure 4. XRD-pattern of bulk Friedland clay.

2.1.2 Mineralogical composition

Mineralogical composition was determined using Rietveld analysis with Siroquant program. First, variable divergence slit data was converted to fixed divergence slit and background was subtracted. Instrument zero, scales, unit cell parameters, orientation and half-width parameters were refined. The results are shown in Tables 4 and 5. As no chemical analysis data was available, the quantification results could not be validated, and thus include large uncertainties. To calculate normative chemical composition, montmorillonite compositions of similar samples from Kumpulainen and Kiviranta (2010) were used.

Table 4. Mineralogical composition (wt.%) determined with Siroquant.

	CL-Fr--BT0004-Sa-R	Be-Mi-NaA-BT0012-Po-R
Smectite	31.7	93.8
Illite	26.2	
Kaolin	9.2	
Quartz	27.9	1.2
Plagioclase		1.0
K-feldspar	0.7	
Calcite		1.6
Dolomite		1.3
Siderite	2.1	
Gypsum	2.3	
Pyrite	0	
Hematite		1.1

Table 5. Calculated chemical composition based on mineralogical composition.

	CL-Fr--BT0004-Sa-R	Be-Mi-NaA-BT0012-Po-R
Na ₂ O	0.26	0.85
MgO	2.39	5.24
CaO	0.85	3.88
Fe ₂ O ₃	3.00	5.72
Al ₂ O ₃	18.25	18.40
SiO ₂	68.32	60.16
H ₂ O	3.45	4.43
CO ₂	0.80	1.32
K ₂ O	2.68	0
SO ₃	0	
TiO ₂		

3 CONCLUSIONS

The results are typical for the materials studied (Kiviranta, 2010). Because chemical composition data was not available, the quantification results could not be validated, and thus include uncertainties.

4 REFERENCES

Kiviranta L. 2010. Basic and further quality control type analyses of two backfill materials. B+Tech Memo (5.7.2010).

Kumpulainen S., Kiviranta L. 2010. Mineralogical and chemical characterization of various bentonite and smectite-rich clay materials. Posiva WR 2010-52. Posiva Oy, Olkiluoto, Finland.

Composition and properties of Milos B, Milos granules and Milos pellets (B+Tech memo 2.11.2011)

Author Sirpa Kumpulainen Leena Kiviranta	Reviewed by Petri Korkeakoski	Approved by Managing director Jorma Autio
date 2.11.2011	date 7.11.2011	date 11.11.2011

COMPOSITION AND PROPERTIES OF MILOS B, MILOS GRANULES AND MILOS PELLETS

1 BACKGROUND INFORMATION

This memo describes the initial composition and properties of Milos B, Milos pellet and Milos granule materials (Figure 1). The work was done as a part of the subproject 166 'Quality control of materials'. The characterization of materials was done in order to define the composition, physical properties and initial state of the backfill for the backfill production line report.

1.1 Origin of materials

In the eastern part of island of Milos in Greece, tertiary Ca-rich bentonite deposits occur. They are thought to form through hydrothermal alteration of pyroclastic tuffs and lavas of andesitic and rhyolitic composition (Christidis et al., 1995). Bentonite deposits are occasionally more than 30 m thick and form irregular bodies in pyroclastics (Christidis & Dunham, 1993). Largest bentonite producer in Milos is S&B Industrial Minerals SA, with annual production of 0.9 Mt. In addition, there are other much smaller producers of Milos bentonite, among those Süd-Chemie, Geohellas, Greek Mining of Milos (subsidiary of Ingenieurburo für Bentonit-Technologie (IBO)) (Roskill, 2008).

1.2 Description of materials

The studied materials, i.e., Milos B, Cebogel pellets and Minelco granules (Figure 1) are all initially Milos bentonite.

Milos B is a working name (used by SKB and Posiva) for medium grade Milos bentonite that is sold also under the name IBECO RWC BF by S&B Industrial Minerals SA.

Cebogel pellets are high grade sodium activated calcium bentonite, mined from Milos, Greece, further processed and compressed in Netherlands or UK by CEBO, a subsidiary of S&B Industrial Minerals SA.

Minelco granules are high grade sodium activated calcium bentonite, excavated by S&B Industrial Minerals in Milos, which are processed, pelletized, and sold by Minelco, a subsidiary of Swedish iron ore and industrial minerals producing LKAB in Luleå, Sweden. According to Dixon et al. (2008), possibly lesser amounts of soda ash have been used to activate the Minelco granules than what have been used for Cebogel material.



Figure 1. Photos of Milos granules, Milos pellets and Milos B from left to right.

2 BASIC TESTS

Water ratio was determined gravimetrically after heating the sample at 105°C for 24h. The swelling index was determined as a volume of swelled material (ml/2g) after period of 24h (ASTM D 5890-06). The liquid limit was determined with a fall-cone method (CEN ISO/TS 17892-12: 2004). Grain density was determined in 1 M NaCl solution (Karnland et al., 2006). The results for initial water ratio (as received), swelling index, liquid limit and grain density of studied materials are listed in Table 1.

Table 1. Water ratio, swelling index, liquid limit, and grain density of studied materials.

Sample name	Milos granules	Milos pellets	Milos B
Water ratio	13.9 %	18.8 %	17.5 %
Swelling index	22 ml/2g	27 ml/2g	13 ml/2g
Liquid limit	464 %	560 %	215 %
Grain density	2.795 g/cm ³	2.837 g/cm ³	2.79 g/cm ³

Granule size distribution of Milos granules and Milos B was determined by dry sieving (CEN ISO/TS 17892-4: 2004). The results are shown in Figure 2.

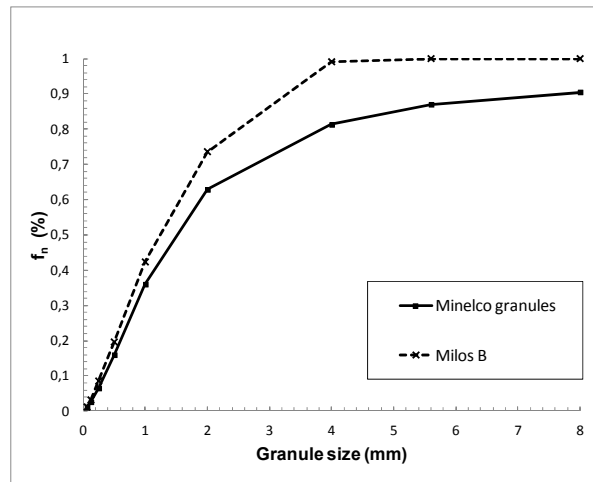


Figure 2. Granule size distribution for Milos granules and Milos B.

Bulk density of 15 Milos pellets was determined with a paraffin oil method (Karnland et al., 2006). The average bulk density was 2.065 g/cm^3 with a standard deviation of 0.037 g/cm^3 .

Dimensions (length and diameter) of individual pellets were determined. The average length was 9.4 mm and average diameter was 6.2 mm. The results are presented in Table 2 and in Figure 3. Both the lengths and diameters of pellets were smaller than the corresponding values given by manufacturer (Cebo Holland product data, 2009). Among the pellets there were also 6 % of bentonite granules, which didn't have cylindrical shape (Figure 3) and have possibly formed as a result of breaking of the pellets.

Table 2. Measured Ceboqel QSE pellet dimensions. The volumes have been calculated based on measured average, minimum and maximum lengths and diameters. The data given by Manufacturer (Cebo Holland product data, 2009) is given in brackets.

Dimension	n	Minimum	Average	Maximum
Length (mm)	346	3.29 (5.00)	9.38	19.47 (20.00)
Diameter (mm)	98	5.28	6.17 (6.50)	6.49
Volume (mm^3)		72	280	644

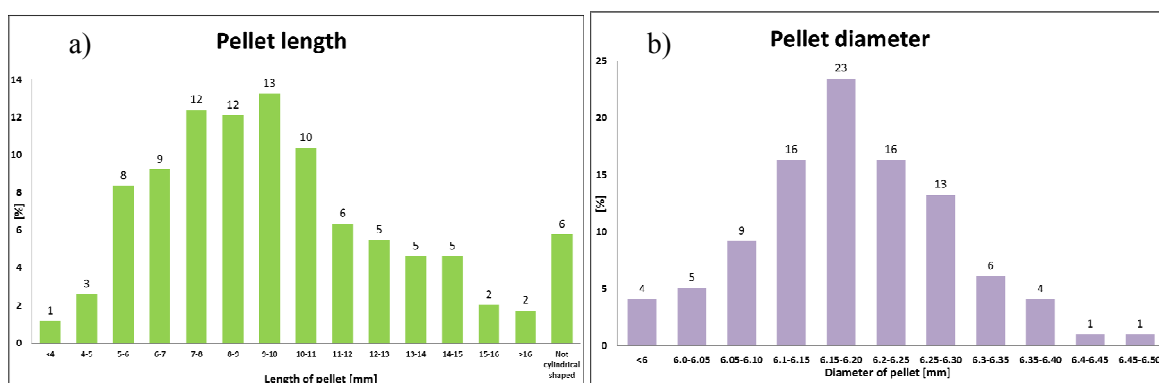


Figure 3. Measured Ceboqel QSE pellet a) length and b) diameter distribution.

3 CHEMICAL COMPOSITION

3.1 Suspension pH and EC

Studied materials were mixed with deionized water. After equilibration period (in air) for one week electric conductivity (EC) and solution pH of clay suspensions (10 g/l) were measured and the results are presented in Table 3.

Table 3. pH and electrical conductivity (EC) of clay suspensions after one week of mixing.

Material	pH	t (°C)	EC (μS/cm)
Milos granules	8.87	29.2	510
Milos pellets	8.89	27.8	675
Milos B	8.34	24.4	223

Table 3 shows that sodium activated materials (pellets and granules) had clearly higher electric conductivities (300-450 μS/cm) than non-activated Milos B. Also the pH of suspensions of activated materials were slightly higher (0.5 pH units) than pH of Milos B suspension.

3.2 Total chemical composition

Table 4. Total chemical composition. The results are in wt.% and normalized to 100 %.

Sample name	Milos granules	Milos pellets	Milos B
Oxides			
SiO ₂	51.2	51.8	44.6
Al ₂ O ₃	15.4	16.4	13.4
Fe ₂ O ₃	4.5 (5.6*)	3.6 (4.2*)	3.0 (5.1*)
FeO	1.0	0.5	1.9
TiO ₂	0.7	0.7	0.6
MgO	4.6	3.6	6.2
CaO	7.0	7.9	9.6
Na ₂ O	2.2	3.3	0.8
K ₂ O	1.2	0.9	1.0
Method	ICP-AES	ICP-AES	ICP-AES
LOI	12.2	11.3	18.7
Total	100.0	100.0	100.0
Elements			
Total C	2.37	2.09	3.79
-Inorg. C	2.34	2.06	3.77
-Org. C	0.03	0.03	0.02
Total S	0.37	0.65	0.12
-Sulphate S	0.08	0.12	0.02
-Sulphide S	0.29	0.53	0.10
Method	Leco	Leco	Leco

Note: *Total iron (includes ferrous iron).

Chemical composition of Milos B, Milos granules and Milos pellets was determined by analyzing LOI, concentration of elements (Si, Al, Fe, Ti, Mg, Ca, Na, K) with ICP-AES, Leco-S, and Leco-C/CO₃. The methods are described in Kumpulainen & Kiviranta (2010). The analyses were done by Labtium Oy. The results are presented in Table 4.

The amount of organic matter in all materials is negligible, the amount of total sulphur is below 1 wt.% and the amount of sulphide bound sulphur below 0.5 wt.%, except in studied pellets it was slightly higher, i.e., 0.53 wt.% (Table 4).

3.3 Exchangeable cations and CEC

Original exchangeable cations were extracted using NH₄Cl in 80 % ethanol (Belyayeva, 1967; Jackson, 1975). The concentrations of cations in the extracted solutions were analysed with ICP-AES by Labtium Oy. Cation exchange capacity (CEC) was measured using Cu(II)-triethylenetetramine method (Meier and Kahr, 1999; Ammann et al., 2005). The results are shown in Table 5.

Table 5. Exchangeable cations [eq/kg] and CEC [eq/kg] of dry (105°C) bulk materials measured with NH₄Cl- and Cu(II)-triethylenetetramine-methods.

Sample	Saturation sites (%)				Exchangeable cations (eq/kg)					CEC (eq/kg)
	Ca	K	Mg	Na	Ca	K	Mg	Na	Sum	Cu-trien
Milos granules	12	2	13	73	0.11	0.02	0.12	0.68	0.93	0.78
Milos pellets	5	2	6	87	0.05	0.02	0.06	0.90	1.03	0.89
Milos B	46	2	22	30	0.35	0.01	0.17	0.23	0.77	0.71

For Milos pellets the sum of initial exchangeable cations was initially 1.21 eq/kg and exchangeable sodium 1.08 eq/kg, which were well above the measured CEC. Based on mineralogical analysis (see section 4.4), Milos pellets contained 2.3 wt.% of hydrated soda, which was apparently remnant of soda activation. Further, it was assumed that soda dissolved during the exchangeable cation extraction. Thus, initial exchangeable sodium cation values were corrected by subtracting the amount of sodium dissolved from the soda (Table 5).

4 MINERALOGICAL COMPOSITION

Mineralogical composition was determined by identifying minerals with x-ray diffraction (XRD) and optical microscopy, and quantifying mineralogical composition with Rietveld refinement. The methods are described in Kumpulainen & Kiviranta (2010). XRD scans were done by GTK.

4.1 Optical microscopy

Coarse fraction of studied materials consisted of carbonates with minor amounts of feldspar, quartz, opaque, iron oxides, opal-A, biotite/chlorite, muscovite, apatite and zircon (Figures 4-6).

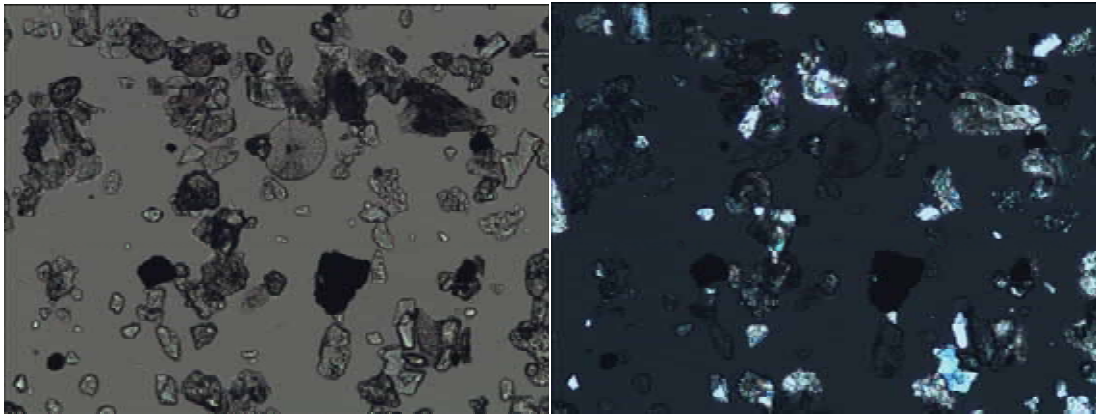


Figure 4. Optical microscopy pictures of coarse grained accessory minerals with x20 magnification of Milos granules. Biogenic opal-A is on middle of the view. Plain polarized light in left and cross polarized light in right.

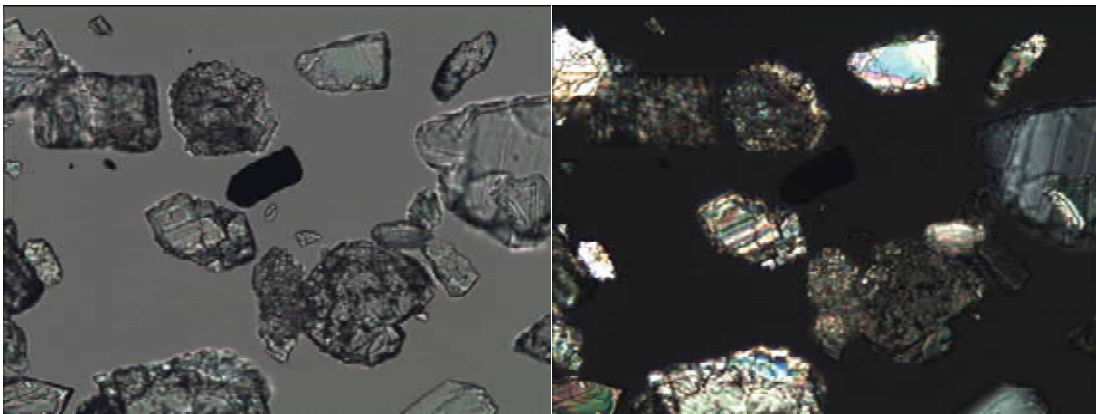


Figure 5. Optical microscopy pictures of coarse grained accessory minerals with x20 magnification of Milos pellets. Plagioclase crystal is on the right edge of the view. Plain polarized light in left and cross polarized light in right.

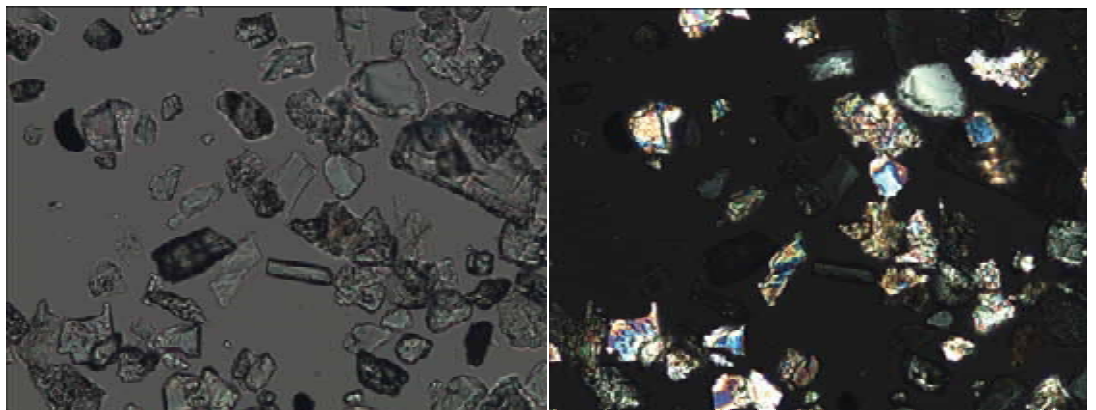


Figure 6. Optical microscopy pictures of coarse grained accessory minerals with x20 magnification of Milos B. Apatite crystal is on the middle of the view. Plain polarized light in left and cross polarized light in right.

4.2 XRD bulk

XRD pattern of randomly oriented sample was measured in order to identify crystalline minerals, to give indication of the presence and quality of clay minerals by defining d(060) line position, and also to produce a data file, which can be used as a basis in the quantification of the mineralogical composition. The method is described in Kumpulainen & Kiviranta (2010). The XRD patterns and interpreted minerals are presented in Figures 7-9. Based on initial XRD identification all samples consisted of dolomite, calcite, smectite, quartz and plagioclase. The position of d(060) lines at 1.496 Å and 1.520 Å for Milos granules, at 1.496 Å and 1.520 Å for Milos pellets, 1.494 Å and 1.519 Å for Milos B indicated the presence of dioctahedral illite/smectite and in addition some other clay mineral (e.g. trioctahedral smectite, glauconite, chlorite, or muscovite), respectively.

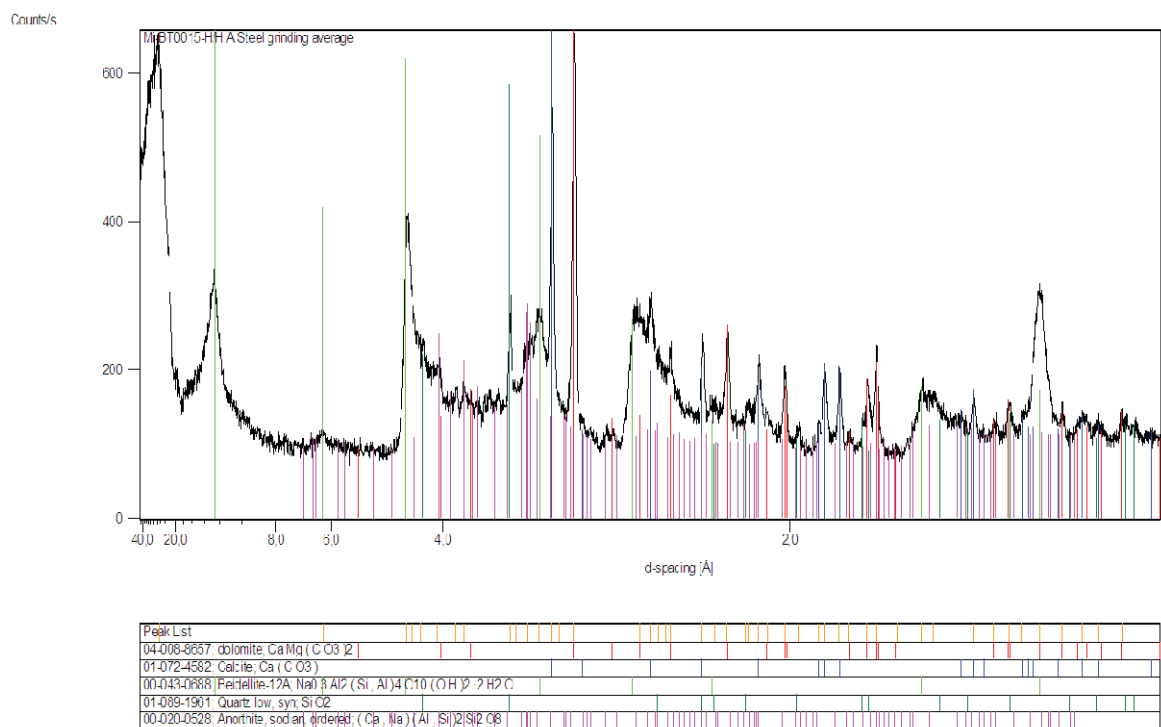


Figure 7. XRD-pattern of bulk samples for Milos granules.

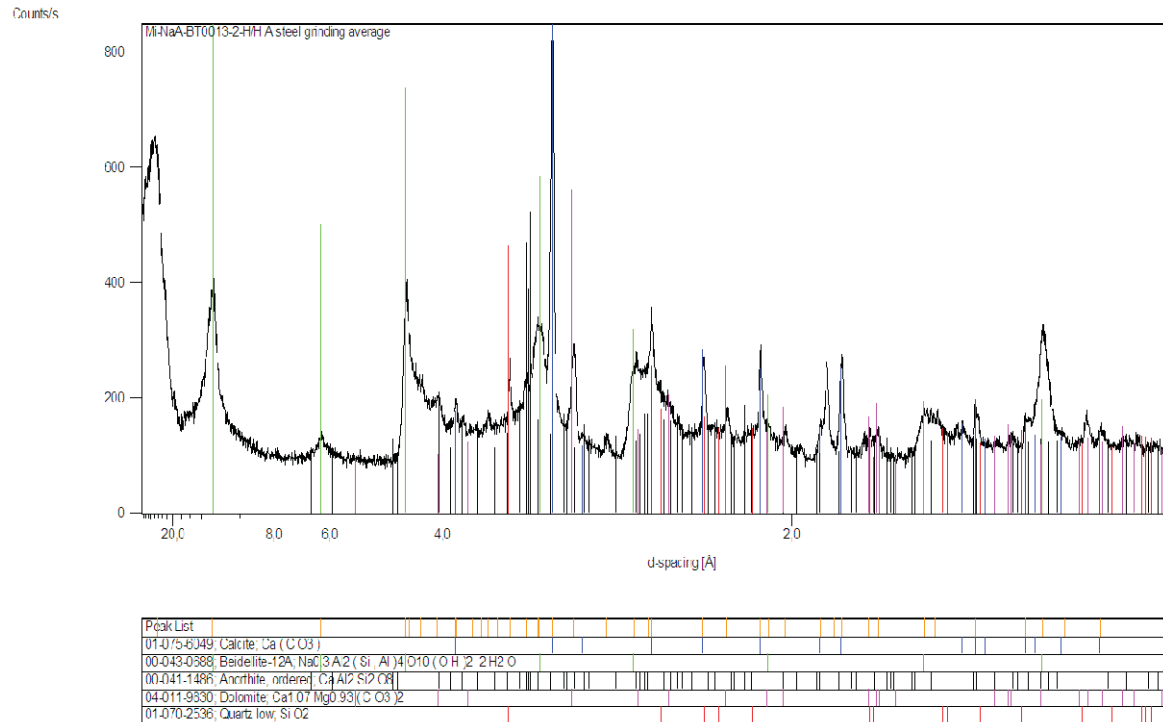


Figure 8. XRD-pattern of bulk samples for Milos pellets.

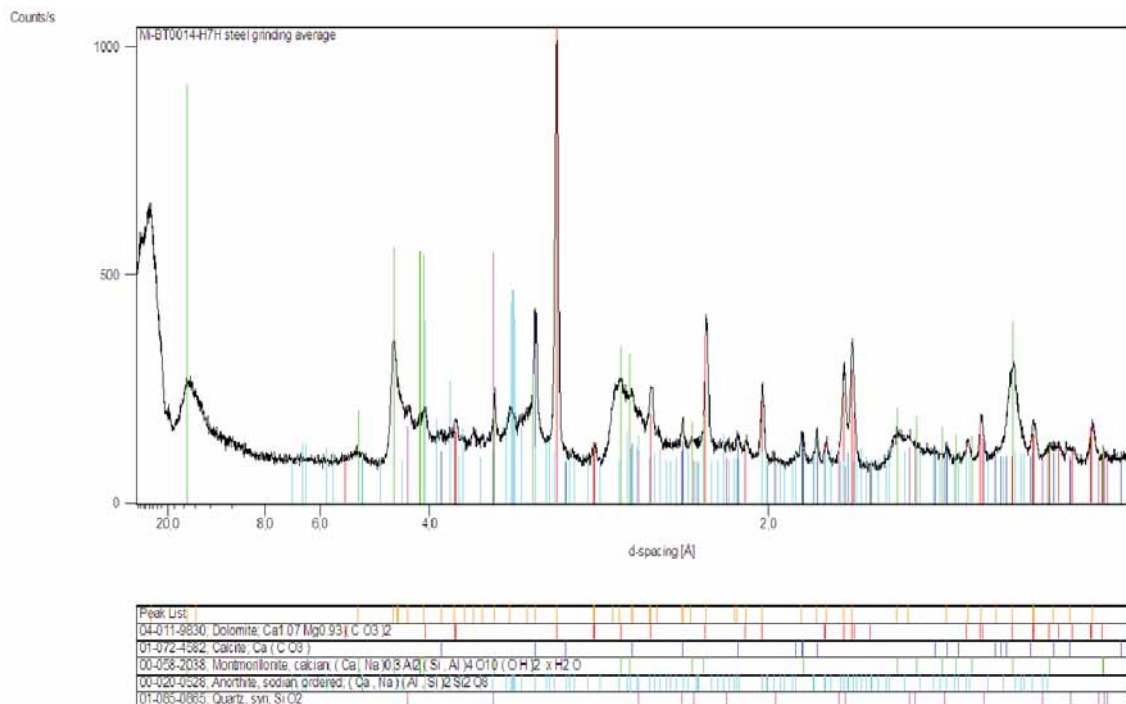


Figure 9. XRD-pattern of bulk samples for Milos B.

4.3 XRD oriented

Oriented mounts were prepared from Mg-exchanged clay fractions (separated by centrifuge sedimentation) in order to identify clay minerals. Oriented mount was scanned by XRD three times: first without any additional treatments to detect the positions of clay mineral (001) lines, then after ethylene glycol (EG) solvation to assess swelling ability of clay minerals (i.e. to identify the presence of smectite), and thirdly after heating at 550 °C to differentiate and identify possible kaolinite from chlorite. The method is described in more detail in Kumpulainen & Kiviranta (2010), and results are shown in Figures 10-12. Based on analyses, clay fraction of Milos granules consists of smectite and illite (Figure 10), clay fraction of Milos pellets consists of smectite (Figure 11), and clay fraction of Milos B consists of smectite, illite and cristobalite (Figure 12).

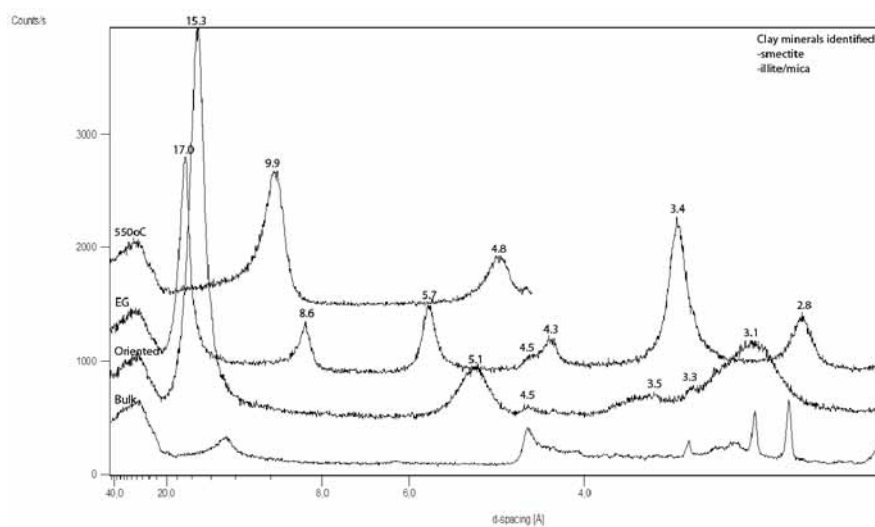


Figure 10. XRD-patterns of clay fraction for Milos granules.

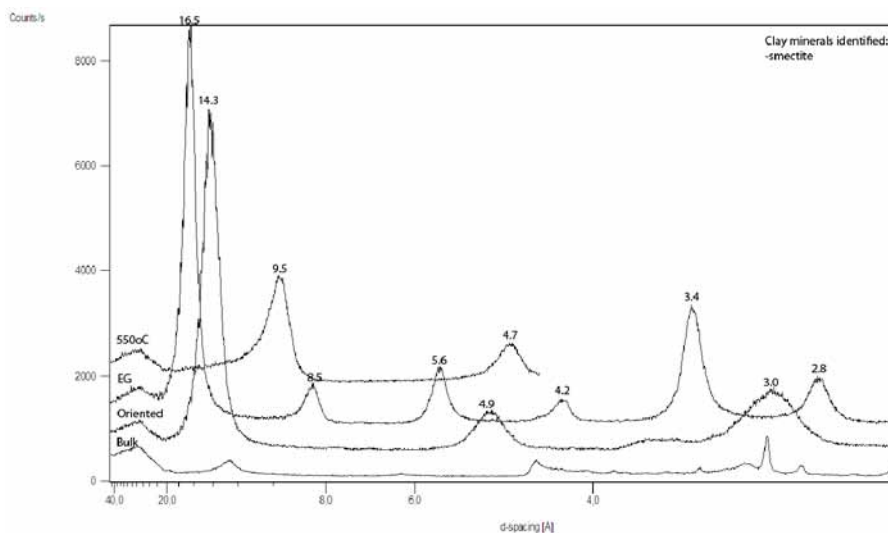


Figure 11. XRD-patterns of clay fraction for Milos pellets.

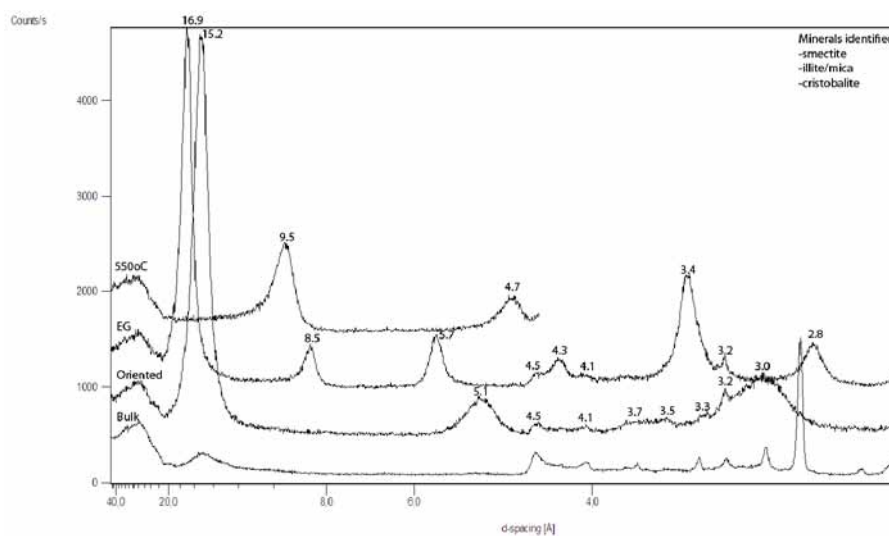


Figure 12. XRD-patterns of clay fraction for Milos B.

4.4 Rietveld analysis

Table 6. Mineralogical compositions (wt.%) of Milos granules, Milos pellets and Milos B.

Sample name	Milos granules	Milos pellets	Milos B
<i>Clay minerals</i>	73.0	72.7	57.5
- Smectite	67.6	69.1	50.0
- Illite	5.4	3.6	7.5
- Biotite/chlorite	tr	tr	tr
- Muscovite	tr		tr
<i>Feldspars</i>	5.7	4.0	4.3
- Plagioclase	3.2	4.0	2.9
- K-feldspar	2.5		1.4
Cristobalite			4.4
Tridymite/opal	tr	1.0	tr
Quartz	1.0	0.6	0.8
<i>Iron oxides</i>	0.5	0.5	0.6
- Hematite	0.5	0.2	tr
- Goethite		0.3	0.6
- Magnetite		tr	tr
Pyrite	0.7	1.3	0.5
Anatase	0.4	0.3	0.4
Soda (hydrated)		2.3	
<i>Carbonates</i>	18.7	17.4	31.3
- Calcite	8.3	13.4	7.9
- Dolomite	10.4	4.0	23.4
Apatite	tr		tr
Zircon		tr	
Total	100	100.1	99.8
Method	XRD/Rietveld	XRD/Rietveld	XRD/Rietveld

Note: tr=trace amounts

Mineralogical composition was determined with Rietveld analysis using Siroquant program. The method is described in Kumpulainen & Kiviranta (2010), and the results are presented in Table 6. Some minerals such as pyrite and anatase were added to the list of quantified minerals based on information from chemical analyses, and some minerals, such as K-feldspar and soda ash were added to the initial list of quantified minerals to get a better fit for the XRD pattern.

Mineralogical quantification shows that all samples consist mostly of smectite (50-69 wt.%), but also quite large amounts of carbonates are present (17-31 wt.%). The amount of non-swelling illite in studied Milos material varied from 3.6 to 7.5 wt.%, and the amount of feldspars from 4.0 to 5.7 wt.%. Milos pellets contained 2.3 wt.% hydrated soda ash as a remnant from soda activation.

The validity of Rietveld analyses were estimated by comparing calculated chemical compositions to the observed chemical composition (Tables 7-9). Comparison (Table 7) shows that mineralogical analysis overestimates the content of smectite and plagioclase, and underestimates the content of iron oxides and silica phases (quartz and opal-A) in Milos granules.

Table 7. Comparison of mineralogy based calculated chemical composition, observed chemical composition, difference (all in wt.%) and possible explanation for the difference of Milos granules.

Oxide	Observed	Calculated	Difference	Possible explanation
Na ₂ O	2.29	2.43	-0.15	
MgO	4.73	5.27	-0.55	Overestimation of smectite
CaO	7.13	8.77	-1.64	Overestimation of plagioclase
Fe ₂ O ₃	5.77	4.33	1.44	Underestimation of iron oxides
Al ₂ O ₃	15.84	17.01	-1.17	Overestimation of plagioclase and smectite
SiO ₂	52.52	51.01	1.51	Underestimation of silica phases
CO ₂	8.81	8.82	-0.02	
SO ₃	0.94	0.95	-0.02	
TiO ₂	0.69	0.44	0.25	
K ₂ O	1.28	0.95	0.32	

For Milos pellets, mineralogical analysis overestimates the content of plagioclase, calcite and pyrite, and underestimates the content of illite and silica phases (quartz and opal-A) (Table 8).

Table 8. Comparison of mineralogy based calculated chemical composition, observed chemical composition, difference (all in wt.%) and possible explanation for the difference of Milos pellets.

Oxide	Observed	Calculated	Difference	Possible explanation
Na ₂ O	3.35	3.01	0.34	
MgO	3.71	3.87	-0.16	
CaO	8.05	9.94	-1.89	Overestimation of plagioclase and calcite
Fe ₂ O ₃	4.31	5.00	-0.69	Overestimation of pyrite and iron oxides
Al ₂ O ₃	16.75	1.67	0.09	
SiO ₂	52.79	50.59	2.20	Underestimation of silica phases
CO ₂	7.78	8.42	-0.64	Overestimation of calcite
SO ₃	1.67	1.84	-0.17	Overestimation of pyrite
TiO ₂	0.68	0.28	0.40	
K ₂ O	0.91	0.35	0.56	Underestimation of illite

For Milos B, mineralogical analysis slightly overestimates the content of plagioclase, dolomite and pyrite, and slightly underestimates the content of iron oxides and silica phases (quartz, cristobalite and opal-A) (Table 9).

Table 9. Comparison of mineralogy based calculated chemical composition, observed chemical composition, difference (all in wt.%) and possible explanation for the difference of Milos B.

Oxide	Observed	Calculated	Difference	Possible explanation
Na ₂ O	0.85	0.76	0.09	
MgO	6.50	7.69	-1.19	Overestimation of dolomite
CaO	10.06	12.93	-2.88	Overestimation of dolomite and plagioclase
Fe ₂ O ₃	5.38	3.47	1.92	Underestimation of iron oxides
Al ₂ O ₃	14.05	13.57	0.48	
SiO ₂	46.67	44.50	2.17	Underestimation of silica phases
K ₂ O	1.10	0.98	0.12	
CO ₂	14.47	14.91	-0.44	
SO ₃	0.30	0.68	-0.38	Overestimation of pyrite
TiO ₂	0.62	0.45	0.17	

5 BULK DENSITY, SWELLING PRESSURE, HYDRAULIC CONDUCTIVITY AND EMDD

Swelling pressure and hydraulic conductivity was determined using de-aired 1 %-salt solution, which had Na:Ca-ratio of 2:1, as saturant and permeant. Dry density was calculated from water ratio and bulk density determined with paraffin oil method (Karnland et al. 2006). Effective montmorillonite dry density (EMDD) was calculated after Dixon et al. (2002), using a water ratio based dry density. The results are presented in Table 10.

There were two types of swelling pressure and hydraulic conductivity measurements of Milos pellets in this study. First, swelling pressure and hydraulic conductivity of pellets was measured from a sample that was used as received and compacted to a target density, and then from a sample that was pulverized and compacted to a same density as the not ground sample. The results (Table 10) showed that there was no noticeable difference in the swelling pressure or hydraulic conductivity of these samples.

Two types of swelling pressure and hydraulic conductivity measurements were done with variable sample diameters (24 and 50 mm) using Milos B. The results (Table 10) showed that there was no difference in the hydraulic conductivity or swelling pressure of these samples.

Table 10. Bulk density, swelling pressure, hydraulic conductivity and EMDD for Milos granules, Milos pellets and Milos B.

Material	Milos granules	Milos pellets			Milos B	
Sample name	Milos granules	Mi-NaA-BT0013-2-Pp-1	Mi-NaA-BT0013-2-Pp-2	Mi-NaA-BT0013-2-Powder	Mi--BT0014-1	Mi--BT0014-2
Sample diameter	50 mm	50 mm	50 mm	50 mm	24 mm	50 mm
Saturating solution	10 g/l salt (2:1 NaCl: CaCl ₂)	10 g/l salt (2:1 NaCl: CaCl ₂)	10 g/l salt (2:1 NaCl: CaCl ₂)	10 g/l salt (2:1 NaCl: CaCl ₂)	10 g/l salt (2:1 NaCl: CaCl ₂)	10 g/l salt (2:1 NaCl: CaCl ₂)
Bulk density - paraffin method -calculated from w	1.830 g/cm ³ 1.882 g/cm ³	1.684 g/cm ³ 1.723 g/cm ³	1.622 g/cm ³ 1.653 g/cm ³	1.631 g/cm ³ 1.652 g/cm ³	1.877 g/cm ³ 1.963 g/cm ³	1.884 g/cm ³ 1.955 g/cm ³
Dry density - paraffin method -calculated from w	1.336 g/cm ³ 1.374 g/cm ³	1.091 g/cm ³ 1.116 g/cm ³	0.989 g/cm ³ 1.008 g/cm ³	0.994 g/cm ³ 1.007 g/cm ³	1.436 g/cm ³ 1.502 g/cm ³	1.435 g/cm ³ 1.489 g/cm ³
Water ratio	37.0 %	54.4 %	63.9 %	64.1 %	30.7 %	31.3 %
Swelling pressure	1.28 MPa	0.129 MPa	0.116 MPa	0.115 MPa	1.15 MPa	1.40 MPa
Hydraulic conductivity	2.35*10 ⁻¹² m/s	9.66*10 ⁻¹² m/s	1.53*10 ⁻¹¹ m/s	7.08*10 ⁻¹² m/s	1.69*10 ⁻¹² m/s	2.47*10 ⁻¹² m/s
EMDD	1.099 g/cm ³	0.855 g/cm ³	0.765 g/cm ³	0.781 g/cm ³	0.967 g/cm ³	0.966 g/cm ³

6 REFERENCES

Ammann L., Bergaya F., Lagaly G. 2005. Determination of the cation exchange capacity of clays with copper complexes revisited. *Clay Minerals*, 40, 441-453.

ASTM D 5890-06. Standard Test Method for Swell Index of Clay Mineral Component of Geosynthetic Clay Liners.

Belyayeva N.I. 1967. Rapid method for the simultaneous determination of the exchange capacity and content of exchangeable cations in solonchic soils. *Soviet Soil Science*, 1409-1413.

Cebo Holland product data 2009. Published in Hansen J., Korkiala-Tanttu L., Keski-Kuha E., Keto P. 2010. Deposition tunnel backfill design for a KBS-3V repository. Posiva WR 2009-129, Appendix V.

Christidis G. & Dunham A.C. 1993. Compositional variations in smectites: Part I. Alteration of intermediate volcanic rocks. A case study from Milos Island, Greece. *Clay Minerals* 28, 255-273.

Christidis G.E., Scott P.W., Marcopoulos T. 1995. Origin of the bentonite deposits of Eastern Milos, Aegea, Greece: Geological, mineralogical and geochemical evidence. *Clays and Clay Minerals* 43, 63-77.

Dixon D., Anttila S., Viitanen M., Keto P. 2008. Tests to determine water uptake behaviour of tunnel backfill. SKB R-08-134.

Dixon D.A., Chandler N.A., Baumgartner P. 2002. The influence of groundwater salinity and interfaces on the performance of potential backfilling materials. *In* Proceedings of the 6th International Workshop on design and Construction of Final Repositories, Backfilling in Radioactive Waste Disposal, Brussels, 11–13 March 2002. ONDRAF/NIRAS, Brussels, Belgium. Transactions, Session IV, Paper 9.

Finnish standard CEN ISO/TS 17892-4: 2004. Geotechnical investigation and testing. Laboratory testing of soil. Part 4: Determination of particle size distribution.

Finnish standard CEN ISO/TS 17892-12: 2004. Geotechnical investigation and testing. Laboratory testing of soil. Part 12: Determination of Atterberg limits.

Jackson M.L. 1975. Soil chemical analysis – advanced course. Second edition. Madison, Wisconsin. 991p.

Karnland O., Olsson S., Nilsson U. 2006. Mineralogy and sealing properties of various bentonites and smectite-rich clay materials. SKB TR-06-30. Swedish Nuclear Fuel and Waste Management Company (SKB), Stockholm, Sweden.

Kumpulainen S., Kiviranta L. 2010. Mineralogical and chemical characterization of various bentonite and smectite-rich clay materials. Posiva WR 2010-52. Posiva Oy, Olkiluoto, Finland.

Meier L.P., Kahr G. 1999. Determination of the cation exchange capacity (CEC) of clay minerals using the complexes of copper(II) ion with triethylenetetramine and tetraethylenepentamine. *Clays and Clay Minerals*, 47, 386-388.

Roskill 2008. The Economics of bentonite, 2008. 11th edition. Roskill Information Services Ltd. 281p.